



Novel quinolone-based potent and selective HDAC6 inhibitors: synthesis, molecular modeling studies and biological investigation

This is the peer reviewed version of the following article:

Original:

Relitti, N., Saraswati, A.P., Chemi, G., Brindisi, M., Brogi, S., Herp, D., et al. (2021). Novel quinolone-based potent and selective HDAC6 inhibitors: synthesis, molecular modeling studies and biological investigation. EUROPEAN JOURNAL OF MEDICINAL CHEMISTRY, 212, 1-20 [10.1016/j.ejmech.2020.112998].

Availability:

This version is available <http://hdl.handle.net/11365/1123251> since 2021-05-28T14:07:12Z

Published:

DOI: <http://doi.org/10.1016/j.ejmech.2020.112998>

Terms of use:

Open Access

The terms and conditions for the reuse of this version of the manuscript are specified in the publishing policy. Works made available under a Creative Commons license can be used according to the terms and conditions of said license.

For all terms of use and more information see the publisher's website.

(Article begins on next page)

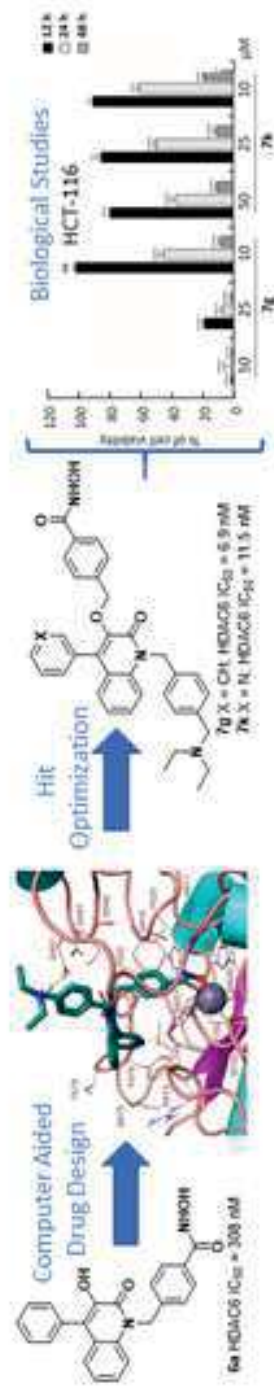
European Journal of Medicinal Chemistry

Novel quinolone-based potent and selective HDAC6 inhibitors: synthesis, molecular modelling studies and biological investigation

--Manuscript Draft--

| | |
|------------------------------|---|
| Manuscript Number: | EJMECH-D-20-02294R2 |
| Article Type: | Full Paper |
| Keywords: | HDAC6 inhibitors; HDAC; quinolone synthesis; cancer; structure-activity relationships; molecular modeling |
| Corresponding Author: | Giuseppe Campiani, Ph.D. European Research Centre for Drug Discovery & Development Siena, ITALY |
| First Author: | Nicola Relitti |
| Order of Authors: | Nicola Relitti A. Prasanth Saraswati Giulia Chemi Margherita Brindisi Simone Brogi Daniel Herp Karin Schmidtkunz Fulvio Saccoccia Giovina Ruberti cristina ulivieri Francesca Vanni Federica Sarno Lucia Altucci Stefania Lamponi Manfred Jung Sandra Gemma stefania butini, Ph.D. Giuseppe Campiani |
| Abstract: | <p>In this work we describe the synthesis of potent and selective quinolone-based histone deacetylase 6 (HDAC6) inhibitors. The quinolone moiety has been exploited as an innovative bioactive cap-group for HDAC6 inhibition; its synthesis was achieved by applying a multicomponent reaction. The optimization of potency and selectivity of these products was performed by employing computational studies which led to the discovery of the diethylaminomethyl derivatives 7g and 7k as the most promising hit molecules. These compounds were investigated in cellular studies to evaluate their anticancer effect against colon (HCT-116) and histiocytic lymphoma (U9347) cancer cells, showing good to excellent potency, leading to tumor cell death by apoptosis induction. The small molecules 7a, 7g and 7k were able to strongly inhibit the cytoplasmic and slightly the nuclear HDAC enzymes, increasing the acetylation of tubulin and of the lysine 9 and 14 of histone 3, respectively. Compound 7g was also able to increase Hsp90 acetylation levels in HCT-116 cells, thus further supporting its HDAC6 inhibitory profile. Cytotoxicity and mutagenicity assays of these molecules showed a safe profile; moreover, the HPLC analysis of compound 7k revealed good solubility and stability profile.</p> |

| | |
|-----------------------------|--|
| Suggested Reviewers: | José Marco-Contelles jlmarco@iqog.csic.es |
| | Mary Kay Pflum pflum@wayne.edu |
| | Shozeb Haider shozeb.haider@ucl.ac.uk |
| | Angel De Lera qolera@uvigo.es |



Highlights

- Rational design and synthesis of novel quinolone-based selective HDAC6 inhibitors
- Compounds **7g** and **7k** were the most potent compounds against HDAC6
- These compounds possess a good selectivity towards HDAC6 over the 1 and 8 isoforms
- Compound **7g** showed a strong reduction in cell viability against HCT-116 cells
- Induction of apoptosis was observed after the treatment with **7g** and **7k**

Novel quinolone-based potent and selective HDAC6 inhibitors: synthesis, molecular modelling studies and biological investigation

Nicola Relitti ^{a,1}, A. Prasanth Saraswati ^{a,1}, Giulia Chemi ^{a,2}, Margherita Brindisi ^{a,3}, Simone Brogi ^b, Daniel Herp ^c, Karin Schmidtkunz ^c, Fulvio Saccoccia ^d, Giovina Ruberti ^d, **Cristina Ulivieri ^e, Francesca Vanni ^e**, Federica Sarno^f, Lucia Altucci^f, Stefania Lamponi ^a, Manfred Jung ^c, Sandra Gemma ^a, Stefania Butini ^a, Giuseppe Campiani ^{a,*}

^a *Department of Biotechnology, Chemistry and Pharmacy, DoE Department of Excellence 2018-2022, University of Siena, via Aldo Moro 2, 53100, Siena, Italy*

^b *Department of Pharmacy, University of Pisa, via Bonanno 6, 56126, Pisa, Italy*

^c *Institute of Pharmaceutical Sciences, Albert-Ludwigs-Universität Freiburg, Albertstraße 25, 79104, Freiburg, Germany*

^d *Institute of Biochemistry and Cell Biology, CNR, Campus A. Buzzati-Traverso. Via E. Ramarini 32, 00015 Monterotondo (Rome) Italy*

^e *Department of Life Sciences, University of Siena, via Aldo Moro 2, 53100, Siena, Italy*

^f *Department of Precision Medicine, University of Campania Luigi Vanvitelli, Vico L. de Crecchio 7, 80138, Naples, Italy*

Corresponding author.

E-mail address: campiani@unisi.it (G. Campiani)

¹ These authors equally contributed.

² Present address: Wellcome Centre for Anti-Infectives Research, Drug Discovery Unit, Division of Biological Chemistry and Drug Discovery, University of Dundee, DD1 5EH Dundee, United Kingdom

³ Present address: Department of Pharmacy, University of Napoli Federico II, DoE Department of Excellence 2018-2022, Via D. Montesano 49, 80131, Napoli, Italy

Abstract

In this work we describe the synthesis of potent and selective quinolone-based histone deacetylase 6 (HDAC6) inhibitors. The quinolone moiety has been exploited as an innovative bioactive cap-group for HDAC6 inhibition; its synthesis was achieved by applying a multicomponent reaction. The optimization of potency and selectivity of these products was performed by employing computational studies which led to the discovery of the diethylaminomethyl derivatives **7g** and **7k** as the most promising hit molecules. These compounds were investigated in cellular studies to evaluate their anticancer effect against colon (HCT-116) and histiocytic lymphoma (U937) cancer cells, showing good to excellent potency, leading to tumor cell death by apoptosis induction. The small molecules **7a**, **7g** and **7k** were able to strongly inhibit the cytoplasmic and slightly the nuclear HDAC enzymes, increasing the acetylation of tubulin and of the lysine 9 and 14 of histone 3, respectively. Compound **7g** was also able to increase Hsp90 acetylation levels in HCT-116 cells, thus further supporting its HDAC6 inhibitory profile. Cytotoxicity and mutagenicity assays of

these molecules showed a safe profile; moreover, the HPLC analysis of compound **7k** revealed good solubility and stability profile.

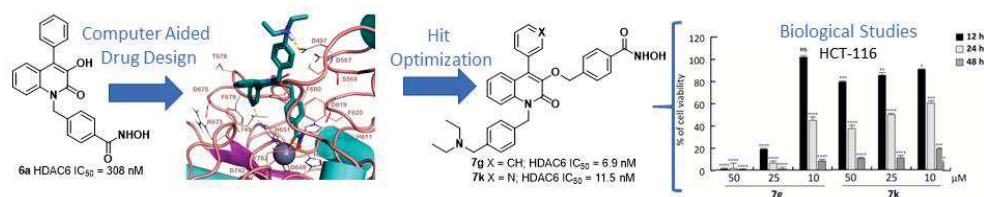
Keywords

HDAC6 inhibitors, HDAC, quinolone synthesis, cancer, structure-activity relationships, molecular modeling

Highlights

- Rational design and synthesis of novel quinolone-based selective HDAC6 inhibitors
- Compounds **7g** and **7k** were the most potent compounds against HDAC6
- These compounds possess a good selectivity towards HDAC6 over the 1 and 8 isoforms
- Compound **7g** showed a strong reduction in cell viability against HCT-116 cells
- Induction of apoptosis was observed after the treatment with **7g** and **7k**
- No mutagenicity and cytotoxicity were observed for these compounds

Graphical abstract



Abbreviations

AcHsp90 (AcLys294), acetylated Hsp90 in lysine 294; AcTub, acetylated α -tubulin; DCM, dichloromethane; DIBAL, diisobutylaluminum hydride; DMF, dimethylformamide; DMSO, dimethyl sulfoxide; H3K9/14ac, acetylated histone H3 in lysine 9 and 14; HCT-116, colon cancer cells; HDAC, histone deacetylase; HDACi, HDAC inhibitors; Hsp90, heat-shock protein 90; PARP, Poly(ADP-ribose) polymerase; PTSA, *p*-toluenesulfonic acid; PTSH, *p*-toluenesulfonyl hydrazide; SAR, structure-activity relationship; SP, standard precision; TFA, trifluoroacetic acid; THF; tetrahydrofuran; U937, histiocytic lymphoma; ZBG, zinc binding group.

1. Introduction

Histone deacetylases (HDACs) are enzymes involved in the removal of acetyl groups from histones, thus modulating gene transcription. Their over-expression has been ascertained in solid cancers, hematological malignancies, and parasitic disorders, making them a viable target for developing novel chemotherapeutic agents [1,2], as well as in rare diseases [3]. Of the 18 identified HDAC isoforms (subdivided into 4 classes, I-IV), HDAC6 is unique owing to the presence of a zinc finger ubiquitin binding domain and its localization. Structurally, it contains two catalytic domains, DD1 and DD2, present at the *N*-terminal and the central region, respectively. With regard to its localization, HDAC6 is a cytoplasmic enzyme (unlike HDAC1, 2 and 3, that are nuclear localized and HDAC8, that can show both nuclear and cytoplasmic spreading) which can

shuttle between cytoplasm and the nucleus in response to cellular signaling [4]. Apart from its action on histones it also exerts deacetylase activity on non-histone substrates such as α -tubulin, heat-shock protein 90 (Hsp90), peroxiredoxin, cortactin, and tau [3]. This specific feature of HDAC6 is responsible for its unique role in the pathogenesis of cancer and a number of rare diseases such as idiopathic pulmonary fibrosis, inherited retinal disorders, Rett syndrome, and Charcot-Marie-Tooth disease [3,5]. Comparatively, HDAC10 that has a closer structural correlation with HDAC6 has a very weak activity as a lysine deacetylase and its role has so far been described mostly for autophagy promotion [6].

Several HDAC inhibitors (HDACi) have successfully reached the clinic and are being used as therapeutic tools to treat different malignancies. Representative HDACi include: vorinostat (**1**, SAHA, **1**) [7] and romidepsin (**2**) [8] for the treatment of cutaneous T-cell lymphomas, panobinostat (**3**) [9] for multiple myeloma, and belinostat (**4**) [10] for relapsed or refractory peripheral T-cell lymphoma. These compounds behave as pan-HDACi since they inhibit several HDAC isoforms, thus causing many side effects. The discovery of Tubastatin A (**5**) a tetrahydropyrido[4,3-*b*]indole hydroxamic acid, as a selective HDAC6i has paved the way for the development of isoform-selective HDACi. However, a potent inhibition of HDAC10 isoform has been reported after exposure with **5** [11–13]. Identification of isoform-selective compounds is vital for dissecting the biological roles of specific HDACs and for developing safer therapeutic tools. The general pharmacophoric model of HDACi encompasses three key components namely: the surface recognition group (cap), the zinc binding group (ZBG) and a linker bridging the two portions. Based on this model several selective HDAC6 inhibitors have been developed mainly by modifying the cap and the linker portions, while retaining hydroxamate as the ZBG [2,14,15].

Many natural products have been identified possessing potent anticancer properties, which have inspired chemists to use them as building blocks in the synthesis of novel chemotherapeutics [16–19]. In this context, functionalized 4-arylquinolin-2(1*H*)-ones represent an attractive scaffold for developing biologically active molecules, including the orally active anticancer agent tipifarnib, that is currently undergoing clinical investigation [20]. Based on an exhaustive literature search, we identified the quinolone moiety as a promising cap group due to its lipophilicity *in vitro*. This system ideally fits in the cap region of the HDACi pharmacophore [21]. Many quinolone containing compounds are well known as chemotherapeutics (e.g. ciprofloxacin, norfloxacin) and anticancer agents (voreloxin) [22]. Quinoline based anticancer agents exert their activity by playing a role in the DNA intercalation process, inhibiting topoisomerase II activity and tubulin polymerization [23].

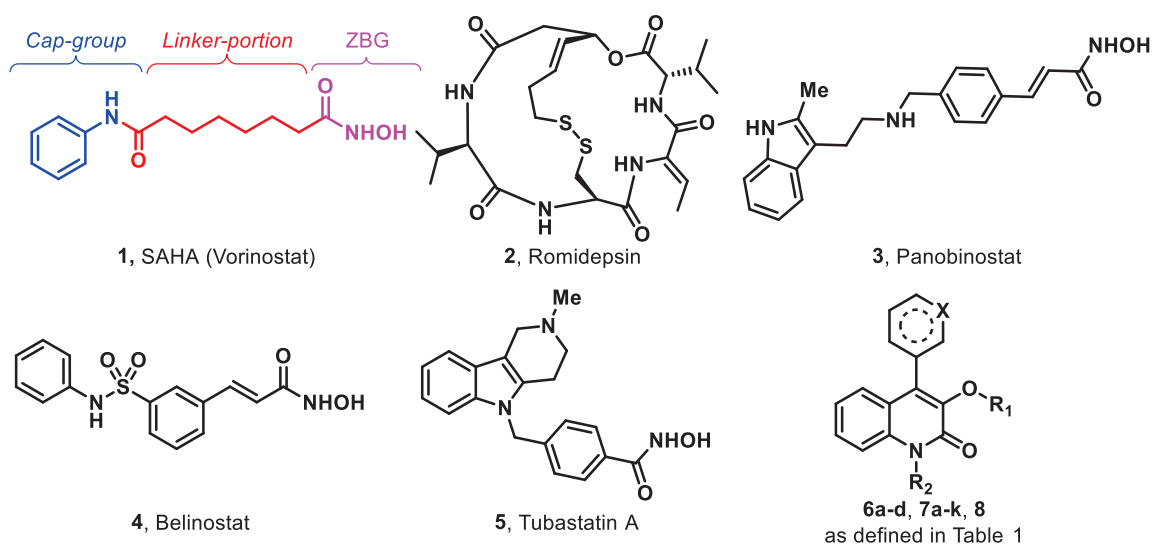


Figure 1. Representative structures of HDAC inhibitors (1-5) and general structure of the title compounds 6-8.

In our pursuit to identify novel cap groups for potent and selective HDAC6i [14,15,24], we exploited the potential of a naturally occurring compound containing the quinolone skeleton as an effective versatile and hindered cap-group suitable for a broad variety of scaffold decorations (as shown in the general structure of Figure 1). By a virtual screening approach, we identified several cap-groups; a preliminary computational investigation, using compound 6a, characterized by a viridicatin-based cap-group, showed that it perfectly fits into the hydrophobic sub-pocket delimited by L712 and F642 (*Danio rerio* HDAC6 numbering, corresponding to residues L749 and F679 in *h*HDAC6). Moreover, by our computational approach, we observed that the cap-group of Tubastatin A and 6a into *z*/HDAC6 (PDB ID: 6THV) target the same region of the enzyme as highlighted in Figure 2. Therefore, we selected this interesting quinolone-based cap-group to rationally design and synthesize a new focused library of HDAC6 selective inhibitors as described below. According to our preliminary *in silico* analysis and aiming at obtaining compounds with high selectivity index towards HDAC6 (over HDAC1) to be screened against different cancer cell lines we synthesized a library of quinolone-based hydroxamates. The synthesis of the 3-hydroxy-4-arylquinolin-2(1*H*)-ones moiety was carried out by the application of a multicomponent ring-expansion recently reported by Tangella *et al.* This protocol permits the conversion of isatin to viridicatin alkaloids after the *in situ* generation of α -aryldiazomethanes in presence of an aldehyde. ~~derivatives and inspired from a multicomponent protocol, useful to access the 3-hydroxy-4-arylquinolin-2(1*H*)-ones, we constructed a series of cap groups~~ [25]. This protocol enabled us to develop novel HDAC6i (compounds 6a-d, 7a-k and 8, Table 1) bearing *N*- or *O*-appended linker moieties, and a variety of focused modifications at both their heterocyclic core and the aromatic portions.

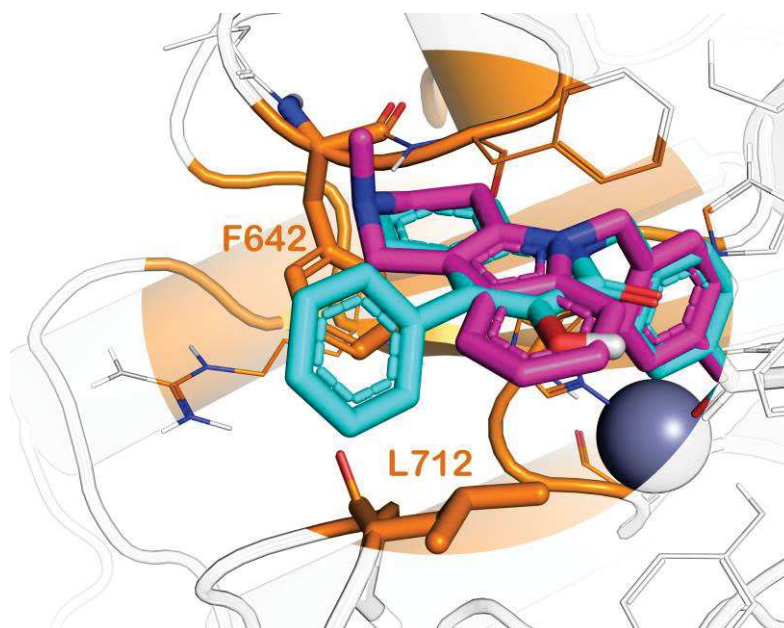
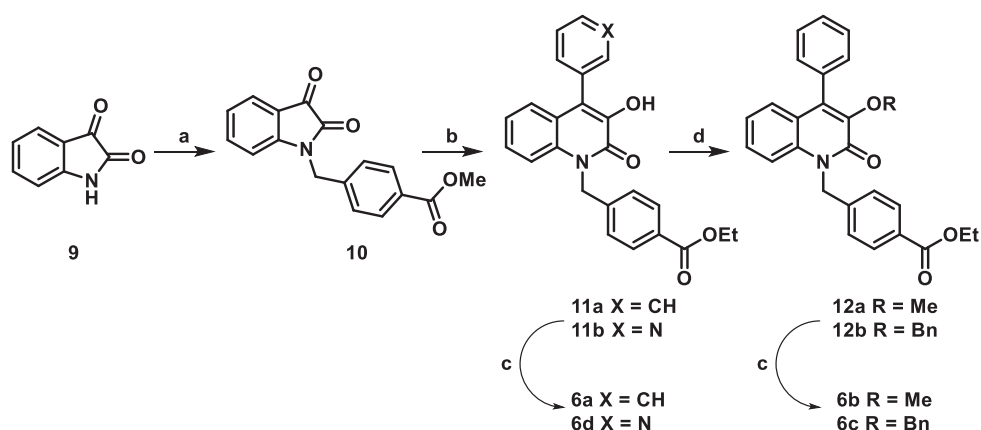


Figure 2. Docked pose of **6a** into *z*HDAC6 (PDB ID: 6THV), superposed to the crystallized inhibitor Tubastatin A belonging to 6THV. Focus on residues in sticks that are the constituents of the hydrophobic sub-pocket explored by the viridicatin cap-group (residues L712 and F642 in *z*HDAC6 correspond to L749 and F679 in *h*HDAC6) is presented. The picture was generated by means of PyMOL.

2. Chemistry

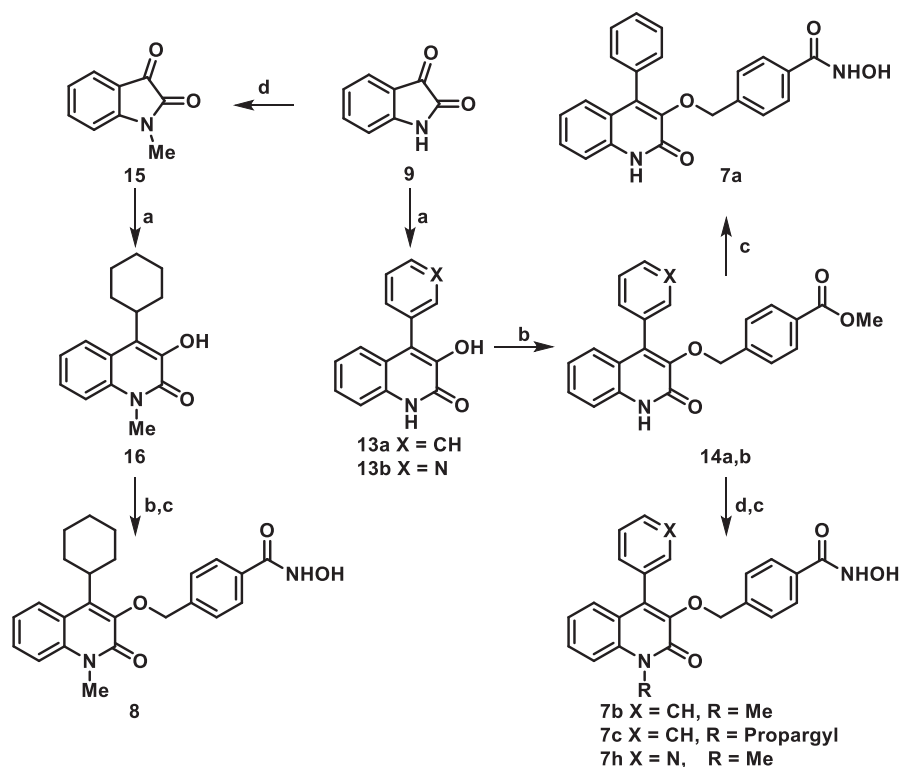
The structures of final compounds **6a-d**, **7a-k** and **8** are shown in Table 1. In order to achieve the synthesis of the quinolone core of the compounds, the ring expansion procedure described by Tangella *et al* was applied [25]. It is a multicomponent reaction involving: an aldehyde, activated with *p*-toluenesulfonyl hydrazide (PTSH), and a *N*-substituted isatin in the presence of K_2CO_3 as base.

In Scheme 1 the synthesis of the final compounds **6a-d** is described. Isatin (**9**) was alkylated with methyl 4-(bromomethyl)benzoate and the resulting product **10** was subjected to the ring expansion procedure with benzaldehyde or 3-pyridinecarboxaldehyde obtaining compounds **11a,b**, respectively. As expected, a transesterification with EtOH occurred in this step. Intermediates **11a,b** were converted to their corresponding hydroxamic acid derivatives **6a,d** after treatment with a strong excess of aqueous NH_2OH in the presence of KOH. Intermediate **11a** was also submitted to *O*-alkylation with MeI or benzyl bromide providing derivatives **12a,b**, respectively. These latter were converted into final compounds **6b,c** upon reaction with NH_2OH and KOH.



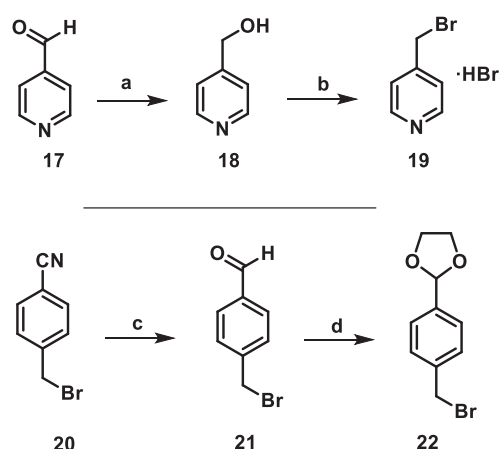
Scheme 1. Synthesis of compounds 6a-d. Reagents and conditions: (a) methyl 4-(bromomethyl)benzoate, NaH, DMF, 0 to 25 °C, 12 h, quantitative yield; (b) PTSH, benzaldehyde or 3-pyridinecarboxaldehyde, K₂CO₃, EtOH, 80 °C, 12 h, 32-64%; (c) NH₂OH (50% water solution), KOH, DCM, MeOH, 25 °C, 3 h, 82-97%; (d) MeI, NaH, THF, 0 to 25 °C, 12 h; or BnBr, KI, K₂CO₃, DMF, 80 °C, 12 h, 29-64%.

In Scheme 2 is reported the synthesis of compounds **7a-c,h** and **8**. The ring expansion performed on isatin (**9**) in the presence of benzaldehyde or 3-pyridinecarboxaldehyde provided quinolone derivatives **13a,b**, respectively. These latter were subjected to alkylation reaction with methyl 4-(bromomethyl)benzoate in the presence of K₂CO₃ as the base to furnish the *O*-alkylated intermediates **14a,b**. Treatment of **14a** with NH₂OH in the presence of KOH led to compound **7a**. Alternatively, alkylation of the lactam nitrogen of **14a,b** with MeI or propargyl bromide followed by reaction with NH₂OH, led to the *N*-alkyl derivatives **7b,c,h** [26]. For the synthesis of compound **8**, isatin was alkylated with MeI and successively subjected to the ring expansion reaction with cyclohexanecarboxaldehyde obtaining compound **16**. From this intermediate, compound **8** was obtained as previously described.



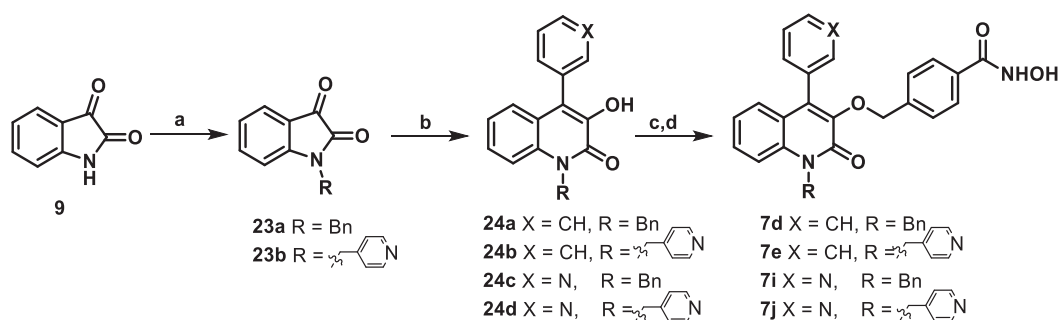
Scheme 2. Synthesis of compounds 7a-c,h and 8. Reagents and conditions: (a) PTSH, benzaldehyde or 3-pyridinecarboxaldehyde or cyclohexanecarboxaldehyde, K_2CO_3 , EtOH, 80 °C, 12 h, 30-45%; (b) methyl 4-(bromomethyl)benzoate, K_2CO_3 , KI, DMF, 80 °C, 12 h, 20-74%; (c) NH_2OH , KOH, DCM, MeOH, H_2O , 25 °C, 3 h, 50-98%; (d) MeI/ propargyl bromide, NaH, THF, 0 to 25 °C, 12 h, 56% to quantitative yield.

In Scheme 3 is reported the synthesis of bromides **19** and **22** used as alkylating agents for the synthesis of final compounds **7e**, **7g** and **7k**. Following the procedure described by Liu et al. 4-pyridinecarboxaldehyde (**17**) was reduced to alcohol **18** with $NaBH_4$ and then converted to the corresponding bromide **19** after treatment with PBr_3 [27]. For the synthesis of the intermediate **22**, 4-(bromomethyl)benzonitrile (**20**) was reduced with DIBAL to the corresponding benzaldehyde **21**, that was successively converted to dioxolane **22** with ethylene glycol in the presence of PTSA [28].



Scheme 3. Synthesis of bromo-derivatives 19 and 22. Reagents and conditions: (a) $NaBH_4$, MeOH, 0 to 25 to 25 °C, 2 h, 80%; (b) 48% HBr, 100 °C, 4 h then PBr_3 , DCM, 45 °C, 4 h, 93%; (c) DIBAL, DCM, -78 to 0 °C, 1 h, quantitative yield; (d) ethylene glycol, PTSA, toluene, 110 °C, 12 h, 69%.

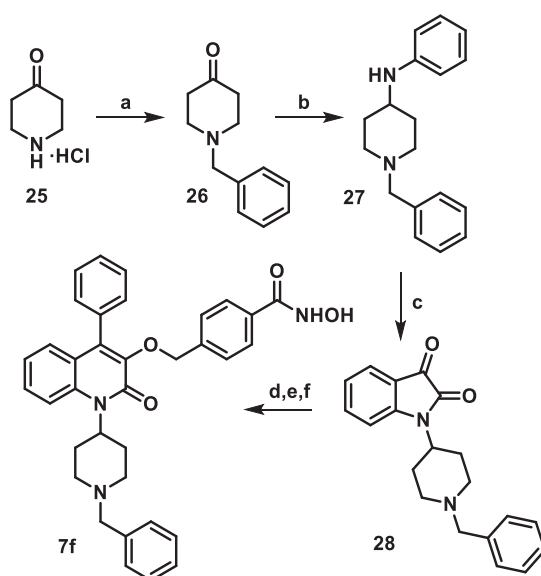
In Scheme 4 the synthesis of final compounds **7d,e,i,j** is described. Isatin was alkylated with benzyl bromide or bromide **19** using NaH as the base to generate intermediates **23a,b** [26]. These compounds were subjected to the previously described ring expansion procedure with benzaldehyde or 3-pyridinecarboxaldehyde to provide the desired 2-quinolones **24a-d** that were converted to the final compounds **7d,e,i,j** in the presence of NH_2OH .



Scheme 4. Synthesis of compounds 7d,e,i,j. Reagents and conditions: (a) BnBr or **19**, NaH, DMF, 0 to 25 °C, 12 h, 38-74%; (b) PTSH, benzaldehyde or 3-pyridinecarboxaldehyde, K_2CO_3 , EtOH, 80 °C, 12 h, 24-44%; (c) methyl 4-

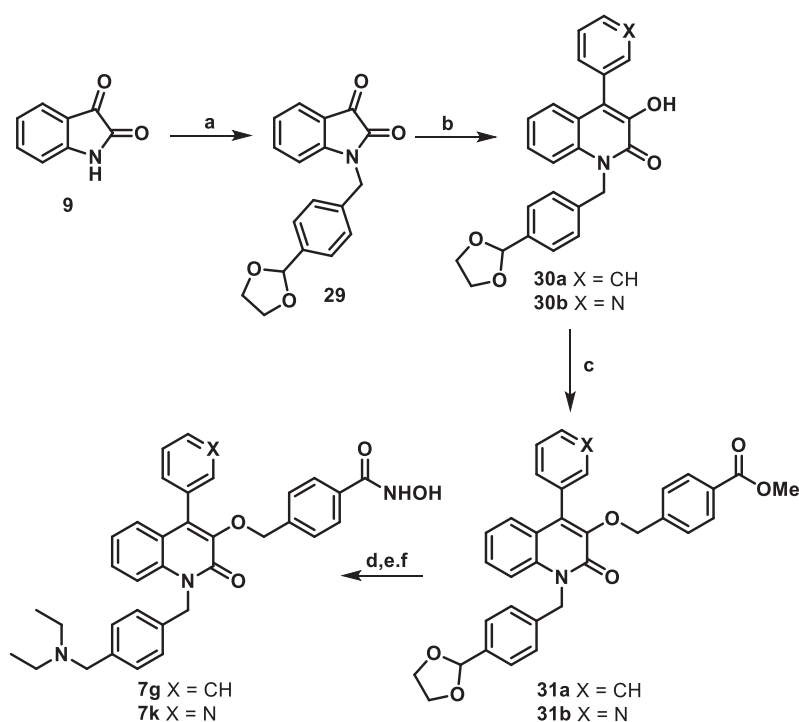
(bromomethyl)benzoate, K_2CO_3 , KI, DMF, 80 °C, 12 h, 62-30%; (d) NH_2OH , KOH, DCM, MeOH, H_2O , 25 °C, 3 h, 45-90%.

The synthesis of compound **7f** is described in Scheme 5. Since alkylation of the isatin with 1-benzyl-4-bromo or iodopiperidine failed in all the attempted conditions, *N*-alkylated isatin **28** was prepared starting from piperidone (**25**) following a procedure described in a patent by Spear et al. [28]. **25** was first *N*-benzylated and then subjected to a reductive amination protocol with aniline in presence of $NaBH(OAc)_3$ providing intermediate **27**. This compound was treated with oxalyl chloride, obtaining an unstable intermediate that was immediately treated with $AlCl_3$ in DCM to afford isatin derivative **28** under Friedel-Craft conditions. Ring expansion, alkylation, and final reaction with NH_2OH were then performed as previously described, leading to the formation of compound **7f**.



Scheme 5. Synthesis of compound 7f. Reagents and Conditions: (a) Benzyl bromide, K_2CO_3 , DMF, 80 °C, 12 h, 70%; (b) aniline, $NaBH(OAc)_3$, DCM, AcOH, 0 to 25 °C, 12 h, 89%; (c) oxalyl chloride, DCM, 25 °C, 2 h; then $AlCl_3$, DCM, 40 °C, 2 h, 52%; (d) PTSH, benzaldehyde, K_2CO_3 , EtOH, 80 °C, 12 h, 55%; (e) methyl 4-(bromomethyl)benzoate, K_2CO_3 , KI, DMF, 80 °C, 12 h, 15%; (f) NH_2OH , KOH, DCM, MeOH, H_2O , 25 °C, 3 h, 62%.

In Scheme 6 the synthesis of the final compounds **7g,k** is described. Isatin was alkylated with bromide **22** affording intermediate **29**. This compound was subjected to the previously described ring expansion procedure to get the desired quinolones **30a,b**. These intermediates were alkylated with methyl 4-(bromomethyl)benzoate obtaining **31a,b** which were subsequently deprotected in acidic medium, and the corresponding free aldehydes were subjected to a reductive amination protocol with diethylamine in the presence $NaBH(OAc)_3$, affording the corresponding diethylamino derivatives, that were converted to the final compounds **7g,k** as previously described.







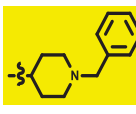
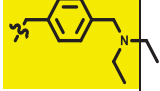


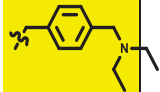
Scheme 6. Synthesis of compounds 7g,k. Reagents and conditions: (a) **22**, NaH, DMF, 0 to 25 °C, 12 h, quantitative yield; (b) PTSH, benzaldehyde or 3-pyridinecarboxaldehyde, K₂CO₃, EtOH, 80 °C, 12 h, 48%; (c) methyl 4-(bromomethyl)benzoate, K₂CO₃, KI, DMF, 80 °C, 12 h, 55-80%; (d) 6 N HCl, THF, 25 °C, 1 h, quantitative yield; (e) diethylamine, NaBH(OAc)₃, DCM, AcOH, 0 to 25 °C, 12 h, 47-59%; (f) NH₂OH, KOH, DCM, MeOH, H₂O, 25 °C, 3 h, 74-80%.

3. Results and Discussion

The compounds herein developed were firstly tested in enzymatic assay to evaluate their HDAC6 inhibitory profile compared with the HDAC1 and 8 isoforms. Successively, the ability of the best performing compounds to induce the acetylation of histone, tubulin and HSP90 was evaluated, followed by assessment of their anticancer properties in two cell lines (HCT-116 and U937). We have also determined key pharmacokinetic parameters (solubility and chemical stability), toxicity and mutagenicity of selected compounds.

Table 1. Novel HDAC6 inhibitors **6a-d**, **7a-k** and **8** against *h*HDAC1, as IC₅₀ (μM), and *h*HDAC6, as IC₅₀ (nM).^a

| Cpd | R | X | HDAC1 IC ₅₀ | HDAC6 IC ₅₀ | HDAC6/HDAC1 |
|-------------|----|---|------------------------|------------------------|-------------|
| 6a-d | OR | X | | | |
| 7a-k | R | X | | | |
| 8 | Me | | | | |

| | | | (μM) | (nM) | |
|----|---|----|---------------------------------------|------------------|------|
| 6a | H | CH | 11 ± 1 | 308 ± 51 | 3.6 |
| 6b | Me | CH | 4.5 ± 0.31 | 61.6 ± 7.5 | 73 |
| 6c |  | CH | 5.5 ± 0.3 | 84.5 ± 7.9 | 65 |
| 6d | H | N | 50 96% 25 82% 10 36% 1 < 10% | 295.6 ± 24.4 | n.d. |
| 7a | H | CH | 6.6 ± 0.4 | 146.9 ± 14.2 | 45 |
| 7b | Me | CH | 50 80% 25 46% 10 26% 1 < 10% | 518.9 ± 17.1 | n.d. |
| 7c |  | CH | 6.1 ± 0.9 | 82.3 ± 11.4 | 74 |
| 7d |  | CH | 50 97% 25 93% 10 76% 1 17% | 176.0 ± 14.7 | n.d. |
| 7e |  | CH | 1.2 ± 0.2 | 84.1 ± 9.9 | 14 |
| 7f |  | CH | 50 79% 25 67% 10 46% 1 < 10% | 870.4 ± 87.8 | n.d. |
| 7g |  | CH | 0.322 ± 0.073 | 6.9 ± 0.9 | 46 |
| 7h | Me | N | 5.01 ± 0.44 | 46 ± 5 | 109 |
| 7i |  | N | 2.5 ± 0.41 | 25.6 ± 3.1 | 96 |
| 7j |  | N | 1.7 ± 0.31 | 45.3 ± 5.6 | 38 |
| 7k |  | N | 0.319 ± 0.08 | 11.5 ± 1.5 | 29 |
| 8 | - | - | 3.0 ± 0.18 | 33.0 ± 2.6 | 91 |

^aEach value is the mean of at least three determinations; compounds were assayed at eight concentrations; results are expressed with SD.

3.1. Structure-activity relationships (SAR)

From the enzymatic assay emerged a significant affinity of the molecules for the HDAC6 with selectivity over HDAC1 and 8 isoforms (Tables 1 and 2). Starting from compound **6a** (HDAC6 IC₅₀ = 308 nM) we decided to explore the effect of the introduction of alkyl groups such as methyl or benzyl substituent on the oxygen at C3 (**6b,c**). These modifications led to a significant improvement in both the HDAC6 inhibition potency (HDAC6 IC₅₀ of 61 and 84 nM, for **6b** and **6c** respectively) and the selectivity over HDAC1 isoform. Successively we decided to explore the effect of replacing the 4-phenyl group with a more basic 3-pyridyl group (compound **6d**); this modification did not improve potency and led to a HDAC6 inhibition (295 nM) similar to **6a**. We then decided to interrogate the outcome of a switch of the acidic ZBG from the N1 to the oxygen atom at C3; thus, we developed a series of analogues typified by **7a**. This new prototypic compound led to improved potency at HDAC6 over **6a** (**7a** HDAC6 IC₅₀ = 147 nM). Following exploration of several substituents at N1 generated compounds **7b-g**. This focused series of derivatives demonstrated that the introduction of a basic lateral chain such as 4-pyridyl (**7e**) or *N,N*-diethylaminomethylbenzyl (**7g**) determined a strong increase in HDAC6 inhibition (**7e,g** HDAC6 IC₅₀ equal to 84 and 7 nM, respectively). Also, it was shown that the introduction of large and/or alkyl substituents generated analogues with weaker potency against HDAC6 (**7b-d,f** IC₅₀ ranging from 82 to 870 nM). The substitution of the phenyl ring at C4 with a 3-pyridyl group (compounds **7h-k**) resulted in a general increase of HDAC6 inhibition, when compared to **7a**, with IC₅₀ values ranging from 12 to 46 nM. As observed for **7g**, also compound **7k**, bearing a *N,N*-diethylaminomethylbenzyl at N1, showed the highest potency of this subgroup of analogues. From **7a**, the introduction of a methyl group at N1 and the replacement of the phenyl group at C4 with a cyclohexyl group led to compound **8**. This compound showed a good inhibitory profile for HDAC6 together with a significant selectivity over HDAC1 (IC₅₀ = 33 nM and selectivity index of 91).

In order to gain a full picture in terms of SAR analysis for the new series of compounds, we flanked *in vitro* data with computational studies. Starting from the molecular docking calculations using Glide employing Standard Precision (SP) as scoring function and visual inspection we were able to understand the general trend of the preferred binding modes of quinolone derivatives on HDAC1 and HDAC6 isoforms (for more details see the appropriate sections in the supplementary material file). Keeping on with the already described inhibitors, for our newly developed derivatives we retained the *para*-substituted phenylhydroxamic acid functionality, anchored to the benzyl linker, as the ZBG. Among the derivatives the polar contacts established by the hydroxamic acid of the ZBG were similar and represented by three H-bonds established between the carbonyl and Y782, the NH and G619, the OH and H610. Considering the specific contacts, we primarily focused our attention to the best positioning of the ZBG on the quinolone scaffold (heterocyclic nitrogen vs exocyclic hydroxyl group). Merging the results of the docking studies and the enzymatic tests we observed that: when the ZBG is placed on the nitrogen atom as for compounds **6a-d** the activity on HDAC6 slightly decreases when compared to the substitution on the oxygen atom (3-OH) (i.e. compounds **7a-k** and **8**). The binding mode of compounds is depicted in Figures 3 and Figures S1, S3. The whole orientation of the scaffolds of compound **6a,b** (Figures 3A,B), presented a similar binding mode, differing from that of the other analogues as represented in Figures 3C-F and Figures S1-S3 (see details in the Supplementary Material

sections). Compound **7a** (Figure 3C), with no substituents on *N1*, was able to establish two π - π stackings with F620, F680 through the phenyl ring of the ZBG, and an additional H-bond between H651 and the carbonyl of the quinolone core. The binding mode of compounds **7b-d,h,i,j** is discussed in the Supplementary Material section.

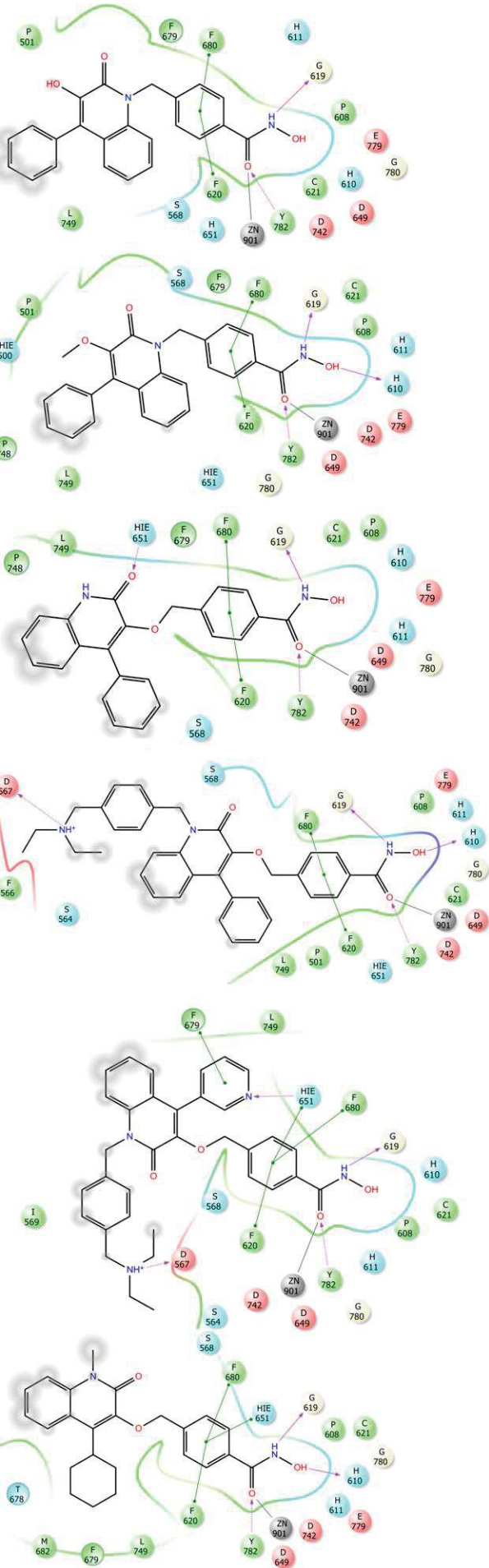
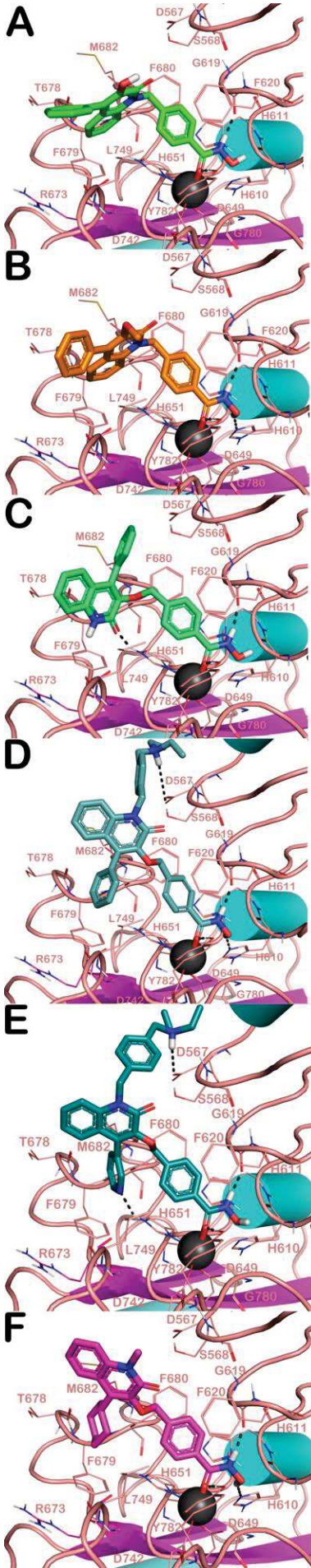


Figure 3. Docked poses into HDAC6 (PDB ID: 5EDU) of compounds **6a,b**, **7a**, **7g**, **7k** and **8** (panels A-F, respectively). Compounds are represented as sticks. The residues of the active sites are represented as lines and the whole protein is represented as cartoon. The Zn²⁺ ion is represented as a gray sphere. The polar contacts are depicted as dotted lines while the coordination bond as plain lines. The pictures were generated by means of PyMOL.

With the dual aim of increasing polar contacts within HDAC6 binding site while improving water solubility of these molecules, we introduced some functionalities on the quinolone scaffold leading to compounds **6d**, **7e-k** bearing pyridine at C4, benzylpiperidine and diethylaminomethylbenzyl groups at N1 (Figures 3D-E for compounds **7g** and **7k**). The introduction of a pyridin-3-yl instead of the phenyl ring at C4 (compound **6d**, Figure S1B), gave better results in terms of selectivity between the two investigated isoforms, compared to the parent compound **6a**. These findings prompted us to evaluate the introduction of the 4-methylenepyridine system at N1 on the series of compound **7**. Although establishing a polar contact through the nitrogen of the pyridine with the backbone of F680, compound **7e** (Figure S3A) did not show a satisfactory profile towards the HDAC6 isoform, since a similar set of contacts were also established with the HDAC1 isoform. The insertion of the different basic functionalities like the benzylpiperidine, as for compound **7f** (Figure S3B), resulted in an increase in the length of the molecule that precluded the formation of any relevant H-bond, decreasing the HDAC6 inhibitory potency. On the contrary, the insertion of a diethylaminomethylbenzyl portion at N1 as in compound **7g** (Figure 3D) provided the most potent HDAC6 inhibitor, with a potency in the low nanomolar range. As expected, the more flexible and protonatable diethylaminomethylbenzyl substituent allowed to form not only a new and not previously observed H-bond with the D567 residue, but also a strong salt bridge with the same residue. In summary, the introduction of a flexible and protonatable moiety, able to establish a salt bridge and a polar contact with D567 in HDAC6, is a preferred choice to improve the potency of enzyme inhibition. On the other hand, isoform selectivity was improved by introducing at C4 the pyridin-3-yl, retaining a significant potency (**7h-i**, Figure S3C,D) and with over 100-fold selectivity ratio towards HDAC6 over HDAC1. Compound **7k** (Figure 2E) showed a different binding mode compared to the other compounds of the series. With the introduction of the pyridine-4-yl, and additional bond with H651 was established, maintaining the same inhibitory profile. Furthermore, taking into consideration the hydrophobic residues present in the interaction site of HDAC6, we introduced a cyclohexyl ring at C4 in place of the aromatic system, obtaining **8**, the binding mode of which is shown in Figure 2F. Owing to ring flexibility and lower steric hindrance of the methyl at N1 of **8**, different residues were engaged through hydrophobic interactions, namely F679, F680 and L749.

In addition, we performed molecular docking calculation for assessing the putative binding mode of the developed compounds into HDAC1 enzyme. The output of this calculation is depicted in Figures S4-S6, and the binding mode of all molecules is reported in the Supplementary Material.

3.2. *hHDAC8* inhibition assays

Binding affinity studies towards *h*HDAC8 isoform were conducted on the best HDAC6 inhibitors (**7g,k** and **8**) to have an indication of the potency and selectivity of these new quinolone-based derivatives also against this isoform. Among the three tested derivatives, compound **7g** demonstrated the highest selectivity with an IC₅₀ value of 0.55 μM (Table 2) and an index of 80 (HDAC8/HDAC6), while compound **8** was the least potent with an IC₅₀ value of 1.64 μM and a selectivity index of 50. These results highlighted a significant selectivity profile of these compounds towards HDAC6.

Table 2. Inhibitory activity of compounds **7g,k** and **8** as IC₅₀ (μM), and apparent inhibitor constant (K^{app}) against the *h*HDAC8 enzyme

| Cpd | 7g | 7k | 8 | TubA |
|------------------------------------|-------------|-------------|------------|-------------------|
| IC ₅₀ (μM) ^a | 0.55 ± 0.15 | 0.49 ± 0.20 | 1.64 ± 0.3 | 0.695 |
| K ^{app} (μM) ^a | 0.36 ± 0.1 | 0.40 ± 0.1 | 1.93 ± 0.2 | n.d. ^b |
| HDAC8/HDAC6 | 80 | 42 | 50 | 23 |

^aAll compounds were assayed at least two times, and the results are expressed with standard deviations.

^bn.d. Not determined

3.3. Cell-based studies

The anticancer effect of compounds **7g** and **7k**, the best performing small-molecules emerged from the HDAC6 *in vitro* experiments, and one of the starting hit **7a**, were evaluated in cell-based MTT assays against a colon cancer cell line (HCT-116) and a histiocytic lymphoma cell line (U937). All compounds showed a good cytotoxic activity in HCT-116 when used at 50 μM for 24 h and 48 h of induction (Table 3 and Table S1). However, **7g** resulted to be the best molecule tested, with an IC₅₀ of 3.6 μM after 48 h of induction, causing a strong block of cell proliferation already at 25 μM (80%), and at 10 μM, after 24 and 48 h 50% and 90% respectively. Compound **7k**, showed a potent cytotoxicity against HCT-116 cells after 48 h of induction at all concentrations, showing 10 to 20% of cell survival. In accordance with HDAC enzymatic results, compound **7a** resulted the least potent molecule, showing the best results only when tested at 50 μM for 48 h (10% cell viability). In U937 cells, these compounds were found to be less active, inducing the 60-70% of cell proliferation reduction after 48 h at 50 μM (Table 3 and Table S2). Compound **7a** was the most potent in this cell line with respect to the other compounds.

Table 3. IC₅₀ of **7a**, **7k** and **7g** in HCT-116 and U937 cell lines.

| | IC ₅₀ (μM) | | | | | | |
|-----------|-----------------------|-------------|--------------|------|------|-------------|--------|
| | HCT-116 | | | U937 | | | NIH3T3 |
| | 12 h | 24 h | 48 h | 12 h | 24 h | 48 h | 24 h |
| 6b | n.d. | n.d. | n.d. | n.d. | n.d. | n.d. | 90 |
| 7a | n.d. | 33.4 ± 0.1 | 15.02 ± 0.12 | n.d. | n.d. | 27.9 ± 0.05 | n.d. |
| 7k | n.d. | 25.7 ± 0.25 | 8.4 ± 0.56 | n.d. | n.d. | 45.5 ± 0.37 | 90 |
| 7g | 13.5 ± 0.2 | 11.6 ± 0.3 | 3.6 ± 0.29 | n.d. | n.d. | 40.6 ± 0.24 | n.d. |

| | | | | | | | |
|---|------|------|------|------|------|------|----|
| 8 | n.d. | n.d. | n.d. | n.d. | n.d. | n.d. | 18 |
|---|------|------|------|------|------|------|----|

n.d. Not determined

To assess the nature of cellular death occurring after **7a**, **7g** and **7k** treatment, Poly(ADP-ribose)-Polymerase (PARP) was evaluated in HCT-116 (Figure 4E,F) and U937 (Figure 5E,F) cell lines. A significant increase of PARP cleavage levels was observed in the samples after 24 h of treatment with **7g** and **7k**, tested at 10 μ M, demonstrating the activation of apoptotic process [29].

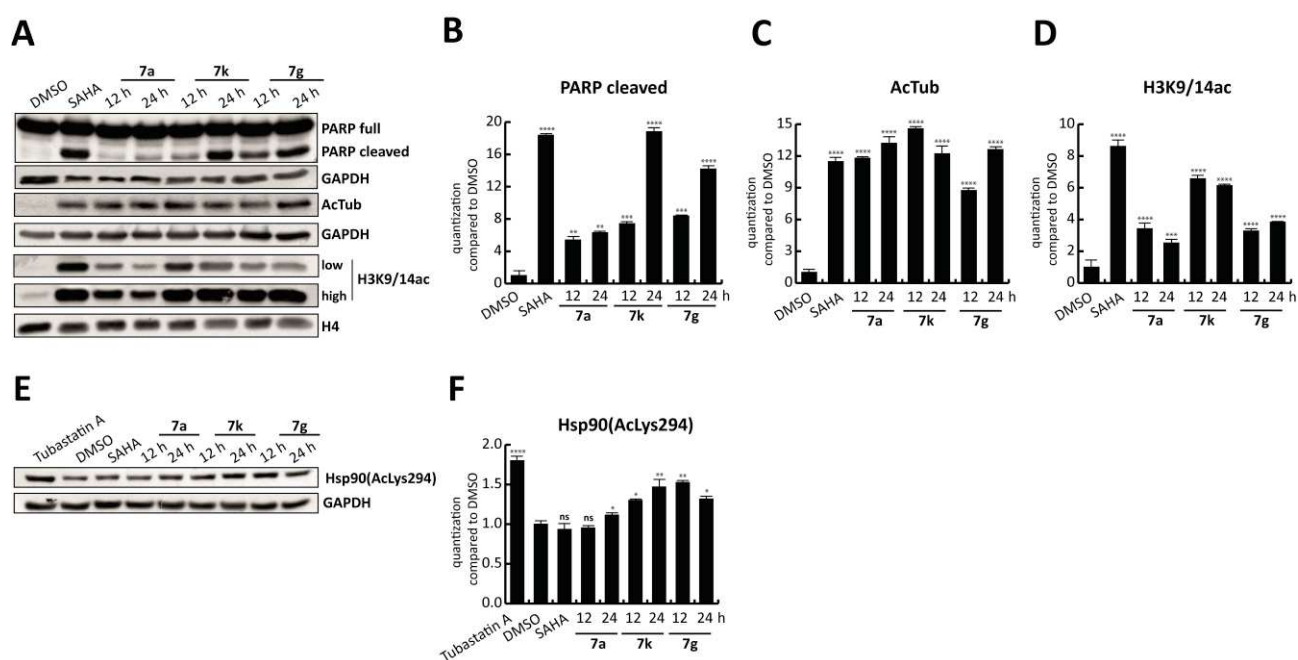


Figure 4. Western blot analysis for cleaved PARP, AcTub, H3K9/14ac and Hsp90(AcLys294) on HCT-116 cancer cell line treated with the compounds **7a**, **7g** and **7k** at 10 μ M for 12 and 24 h. Tubastatin A (5 μ M for 24 h) and SAHA (5 μ M for 24 h) were the positive controls. GAPDH and H4 were used for the normalization. Target levels were quantized using ImageJ software. **** p-value \leq 0.0001, *** p-value \leq 0.001, ** p-value \leq 0.01, * p-value \leq 0.05, ns p-value $>$ 0.05 vs control cells.

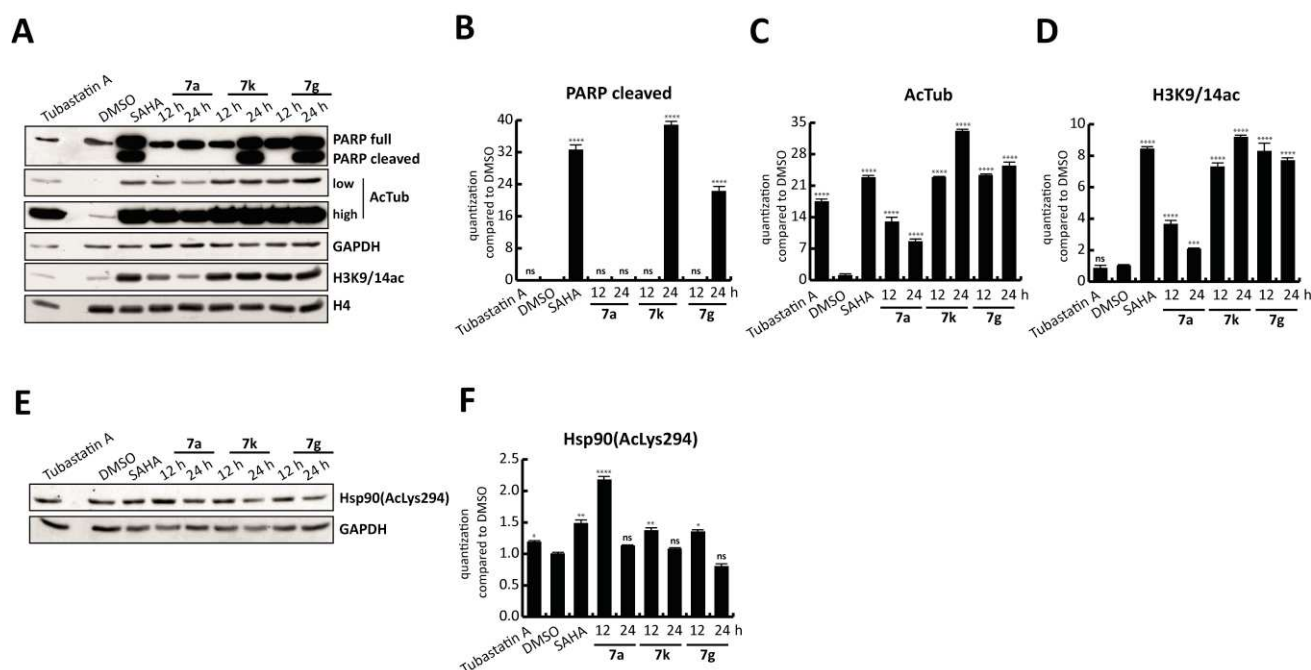


Figure 5. Western blot analysis for cleaved PARP, AcTub, H3K9/14ac and Hsp90(AcLys294) on U937 cancer cell line treated with the compounds **7a**, **7g** and **7k** at 10 μ M for 12 and 24 h. Tubastatin A (5 μ M for 24 h) and SAHA (5 μ M for 24 h) were the positive controls. GAPDH and H4 were used for the normalization. Target levels were quantized using ImageJ software. **** p-value \leq 0.0001, *** p-value \leq 0.001, ** p-value \leq 0.01, * p-value \leq 0.05, ns p-value $>$ 0.05 vs control cells.

To evaluate the capability of the compounds **7a**, **7g** and **7k** to inhibit the HDACs, Western blot studies were conducted in both cell lines analyzing the acetylation levels of alpha-tubulin and of the lysine 9 and 14 of histone 3 (Figure 4 and 5). All molecules, tested at 10 μ M, strongly enhanced the levels of AcTub in HCT-116 (Figure 4C) and U937 (Figure 5C), with a fold \geq 9, indicating the inhibition of cytoplasmic HDACs. The analysis of histone acetylation levels showed that the amount of H3K9/14ac increased after **7a**, **7g** and **7k** treatment, respect to the control, suggesting a possible inhibition of nuclear HDACs may have also occurred. However, in HCT-116 (Figure 4D) compounds **7a** and **7g** appeared to be more selective for cytoplasmic HDACs, increasing the H3K9/14ac of 2/4-fold, compared to **7k** ($>$ 6-fold). In U937 cells (Figure 5D) only compound **7a** showed a low potency against nuclear HDACs.

The interplay between HDAC6 and Hsp90 has been widely demonstrated in the last decade. It was observed that the over-acetylation of Hsp90, due to the inactivation or knockdown of HDAC6, determined the loss of chaperone activity of this protein [30]. Therefore, we decided to evaluate Hsp90(AcLys294) after treatment with **7a**, **7g**, and **7k**. In HCT-116 (Figure 4E, F), but not in U937 (Figure 5E, F), **7a**, **7g** and **7k** increased the levels of Hsp90(AcLys294) when tested at 10 μ M for 12 or 24 h, suggesting the inhibition of HDAC6. In U937, instead, only **7a** raised the Hsp90ac levels respect to the control (Figure 5).

3.4. In silico prediction of selected drug-like properties and experimental evaluation of physico-chemical properties

We predicted the ADME properties and the **heart** toxicity potential of the newly developed compounds by means of QikProp, a software implemented in Maestro suite (QikProp, version 4.3, Schrödinger, LLC, New York, NY, 2015). The output of the calculation is reported in Table **S3**. The predicted values for every molecule can be considered acceptable since they were within the recommended range of the software.

Selected parameters were also assessed experimentally. The *in vitro* solubility and chemical stability of selected compounds **6b**, **7e**, and **7k** were measured by means of HPLC methods as reported in previous work from us [31,32]. As expected, the presence of basic groups on compounds **7e,k** improved the solubility profile at pH = 3 with respect to compound **6b**. Gratifyingly, our analysis also revealed that both **7e,k** exhibited a favorable chemical stability profile at acidic pH. In particular, the chemical stability was almost quantitative for the selected compounds with more than 95% of the compound remaining unaltered at pH = 3 after 24 h (**Table S4**).

3.5. Mutagenicity profile evaluation for **6b**, **7k**, and **8**.

Potential mutagenicity associated with the use of hydroxamic acid-based compounds poses a significant challenge in terms of their drug-like profile [33]. To date, givinostat is the only compound under clinical trials that exhibited no mutagenic effect, while the other FDA approved drugs **1-4** have shown mutagenicity [34]. Therefore, we investigated for compounds **6b**, **7k** and **8** the mutagenic effect in the *Salmonella typhimurium* strains TA98 and TA100. The Ames test is employed to detect potential risks of mutagenicity at the early stages of drug development. The assay can be performed with or without the S9 fraction of rat liver. This latter condition allows an in-depth investigation for evaluating the risk of mutagenicity derived from the metabolites of the compounds under study. After applying both the experimental conditions, no mutagenic effect was observed for compounds **6b**, **7k** and **8** in the *Salmonella typhimurium* strains TA98 and TA100 at all concentrations (5-230 μ M) (Figures S7-S9).

3.6. Lossen rearrangement study on compound **7k**.

It has been observed that the leading cause of mutagenicity associated with the use of HDACi is related to a Lossen's rearrangement involving the hydroxamate group with the formation of the corresponding isocyanate. This intermediate can trigger mutagenicity by damaging the DNA due to its susceptibility to undergo nucleophilic attack [34]. In laboratory, this reaction can be performed on *O*-activated hydroxamic acids under basic conditions. However, under physiological conditions, it has been reported that in case of 2-naphthohydroxamic acid this reaction occurs by the involvement of acetyl-CoA, which activates the oxygen by the addition of an acetyl group [35]. Because of the low acidity of hydroxamic acids, it has been speculated that hydroxamate-based HDACi can reach the catalytic site as neutral molecules and get deprotonated only after a strong metal chelation (e.g. zinc and potassium) [34,36]. In this way, a metal-assisted Lossen's rearrangement may occur leading to the formation of the isocyanate.

In order to check the susceptibility of our compounds to undergo Lossen's rearrangement we investigated **7k** in terms of the formation of the corresponding isocyanate (by checking the conversion to its aniline

counterpart) by exposing it to one equivalent of K_2CO_3 in DMSO at 40 °C (Figures S10, S11). After 18 h we observed by ESI-MS analysis that the predominant peaks were: the starting material (**7k**, $[M+H]^+ = 563.2$) and the corresponding carboxylic acid ($[M+H]^+ = 548.2$, Figure S11). From this study we can assume that the absence of mutagenicity detected in the Ames assay can be explained by a low vulnerability of our compounds to undergo Lossen's rearrangement, thus confirming a safe profile for the HDACi described in this paper.

3.7. Cytotoxic profile evaluation for **6b**, **7g**, **7k** and **8**.

Compounds **6b**, **7k** and **8** were further characterized in a cytotoxicity assay to establish their effect on mouse fibroblasts NIH3T3 cells. Cell viability was measured by the Neutral Red Uptake test and data normalized as % control. TC_{50} values of 90 μM were observed for **6b**, **7k** and 18 μM for **8**, thus indicating a safe profile in normal cells for compounds **6b** and **7k**, while a low cytotoxicity in NIH3T3 cells was observed with compound **8** (Table 3 and Table S5). A second cytotoxicity study was performed on human peripheral blood mononuclear cells (PBMC) after the treatment with compounds **7g** and **7k** for 24 and 48 h. Cell viability was measured by using Guava® ViaCount™ Reagent. From cell viability study, was observed that compound **7k**, after 24 h treatment, exhibited a low cytotoxic action only when tested at 90 μM , thus confirming a safe profile for this compound. On the other hand, compound **7g**, after 24 h treatment, demonstrated a strong reduction in cell viability already when tested at 45 μM (Figure S12, panel A). No significant difference in cytotoxicity were observed when the cells were treated for longer times (48 h, Figure S12, panel B).

4. Conclusion

In this work we describe the synthesis of quinolone-based HDAC inhibitors preferentially targeting the isoform 6. The synthesis of the cap group was achieved by applying a multicomponent reaction involving several substituted isatins, PTSH and a suitable aldehyde. This versatile synthetic strategy could be applied for future scaffold modifications and for the development of optimized analogs. The design of the described molecules was facilitated by applying a computational chemistry approach. The final compounds obtained showed inhibition values in the nanomolar range for HDAC6 with a selectivity index up to 109-fold for HDAC6 over HDAC1. Moreover, selected analogues showed a weak affinity for the *h*HDAC8 enzyme. The most potent HDAC6 inhibitors were subjected to cell-based assays to check their anticancer potential. In particular, compound **7g** gave the best result in terms of cytotoxicity against colon cancer cells, inducing 90% cell death after 48 h at 10 μM , and after 12 h when tested at 50 and 25 μM , by triggering apoptosis. The influence of the compounds on tubulin, histone and Hsp90 acetylation status was evaluated to establish their selectivity towards HDAC6. Notably, all the tested compounds enhanced the levels of AcTub as a result of the inhibition of cytoplasmic HDACs. In HCT-116, **7a** and **7g** showed a lower increase of H3K9/14ac, thus indicating a lower selectivity for nuclear HDACs. Additionally, compounds **7g** and **7k** led to the increase of Hsp90(AcLys294), a selective substrate of HDAC6. By applying HPLC protocols, compound **7k** was found soluble and stable in aqueous solution at pH = 3. Compounds **6b**, **7k** and **8** did not display any cytotoxic or

mutagenic profile as assessed by cytotoxicity studies on mouse fibroblasts and Ames test on *Salmonella typhimurium* strains. The absence of mutagenicity was further confirmed by the low susceptibility of compound **7k** to undergo Lossen's rearrangement to generate its isocyanate derivative. Taken together, these data highlight a promising antitumor potential for these quinolone-based HDAC6 selective inhibitors. These evidences may pave the way to the development of more potent and selective optimized hits useful for a H2L transition and for further biological investigation.

5. Experimental data

5.1. General information

Unless otherwise specified, materials were purchased from commercial suppliers and used without further purification. Reaction progress was monitored by TLC using silica gel 60 F254 (0.040–0.063 mm) with detection by UV. Silica gel 60 (0.040–0.063 mm) was used for column chromatography. ¹H NMR and ¹³C NMR spectra were recorded on a Varian 300 MHz spectrometer or a Bruker 400 MHz spectrometer by using the residual signal of the deuterated solvent as internal standard. Splitting patterns are described as singlet (s), doublet (d), triplet (t), quartet (q) and broad (br); the values of chemical shifts (δ) are given in ppm and coupling constants (J) in Hertz (Hz). HPLC were performed with a Shimadzu Prominence apparatus equipped with a scanning absorbance UV-VIS detector (Diode Array SPD-M20A) also equipped with a thermostatic chamber or with Agilent 1100 Series equipped with UV-VIS detector. ESI-MS spectra were performed by an Agilent 1100 Series LC/MSD spectrometer. HRESIMS were carried out by a Thermo Finnigan LCQ Deca XP Max ion-trap mass spectrometer equipped with Xcalibur software, operated in positive ion mode. Infrared (IR) spectra were recorded in the neat on an Agilent Cary 630 Spectrometer FT-IR instrument and are reported in reciprocal centimeters (cm⁻¹). Melting points were detected by a BÜCHI melting point B-450 and reported and °C. The yields are referred to purified products and are not optimized. All moisture-sensitive reactions were performed under argon atmosphere using oven-dried glassware and anhydrous solvents. Final compounds were analyzed by combustion analysis (C, H, N) to confirm purity >95%.

5.2. Chemistry

5.2.1 Methyl 4-((2,3-dioxindolin-1-yl)methyl)benzoate (**10**).

To a solution of isatin (300 mg, 2.03 mmol) in dry DMF, cooled at 0 °C, a 60% dispersion of NaH, in mineral oil (95 mg, 2.38 mmol) was added and stirred for 5 min at 0 °C. Then, methyl 4-(bromomethyl)benzoate (2.34 g, 10.20 mmol) was added and the reaction was allowed to reach 25 °C and stirred for 12 h. Thereafter, a saturated solution of NH₄Cl (5 mL) was added and the mixture was extracted with EtOAc (3 x 5 mL). The combined organic layers were washed with brine, dried over Na₂SO₄ and concentrated *in vacuo*. The residue was used in the next step without further purifications and affording **10** (2.00 g, quantitative yield) as a red solid. ¹H NMR (300 MHz, CDCl₃) δ 8.02 (d, J = 8.3 Hz, 2H), 7.63 (dd, J

= 7.5, 0.8 Hz, 1H), 7.48 (td, $J = 7.8, 1.3$ Hz, 1H), 7.39 (d, $J = 8.5$ Hz, 2H), 7.11 (td, $J = 7.6, 0.8$ Hz, 1H), 6.70 (d, $J = 7.9$ Hz, 1H), 4.98 (s, 2H), 3.90 (s, 3H). ESI-MS m/z : $[M + H]^+$ 296.0.

5.2.2. Ethyl 4-((3-hydroxy-2-oxo-4-phenylquinolin-1(2H)-yl)methyl)benzoate (**11a**).

A solution of benzaldehyde (379 mg, 3.57 mmol) and PTSH (665 mg, 3.57 mmol) in EtOH (17 mL) was stirred at 25 °C for 2 h. After this, **10** (575 mg, 3.57 mmol) and K_2CO_3 (987 mg, 7.14 mmol) were added and the reaction was stirred at 80 °C for 12 h. The solvent was evaporated, and the crude was purified by chromatography on silica gel (20% EtOAc in petroleum ether) giving **11a** (430 mg, 64%) as a red solid. 1H NMR (300 MHz, $CDCl_3$) δ 8.02 (d, $J = 8.3$ Hz, 2H), 7.65 – 6.99 (m, 11H), 5.74 (s, 2H), 4.49 – 4.25 (m, 2H), 1.37 (t, $J = 7.1$ Hz, 3H); ^{13}C NMR (75 MHz, $CDCl_3$) δ 166.2, 159.3, 140.8, 140.7, 133.6, 132.8, 130.8, 130.2, 129.9, 129.7, 128.6, 128.4, 127.5, 126.5, 124.2, 123.3, 122.3, 114.9, 61.0, 46.9, 14.3; ESI-MS m/z : $[M + H]^+$ 400.1; mp 187.3-190.0 °C.

5.2.3. Ethyl 4-((3-hydroxy-2-oxo-4-(pyridin-3-yl)quinolin-1(2H)-yl)methyl)benzoate (**11b**).

Starting from **10** (100 mg, 0.33 mmol) the title compound was obtained following the procedure described to get **11a**. The residue was purified by chromatography on silica gel (2% MeOH in DCM) affording **11b** (43 mg, 32%) as a red solid. 1H NMR (300 MHz, $DMSO-d_6$) δ 9.70 (s, 1H), 8.65 (d, $J = 4.8$ Hz, 1H), 8.57 (s, 1H), 7.92 (d, $J = 8.6$ Hz, 2H), 7.83 (dd, $J = 7.8, 1.9$ Hz, 1H), 7.56 (dd, $J = 7.8, 4.8$ Hz, 1H), 7.44 – 7.23 (m, 4H), 7.21 – 7.00 (m, 2H), 5.74 (s, 2H), 4.27 (q, $J = 7.1$ Hz, 2H), 1.27 (t, $J = 7.1$ Hz, 3H); ESI-MS m/z : $[M + H]^+$ 401.1.

5.2.4. N-Hydroxy-4-((3-hydroxy-2-oxo-4-phenylquinolin-1(2H)-yl)methyl)benzamide (**6a**).

To a solution of **11a** (55 mg, 0.14 mmol) in a 2:1 mixture of DCM (4 mL): MeOH (2 mL), a 50% solution of NH_2OH in water (660 μL , 10.00 mmol) and a 4 M solution of KOH in methanol (1.25 mL, 5.00 mmol) were added dropwise. The reaction was stirred at 25 °C for 3 h, then it was neutralized with 6 N HCl and concentrated *in vacuo*. The residue was purified by chromatography on silica gel (0.1% NH_4OH , 10% MeOH in DCM) affording **6a** (44 mg, 82%) as a white solid. 1H NMR (300 MHz, $DMSO-d_6$) δ 11.14 (s, 1H), 9.36 (s, 1H), 8.98 (s, 1H), 7.75 – 7.24 (m, 11H), 7.11 (d, $J = 4.1$ Hz, 2H), 5.69 (s, 2H); ^{13}C NMR (75 MHz, $DMSO-d_6$) δ 164.4, 158.9, 142.0, 140.2, 134.0, 133.9, 132.2, 130.4, 128.9, 128.2, 127.8, 127.3, 127.0, 125.7, 124.3, 123.1, 122.2, 115.6, 45.9; ESI-MS m/z : $[M - H]^-$ 385.0. FT-IR (neat) ν_{max} 3375, 3291, 3036, 1616, 1566, 1496, 1257, 1015 cm^{-1} ; mp 192.7-195.8 °C, decomposition; Anal. ($C_{23}H_{18}N_2O_4$) C, H, N.

5.2.5. N-Hydroxy-4-((3-hydroxy-2-oxo-4-(pyridin-3-yl)quinolin-1(2H)-yl)methyl)benzamide (**6d**).

Starting from **11b** (20 mg, 0.05 mmol) the title compound was obtained following the procedure described to get **6a**. The residue was purified by chromatography on silica gel (0.1% NH_4OH , 10% MeOH in DCM) affording **15** (16 mg, 84%). 1H NMR (300 MHz, $DMSO-d_6$) δ 11.15 (s, 1H), 9.74 (s, 1H), 8.99 (s, 1H), 8.65 (d, $J = 3.5$ Hz, 1H), 8.57 (s, 1H), 7.83 (d, $J = 7.7$ Hz, 1H), 7.69 (d, $J = 8.1$ Hz, 2H), 7.62 – 7.50 (m, 1H), 7.46

– 7.24 (m, 4H), 7.22 – 6.96 (m, 2H), 5.70 (s, 2H); ¹³C NMR (75 MHz, DMSO-*d*₆) δ 164.3, 158.7, 150.8, 149.4, 142.9, 140.1, 138.2, 133.9, 132.3, 130.0, 127.8, 127.5, 127.0, 125.3, 124.0, 123.4, 121.9, 121.0, 115.7, 46.0; ESI-MS *m/z*: [M - H]⁺ 386.0. Anal. (C₂₂H₁₇N₃O₄) C, H, N.

5.2.6. Ethyl 4-((3-methoxy-2-oxo-4-phenylquinolin-1(2H)-yl)methyl)benzoate (**12a**).

To a solution of **11a** (100 mg, 0.25 mmol) in dry THF (3 mL) cooled at 0 °C, a 60% dispersion of NaH in mineral oil (15 mg, 0.38 mmol) was added. The mixture was stirred at 0 °C for 30 min, then MeI (78 μL, 1.25 mmol) was added. The reaction was allowed to reach 25 °C and stirred for 12 h. After this time a saturated solution of NH₄Cl (5 mL) was added and the mixture was extracted with EtOAc (3 x 5 mL). The combined organic layers were dried over Na₂SO₄ and concentrated in vacuo. The residue was purified by chromatography on silica gel (25% EtOAc in Petroleum ether) affording **12a** (30 mg, 29%) as a colorless oil. ¹H NMR (300 MHz, CDCl₃) δ 8.11 – 7.90 (m, 2H), 7.58 – 7.44 (m, 3H), 7.44 – 7.14 (m, 7H), 7.15 – 6.99 (m, 1H), 5.69 (s, 2H), 4.34 (q, *J* = 7.1 Hz, 2H), 3.80 (s, 3H), 1.35 (t, *J* = 7.1 Hz, 3H); ESI-MS *m/z*: [M + H]⁺ 414.0.

5.2.7. Ethyl 4-((3-(benzyloxy)-2-oxo-4-phenylquinolin-1(2H)-yl)methyl)benzoate (**12b**).

To a solution of **11a** (50 mg, 0.125 mmol) and benzyl bromide (16 μL, 0.137 mmol) in anhydrous DMF (2 mL) was added K₂CO₃ (34 mg, 0.25 mmol) followed by KI (2 mg, 0.01 mmol). Reaction was refluxed for 8 h at 80 °C. Reaction mixture was then partitioned between aqueous saturated NH₄Cl and EtOAc, and the organic layer was washed with a saturated solution of NaHCO₃ (5 mL) and brine (5 mL), dried over Na₂SO₄ and concentrated *in vacuo*. The residue was purified by chromatography on silica gel (25% EtOAc in petroleum ether) affording **12b** (39 mg, 64%) as a pale-yellow oil. ¹H NMR (300 MHz, CDCl₃) δ 8.03 (d, *J* = 8.3 Hz, 2H), 7.56 – 7.40 (m, 3H), 7.40 – 7.13 (m, 10H), 7.13 – 6.94 (m, 3H), 5.73 (s, 2H), 5.15 (s, 2H), 4.37 (q, *J* = 7.1 Hz, 2H), 1.38 (t, *J* = 7.1 Hz, 3H); ESI-MS *m/z*: [M + H]⁺ 490.0.

5.2.8. *N*-Hydroxy-4-((3-methoxy-2-oxo-4-phenylquinolin-1(2H)-yl)methyl)benzamide (**6b**).

Starting from **12a** (30 mg, 0.07 mmol) the title compound was obtained following the procedure described to get **6a**. The residue was purified by chromatography on silica gel (0.1% NH₄OH, 10% MeOH in DCM) affording **6b** (28 mg, 97%) as a white solid. ¹H NMR (300 MHz, CDCl₃) δ 11.15 (s, 1H), 9.00 (s, 1H), 7.69 (d, *J* = 7.9 Hz, 2H), 7.61 – 7.21 (m, 9H), 7.21 – 6.95 (m, 2H), 5.65 (s, 2H), 3.71 (s, 3H); ¹³C NMR (75 MHz, DMSO-*d*₆) δ 164.4, 158.8, 144.8, 140.3, 137.7, 136.4, 133.7, 132.2, 129.7, 129.5, 128.9, 128.6, 127.7, 127.2, 127.0, 123.0, 121.1, 115.6, 60.1, 45.6; ESI-MS *m/z*: [M + H]⁺ 401.0; HRMS-ESI *m/z*: calcd for C₂₄H₂₁N₂O₄⁺ [M+H]⁺: 401.1496; found: 401.1488; FT-IR (neat) *v*_{max} 3217, 2920, 2854, 1719, 1630, 1595, 1456, 1259, 1091, 1016 cm⁻¹; mp 161.0-164.0 °C, decomposition; Anal. (C₂₄H₂₀N₂O₄) C, H, N.

5.2.9. 4-((3-(Benzyloxy)-2-oxo-4-phenylquinolin-1(2H)-yl)methyl)-*N*-hydroxybenzamide (**6c**).

Starting from **12b** (27 mg, 489.56 μmol) the title compound was obtained following the procedure described to get **6a**. The residue was purified by chromatography on silica gel (0.1% NH_4OH , 10% MeOH in DCM) affording **6c** (22 mg, 85%) as a light brown solid. ^1H NMR (300 MHz, $\text{DMSO-}d_6$) δ 11.16 (s, 1H), 9.01 (s, 1H), 7.70 (d, $J = 7.9$ Hz, 2H), 7.59 – 6.81 (m, 16H), 5.70 (s, 2H), 5.07 (s, 2H). ^{13}C NMR (75 MHz, $\text{DMSO-}d_6$) δ 164.4, 159.1, 143.4, 140.3, 138.3, 137.3, 136.5, 133.6, 132.2, 129.8, 129.6, 128.8, 128.6 (2C), 128.5, 128.3, 127.7, 127.2, 127.1, 123.0, 121.2, 115.6, 73.5, 45.6; ESI-MS m/z : $[\text{M} + \text{H}]^+$ 476.9; Anal. ($\text{C}_{30}\text{H}_{24}\text{N}_2\text{O}_4$) C, H, N.

5.2.10. 3-Hydroxy-4-phenylquinolin-2(1H)-one (**13a**).

A solution of benzaldehyde (100 mg, 0.94 mmol) and PTSH (175 mg, 0.94 mmol) in EtOH (5 mL) was stirred at 25 °C for 2 h. After this, isatin (138 mg, 0.94 mmol) and K_2CO_3 (260 mg, 1.88 mmol) were added and the reaction was stirred at 80 °C for 12 h. The solvent was evaporated, and the crude was purified by chromatography on silica gel (20% EtOAc in petroleum ether) giving **13a** (95 mg, 42%) as a brown solid. ^1H NMR (300 MHz, $\text{DMSO-}d_6$) δ 12.19 (s, 1H), 9.16 (s, 1H), 7.57 – 7.35 (m, 3H), 7.34 – 7.18 (m, 4H), 7.09 – 6.94 (m, 2H); ESI-MS m/z : $[\text{M} + \text{Na}]^+$ 260.1.

5.2.11. 3-Hydroxy-4-(pyridin-3-yl)quinolin-2(1H)-one (**13b**).

Starting from 3-pyridinecarboxaldehyde (181 mg, 1.69 mmol) and isatin (500 mg, 1.69), the title compound was obtained following the procedure previously described for compound **13a**. The crude was purified by chromatography on silica gel (5% MeOH in DCM) giving **13b** (180 mg, 45%) as a red solid. ^1H NMR (300 MHz, $\text{DMSO-}d_6$) δ 12.27 (s, 1H), 9.49 (s, 1H), 8.62 (dd, $J = 4.8, 1.7$ Hz, 1H), 8.53 (dd, $J = 2.2, 0.8$ Hz, 1H), 7.85 – 7.71 (m, 1H), 7.62 – 7.46 (m, 1H), 7.42 – 7.25 (m, 2H), 7.17 – 7.05 (m, 1H), 7.05 – 6.94 (m, 1H); ESI-MS m/z : $[\text{M} + \text{H}]^+$ 239.0.

5.2.12. Methyl 4-(((2-oxo-4-phenyl-1,2-dihydroquinolin-3-yl)oxy)methyl)benzoate (**14a**).

To a solution of **13a** (100 mg, 0.42 mmol) in dry DMF (4 mL) methyl 4-(bromomethyl)benzoate (145 mg, 0.63 mmol), KI (7 mg, 0.04 mmol) and K_2CO_3 (116 mg, 0.84 mmol) were added. The reaction mixture was stirred at 80 °C for 12 h. Thereafter the mixture was cooled down to 25 °C and a saturated solution of NH_4Cl (10 mL) was added. The mixture was extracted with EtOAc (10 mL) and the organic layer was washed with a saturated solution of NaHCO_3 (5 mL) and brine (5 mL). Then it was dried over Na_2SO_4 and concentrated *in vacuo*. The crude was purified by chromatography on silica gel (33% EtOAc in petroleum ether) giving **14a** (61 mg, 38%) as a pale brown solid. ^1H NMR (300 MHz, CDCl_3) δ 12.95 (s, 1H), 7.88 (d, $J = 8.0$ Hz, 2H), 7.57 – 7.35 (m, 6H), 7.33 – 7.01 (m, 5H), 5.24 (s, 2H), 3.89 (s, 3H); ^{13}C NMR (75 MHz, CDCl_3) δ 167.0, 161.0, 143.7, 142.2, 140.3, 140.3, 135.5, 133.2, 129.7, 129.4, 129.1, 128.7, 128.3, 127.9, 126.7, 122.8, 120.8, 115.9, 73.4, 57.0; ESI-MS m/z : $[\text{M} + \text{H}]^+$ 386.1; m.p.: 195.0-197.9 °C.

5.2.13. Methyl 4-(((2-oxo-4-(pyridin-3-yl)-1,2-dihydroquinolin-3-yl)oxy)methyl)benzoate (**14b**).

Starting from **13b** (180 mg, 0.76 mmol) the title compound was obtained following the procedure previously described for compound **14a**. The crude was purified by chromatography on silica gel (50% EtOAc in petroleum ether) giving **14b** (60 mg, 20%) as a dark yellow oil. ¹H NMR (300 MHz, CDCl₃) δ 12.82 (s, 1H), 8.71 (dd, *J* = 5.0, 1.7 Hz, 1H), 8.61 – 8.47 (m, 1H), 7.98 – 7.81 (m, 2H), 7.64 – 7.32 (m, 4H), 7.24 – 7.01 (m, 4H), 5.45 – 5.15 (m, 2H), 3.89 (s, 3H); ESI-MS *m/z*: [M + H]⁺ 387.0.

5.2.14. *N*-Hydroxy-4-(((2-oxo-4-phenyl-1,2-dihydroquinolin-3-yl)oxy)methyl)benzamide (**7a**).

To a solution of **14a** (19 mg, 0.049 mmol) in a 2:1 mixture of DCM (2 mL): MeOH (1 mL), a 50% solution of NH₂OH in water (329 μL, 4.90 mmol) and a 4 M solution of KOH in methanol (616 μL, 2.45 mmol) were added dropwise. The reaction was stirred at 25 °C for 3 h, then it was neutralized with 6 N HCl and concentrated *in vacuo*. The crude was purified by chromatography on silica gel (0.1% NH₄OH, 10% MeOH in DCM) giving **7a** (11 mg, 55%) as a white solid. ¹H NMR (300 MHz, DMSO-*d*₆) δ 12.13 (s, 1H), 11.11 (s, 1H), 8.96 (s, 1H), 7.55 (d, *J* = 8.3 Hz, 2H), 7.50 – 7.30 (m, 5H), 7.28 – 7.14 (m, 2H), 7.12 – 7.00 (m, 3H), 7.00 – 6.88 (m, 1H), 5.07 (s, 2H). ¹³C NMR (75 MHz, DMSO-*d*₆) δ 164.3, 159.1, 144.2, 140.6, 138.4, 136.3, 133.7, 132.5, 129.8, 129.1, 128.7, 128.5, 128.0, 127.1, 126.2, 122.5, 120.3, 115.6, 72.8; ESI-MS *m/z*: [M + H]⁺ 387.1; FT-IR (neat) ν_{\max} 3204, 3048, 2858, 1653, 1549, 1279, 1202, 1160, 989 cm⁻¹; mp 204.8-205.4 °C, decomposition; Anal. (C₂₃H₁₈N₂O₄) C, H, N.

5.2.15. *N*-Hydroxy-4-(((1-methyl-2-oxo-4-phenyl-1,2-dihydroquinolin-3-yl)oxy)methyl)benzamide (**7b**).

Step 1: To a solution of **14a** (16 mg, 0.04 mmol) in dry THF (1 mL) cooled at 0 °C, a 60% dispersion of NaH in mineral oil (15 mg, 0.06 mmol) was added. The mixture was stirred at 0 °C for 30 min then MeI (8 μL, 0.12 mmol) was added. The reaction was allowed to reach 25 °C and stirred at this temperature for 12 h. Then a saturated solution of NH₄Cl (5 mL) was added and the mixture was extracted with EtOAc (3 x 5 mL). The combined organic layers were washed with brine, dried over Na₂SO₄ and concentrated *in vacuo*. The crude was purified by chromatography on silica gel (50% EtOAc in petroleum ether) affording *methyl 4-(((1-methyl-2-oxo-4-phenyl-1,2-dihydroquinolin-3-yl)oxy)methyl)benzoate* (16 mg, quantitative yield) as a white solid. ¹H NMR (300 MHz, CDCl₃) δ 7.85 (d, *J* = 6.8 Hz, 2H), 7.57 – 7.32 (m, 5H), 7.32 – 7.17 (m, 3H), 7.17 – 6.95 (m, 3H), 5.13 (s, 2H), 3.95 – 3.79 (m, 6H); ESI-MS *m/z*: [M + H]⁺ 400.1.

Step 2: From *methyl 4-(((1-methyl-2-oxo-4-phenyl-1,2-dihydroquinolin-3-yl)oxy)methyl)benzoate* (22 mg, 0.05 mmol) the title compound was obtained following the procedure previously described for compound **7a**. The crude was purified by chromatography on silica gel (0.1% NH₄OH, 10 % MeOH in DCM) giving **7b** (14 mg, 64%). ¹H NMR (300 MHz, DMSO-*d*₆) δ 11.14 (s, 1H), 8.97 (s, 1H), 7.58-7.47 (m, 7H), 7.35 – 7.13 (m, 3H), 7.06 (dd, *J* = 8.2, 2.4 Hz, 3H), 5.04 (s, 2H), 3.76 (s, 3H) ¹³C NMR (75 MHz, MeOD) δ 166.4, 159.7, 143.0, 140.7, 139.2, 137.0, 133.2, 131.5, 129.4, 129.3, 128.1, 128.0, 127.9, 126.9, 126.5, 122.5, 121.0, 114.5, 73.0, 29.4; ESI-MS *m/z*: [M + H]⁺ 401.0; Anal. (C₂₄H₂₀N₂O₄) C, H, N.

5.2.16. *N*-Hydroxy-4-(((2-oxo-4-phenyl-1-(prop-2-yn-1-yl)-1,2-dihydroquinolin-3-yl)oxy)methyl)benzamide (**7c**).

Step 1: To a solution of **14a** (50 mg, 0.13 mmol) in dry DMF cooled at 0 °C, NaH (60% in mineral oil, 7 mg, 0.194) was added. The reaction was allowed to stir for 30 mins at the same temperature, then propargyl bromide (19 µL, 0.129 mmol) was added. The reaction was allowed to reach 25 °C and stirred for 12 h. After this time, a saturated solution of NH₄Cl (5 mL) was added and the mixture was extracted with EtOAc (3 x 5 mL). The combined organic layers were washed with brine, dried over Na₂SO₄ and concentrated *in vacuo*. The crude was purified by chromatography on silica gel (25% EtOAc in petroleum ether) affording *methyl 4-(((2-oxo-4-phenyl-1-(prop-2-yn-1-yl)-1,2-dihydroquinolin-3-yl)oxy)methyl)benzoate* (31 mg, 56% yield) as a brown solid. ¹H NMR (300 MHz, CDCl₃) δ 7.84 (d, *J* = 7.5 Hz, 2H), 7.63 – 7.37 (m, 5H), 7.34 – 7.19 (m, 3H), 7.19 – 7.11 (m, 1H), 7.08 (d, *J* = 8.0 Hz, 2H), 5.23 (d, *J* = 2.5 Hz, 2H), 5.13 (s, 2H), 3.88 (s, 3H), 2.32 (s, 1H); ESI-MS *m/z*: [M + H]⁺ 424.1

Step 2: From *methyl 4-(((2-oxo-4-phenyl-1-(prop-2-yn-1-yl)-1,2-dihydroquinolin-3-yl)oxy)methyl)benzoate* (30 mg, 0.07 mmol) the title compound was obtained following the procedure previously described for compound **7a**. The crude was purified by chromatography on silica gel (0.1% NH₄OH, 10% MeOH in DCM) giving **7c** (17 mg, 57%) as a brown solid. ¹H NMR (300 MHz, MeOD) δ 11.13 (s, 1H), 8.97 (s, 1H), 7.73 – 7.53 (m, 4H), 7.53 – 7.39 (m, 3H), 7.35 – 7.13 (m, 3H), 7.15 – 6.96 (m, 3H), 5.23 (s, 2H), 5.05 (s, 2H), 3.31 (s, 1H); ¹³C NMR (75 MHz, DMSO-*d*₆) δ 164.3, 158.0, 143.4, 140.5, 138.4, 135.9, 133.4, 132.5, 129.7, 128.8 (2C), 128.7, 128.0, 127.3, 127.1, 123.3, 121.0, 115.6, 79.3, 75.3, 73.1, 32.2; ESI-MS *m/z*: [M + H]⁺ 425.0. mp decomposition; Anal. (C₂₆H₂₀N₂O₄) C, H, N.

5.2.17. *N*-Hydroxy-4-(((1-methyl-2-oxo-4-(pyridin-3-yl)-1,2-dihydroquinolin-3-yl)oxy)methyl)benzamide (**7h**).

Starting from **14b** (15 mg, 0.076 mmol) the title compound was obtained following the procedure previously described for compound **7b**, **Step 1**. The crude was purified by chromatography on silica gel (33% EtOAc in petroleum ether) giving *methyl 4-(((1-methyl-2-oxo-4-(pyridin-3-yl)-1,2-dihydroquinolin-3-yl)oxy)methyl)benzoate* (10 mg, 66%) as a yellow solid. ¹H NMR (300 MHz, CDCl₃) δ 8.68 (dd, *J* = 4.9, 1.7 Hz, 1H), 8.48 (dd, *J* = 2.2, 0.9 Hz, 1H), 7.86 (d, *J* = 8.3 Hz, 2H), 7.62 – 7.32 (m, 4H), 7.23 – 7.03 (m, 4H), 5.31 – 5.06 (m, 2H), 3.89 (s, 3H), 3.86 (s, 3H); ESI-MS *m/z*: [M + H]⁺ 401.1. Starting from *methyl 4-(((1-methyl-2-oxo-4-(pyridin-3-yl)-1,2-dihydroquinolin-3-yl)oxy)methyl)benzoate* (15 mg, 0.076 mmol) the title compound was obtained following the procedure previously described for compound **7a**. The crude was purified by chromatography on silica gel (0.1% NH₄OH, 10% MeOH in DCM) giving **7h** (5 mg, 50%) as a white solid. ¹H NMR (300 MHz, MeOD) δ 8.61 (d, *J* = 4.8 Hz, 1H), 8.32 (s, 1H), 7.74 – 7.45 (m, 6H), 7.30 – 7.01 (m, 4H), 5.12 (d, *J* = 4.9 Hz, 2H), 3.88 (s, 3H); ¹³C NMR (75 MHz, MeOD) δ 166.3, 159.2, 149.3, 148.3, 143.4, 140.2, 138.4, 137.1, 134.8, 131.8, 130.1, 129.5, 128.2, 126.6, 126.2, 123.6, 122.8, 120.2, 114.7, 72.8, 29.2; ESI-MS *m/z*: [M + Na]⁺ 424.0; Anal. (C₂₃H₁₉N₃O₄) C, H, N.

5.2.18. 1-Methylindoline-2,3-dione (**15**) [26].

To a solution of isatin (1.0 g, 6.80 mmol) in dry DMF (4 mL), cooled at 0 °C, a 60% dispersion of NaH, in mineral oil (275 mg, 6.80 mmol) was added and stirred for 5 min at 0 °C. Then, methyl iodide (635 μ L, 10.20 mmol) was added and the reaction was allowed to reach 25 °C and stirred for 12 h. Thereafter, a saturated solution of NH₄Cl (5 mL) was added and the mixture was extracted with EtOAc (3 x 5 mL). The combined organic layers were washed with brine, dried over Na₂SO₄ and concentrated *in vacuo*. The crude was purified by chromatography on silica gel (25% EtOAc in petroleum ether) affording **15** (1.15 g, quantitative yield) as a red solid. ¹H NMR (300 MHz, CDCl₃) δ 7.69 – 7.52 (m, 2H), 7.12 (td, *J* = 7.6, 0.9 Hz, 1H), 6.89 (dd, *J* = 8.6, 0.9 Hz, 1H), 3.25 (s, 3H). The experimental data are consistent with those reported in literature [26].

5.2.19. 4-Cyclohexyl-3-hydroxy-1-methylquinolin-2(1H)-one (**16**).

Starting from **15** (575 mg, 3.57 mmol) and cyclohexanecarboxaldehyde (431 μ L, 3.57 mmol) the title compound was obtained following the procedure described to get **13a**. The residue was purified by chromatography on silica gel (20% EtOAc in petroleum ether) affording **16** (270 mg, 30%) as a white solid. ¹H NMR (300 MHz, CDCl₃) δ 7.92 (d, *J* = 8.2 Hz, 1H), 7.54 – 7.20 (m, 4H), 3.82 (s, 3H), 3.16 (m, 1H), 2.35 – 2.12 (m, 2H), 1.99 – 1.83 (m, 2H), 1.75 (m, 4H), 1.42 (m, 2H); ESI-MS *m/z*: [M + H]⁺ 258.1.

5.2.20. 4-(((4-Cyclohexyl-1-methyl-2-oxo-1,2-dihydroquinolin-3-yl)oxy)methyl)-N-hydroxybenzamide (**8**).

Starting from **16** (270 mg, 1.05 mmol) methyl 4-(((4-cyclohexyl-1-methyl-2-oxo-1,2-dihydroquinolin-3-yl)oxy)methyl)benzoate was obtained following the procedure described to get **14a**. The residue was purified by chromatography on silica gel (33% EtOAc in petroleum ether) affording methyl 4-(((4-cyclohexyl-1-methyl-2-oxo-1,2-dihydroquinolin-3-yl)oxy)methyl)benzoate (317 mg, 74%) as a yellow oil. ¹H NMR (300 MHz, CDCl₃) δ 8.15 – 8.01 (m, 2H), 7.96 (s, 1H), 7.61 (d, *J* = 7.9 Hz, 2H), 7.54 – 7.40 (m, 1H), 7.33 (dd, *J* = 8.6, 1.2 Hz, 1H), 7.22 (t, *J* = 7.6 Hz, 1H), 5.26 (s, 2H), 3.89 (s, 3H), 3.73 (s, 3H), 3.20 (d, *J* = 13.8 Hz, 1H), 2.16 – 1.93 (m, 2H), 1.89 – 1.52 (m, 5H), 1.48 – 1.07 (m, 3H); ¹³C NMR (75 MHz, CDCl₃) δ 167.0, 159.1, 142.9, 140.9, 137.3, 129.7, 129.5, 128.6, 127.9, 126.4, 124.6, 122.1, 120.4, 114.6, 72.7, 52.1, 38.4, 30.6, 29.9, 27.2, 26.1; ESI-MS *m/z*: [M + H]⁺ 406.1; mp 79.1-82.2 °C.

This intermediate (100 mg, 0.25 mmol) was converted into compound **8** following the procedure previously described for the synthesis of compound **7a**. The residue was purified by chromatography on silica gel (0.1% NH₄OH, 10% MeOH in DCM) affording **8** (100 mg, 98%) as a brown solid. ¹H NMR (300 MHz, DMSO-*d*₆) δ 11.21 (s, 1H), 9.01 (s, 1H), 8.04 (d, *J* = 8.2 Hz, 1H), 7.77 (d, *J* = 7.9 Hz, 2H), 7.55 (m, 4H), 7.40 – 7.16 (m, 1H), 5.16 (s, 2H), 3.68 (s, 3H), 3.25 (m, 1H), 2.15 – 1.85 (m, 2H), 1.85 – 0.87 (m, 8H); ¹³C NMR (75 MHz, DMSO-*d*₆) δ 164.4, 158.3, 141.0, 140.5, 137.4, 132.6, 129.3, 128.3, 128.1, 127.4, 125.8, 122.7, 119.8, 115.6, 72.4, 37.7, 30.4, 30.1, 27.0, 26.0; ESI-MS *m/z*: [M + H]⁺ 407.1. HRMS-ESI *m/z*: calcd for C₂₄H₂₇N₂O₄⁺ [M+H]⁺: 407.1965; found: 407.1960; FT-IR (neat) ν_{\max} 3314, 3248, 2919, 2849, 1661, 1618, 1585, 1452, 1206, 1106, 1028 cm⁻¹; mp 197.2-200.0 °C, decomposition Anal. (C₂₄H₂₆N₂O₄) C, H, N.

5.2.21. 4-(Hydroxymethyl)pyridine (**18**).

To a solution of **17** (2.0 g, 18.67 mmol) in methanol (20 mL), cooled at 0 °C, NaBH₄ (706 mg, 18.67 mmol) was added. The reaction was stirred for 2 h and allowed to reach to 25 °C. After the complete consumption of starting material, water (20 mL) was added, solvent was evaporated, and the aqueous residue was extracted with EtOAc (3 x 15 mL). The combined organic layers were filtered over Na₂SO₄ and concentrated *in vacuo* to get **18** (1.60 g, 80%) as a colorless oil. ¹H NMR (300 MHz, CDCl₃) δ 8.52 (dd, *J* = 4.6, 1.5 Hz, 2H), 7.40 – 7.19 (m, 2H), 4.74 (s, 2H), 3.20 (s, 1H).

5.2.22. 4-(Bromomethyl)pyridinium bromide (**19**) [27].

Compound **18** (1.810 g, 16.58 mmol) was dissolved in 48% HBr (16 mL) and stirred at reflux for 4 h. The water was removed *in vacuo* to give a thick gum which was treated with ethanol at 5 °C and then filtered. The white crystals were collected and washed with cold ethanol to get 4-(hydroxymethyl)pyridinium bromide (1.9 g). To a suspension of this salt in chloroform (25 mL) PBr₃ (457 μL, 4.85 mmol) was added, and the mixture was stirred at reflux for 4.5 h. After cooling down to 25 °C, the white precipitate was collected and washed with cold chloroform to give **19** (2.3 g, 93%) as a white solid. ¹H NMR (300 MHz, CDCl₃) δ 8.80 (d, *J* = 6.4 Hz, 2H), 8.00 (d, *J* = 6.4 Hz, 2H), 4.61 (s, 2H). The spectroscopic data are consistent with those reported in literature [27].

5.2.23. 4-(Bromomethyl)benzaldehyde (**21**) [37].

To a solution of 4-(bromomethyl)benzotrile (2.0 g, 10.20 mmol) in dry DCM (40 mL), cooled at -78 °C a 1 M solution of DIBAL-H in DCM (11.2 mL, 11.22 mmol) was slowly added. The reaction was allowed to reach 0 °C in 1 h, then it was slowly quenched with 1 N HCl (20 mL). The mixture was extracted with DCM (3 x 20 mL) and the combined organic layers were washed with NaOH (2 x 20 mL), then dried over Na₂SO₄ and concentrated *in vacuo* affording **21** (2.03 g, quantitative yield) as a white solid that was used in the next step without further purification. ¹H NMR (300 MHz, CDCl₃) δ 10.02 (s, 1H), 7.87 (d, *J* = 8.2 Hz, 2H), 7.56 (d, *J* = 8.1 Hz, 2H), 4.52 (s, 2H). The spectroscopic data are consistent with those reported in literature [37].

5.2.24. 2-(4-(Bromomethyl)phenyl)-1,3-dioxolane (**22**) [37].

To a solution of **21** (2.03 g, 10.20 mmol) in toluene, ethylene glycol (1.1 mL, 20.40 mmol) and PTSA (176 mg, 1.02 mmol) were added. The reaction was stirred at 110 °C for 12 h, then a saturated solution of NaHCO₃ (20 mL) was added. The resulting mixture was extracted with EtOAc (3 x 20 mL) and the combined organic layers were dried over Na₂SO₄ and concentrated *in vacuo*. The crude was purified by chromatography on silica gel (20% EtOAc in petroleum ether) affording **22** (1.7 g, 69%) as a colorless oil. ¹H NMR (300 MHz, Acetone-*d*₆) δ 7.56 – 7.39 (m, 4H), 5.75 (s, 1H), 4.66 (s, 2H), 4.20 – 3.88 (m, 4H). The spectroscopic data are consistent with those reported in literature [37].

5.2.25. 1-Benzylindoline-2,3-dione (**23a**) [26].

To a solution of isatin (300 mg, 2.03 mmol) in dry DMF (2 mL), cooled at 0 °C, a 60% dispersion of NaH in mineral oil (95 mg, 2.38 mmol) was added and stirred for 5 min at 0 °C. Then, benzyl bromide (266 μ L, 2.34 mmol) was added and the reaction was allowed to reach 25 °C and stirred for 12 h. Thereafter, a saturated solution of NH₄Cl (5 mL) was added and the mixture was extracted with EtOAc (3 x 5 mL). The combined organic layers were washed with brine, dried over Na₂SO₄ and concentrated *in vacuo*. The crude was purified by chromatography on silica gel (25% EtOAc in petroleum ether) affording **23a** (358 mg, 74% yield) as a yellow solid. ¹H NMR (300 MHz, CDCl₃) δ 7.67 – 7.55 (m, 1H), 7.47 (td, *J* = 7.8, 1.3 Hz, 1H), 7.41 – 7.24 (m, 5H), 7.08 (t, *J* = 7.6 Hz, 1H), 6.77 (d, *J* = 8.0 Hz, 1H), 4.93 (s, 2H); ¹³C NMR (75 MHz, CDCl₃) δ 183.2, 158.3, 150.7, 138.3, 134.5, 129.1, 128.2, 127.4, 125.4, 123.9, 117.7, 111.0, 44.0; ESI-MS *m/z*: [M + H]⁺ 238.0; mp 129.8-130.8 °C. The spectroscopic data are consistent with those reported in literature [26].

5.2.26. 1-(Pyridin-4-ylmethyl)indoline-2,3-dione (**23b**).

To a solution of **19** (860 mg, 3.39 mmol) in diethyl ether (10 mL) a 10% solution of NaHCO₃ (10 mL) was added. The organic layer was extracted, dried over Na₂SO₄, concentrated *in vacuo* and the residue was dissolved in dry DMF (2 mL). In another flask, a solution of isatin (500 mg, 3.39 mmol) in dry DMF (2 mL), cooled at 0 °C, was treated with a 60% dispersion of NaH in mineral oil (163 mg, 4.07 mmol) and stirred at the same temperature for 30 min. After this time, the previously prepared solution of **19** (free base in dry DMF) was added and the reaction was allowed to reach 25 °C and stirred for 12 h. Then a saturated solution of NH₄Cl (5 mL) was added and the mixture was extracted with EtOAc (3 x 5 mL). The combined organic layers were washed with brine (10 mL), dried over Na₂SO₄ and concentrated *in vacuo*. The crude was purified by chromatography on silica gel (EtOAc) affording **23b** (311 mg, 38% yield) as an orange solid. ¹H NMR (300 MHz, CDCl₃) δ 8.50 (d, *J* = 6.1 Hz, 2H), 7.56 (dd, *J* = 7.5, 1.4 Hz, 1H), 7.51 – 7.34 (m, 1H), 7.20 (d, *J* = 6.2 Hz, 2H), 7.06 (t, *J* = 7.6 Hz, 1H), 6.66 (d, *J* = 7.9 Hz, 1H), 4.88 (s, 2H); ESI-MS *m/z*: [M + H]⁺ 239.0.

5.2.27. 1-Benzyl-3-hydroxy-4-phenylquinolin-2(1H)-one (**24a**).

Starting from benzaldehyde (67 mg, 0.62 mmol) and **23a** (150 mg, 0.62 mmol), the title compound was obtained following the procedure previously described for compound **13a**. The crude was purified by chromatography on silica gel (25% in EtOAc in petroleum ether) giving **24a** (78 mg, 38%) as a brown solid. ¹H NMR (400 MHz, DMSO-*d*₆) δ 9.33 (s, 1H), 7.90 – 6.90 (m, 14H), 5.65 (s, 2H); ESI-MS *m/z*: 328.0.

5.2.28. 3-Hydroxy-4-phenyl-1-(pyridin-4-ylmethyl)quinolin-2(1H)-one (**24b**).

Starting from benzaldehyde (53 mg, 0.62 mmol) and **23b** (120 mg, 0.50 mmol), the title compound was obtained following the procedure previously described for compound **13a**. The crude was purified by chromatography on silica gel (EtOAc) giving **24b** (64 mg, 39%) as a brown solid. ¹H NMR (300 MHz,

CDCl₃) δ 8.58 (d, J = 6.2 Hz, 2H), 7.62 – 7.38 (m, 6H), 7.37 – 7.28 (m, 1H), 7.22 – 7.13 (m, 4H), 7.10 (s, 1H), 5.69 (s, 2H); ESI-MS m/z : [M + H]⁺ 329.

5.2.29. *1-Benzyl-3-hydroxy-4-(pyridin-3-yl)quinolin-2(1H)-one (24c)*.

Starting from 3-pyridinecarboxaldehyde (67 mg, 0.62 mmol) and **23a** (150 mg, 0.62 mmol), the title compound was obtained following the procedure previously described for compound **13a**. The crude was purified by chromatography on silica gel (2% MeOH in DCM) giving **24c** (55 mg, 24%) as a red solid. ¹H NMR (300 MHz, CDCl₃) δ 8.73 (s, 2H), 7.88 – 7.77 (m, 1H), 7.53 – 7.43 (m, 1H), 7.41 – 7.22 (m, 9H), 7.21 – 7.11 (m, 1H), 5.70 (s, 2H); ESI-MS m/z : [M + H]⁺ 329.1.

5.2.30. *3-Hydroxy-4-(pyridin-3-yl)-1-(pyridin-4-ylmethyl)quinolin-2(1H)-one (24d)*.

Starting from 3-pyridinecarboxaldehyde (54 mg, 0.503 mmol) and **23b** (120 mg, 0.503 mmol), the title compound was obtained following the procedure previously described for compound **13a**. The crude was purified by chromatography on silica gel (2% MeOH in DCM) giving **24d** (73 mg, 44%) as a red solid. ¹H NMR (300 MHz, CDCl₃) δ 8.85 – 8.40 (m, 4H), 7.80 (d, J = 7.1 Hz, 1H), 7.55 – 7.38 (m, 1H), 7.37 – 7.25 (m, 2H), 7.24 – 7.00 (m, 4H), 5.66 (s, 2H); ESI-MS m/z : [M + H]⁺ 330.1.

5.2.31. *4-(((1-Benzyl-2-oxo-4-phenyl-1,2-dihydroquinolin-3-yl)oxy)methyl)-N-hydroxybenzamide (7d)*.

Starting from **24a** (78 mg, 0.24 mmol) *methyl 4-(((1-benzyl-2-oxo-4-phenyl-1,2-dihydroquinolin-3-yl)oxy)methyl)benzoate* was obtained following the procedure previously described for compound **14a**. The crude was purified by chromatography on silica gel (50% EtOAc in petroleum ether) giving the intermediate (70 mg, 62%) as a dark yellow oil. ¹H NMR (300 MHz, CDCl₃) δ 7.92 – 7.80 (m, 2H), 7.55 – 7.40 (m, 3H), 7.40 – 7.19 (m, 10H), 7.16 – 6.99 (m, 3H), 5.68 (s, 2H), 5.22 (s, 2H), 3.90 (s, J = 8.5 Hz, 3H); ESI-MS m/z : [M + H]⁺ 476.0. Starting from this intermediate (20 mg, 0.04 mmol) the title compound was obtained following the procedure previously described for compound **7a**. The crude was purified by chromatography on silica gel (0.1% NH₄OH, 10% MeOH in DCM) giving **7d** (9 mg, 45%). ¹H NMR (300 MHz, DMSO-*d*₆) δ 11.14 (s, 1H), 8.97 (s, 1H), 7.63 – 7.19 (m, 14H), 7.19 – 7.00 (m, 4H), 5.64 (s, 2H), 5.10 (s, 2H); ¹³C NMR (75 MHz, DMSO-*d*₆) δ 164.3, 159.0, 143.4, 140.5, 138.2, 137.1, 136.6, 133.6, 132.5, 129.8, 129.6, 129.1, 128.8, 128.6 (2C), 128.1, 127.6, 127.2, 127.1, 123.0, 121.1, 115.7, 73.0, 45.8; ESI-MS m/z : [M + H]⁺ 477.0. FT-IR (neat) ν_{\max} 3259, 2923, 2854, 1719, 1634, 1597, 1453, 1013 cm⁻¹; mp decomposing; Anal. (C₃₀H₂₄N₂O₄) C, H, N.

5.2.32.

N-Hydroxy-4-(((2-oxo-4-phenyl-1-(pyridin-4-ylmethyl)-1,2-dihydroquinolin-3-yl)oxy)methyl)benzamide (7e).

Starting from **24b** (71 mg, 0.21 mmol) *methyl 4-(((2-oxo-4-phenyl-1-(pyridin-4-ylmethyl)-1,2-dihydroquinolin-3-yl)oxy)methyl)benzoate* was obtained following the procedure previously described for compound **14a**. The crude was purified by chromatography on silica gel (50% EtOAc in petroleum ether)

giving the intermediate (31 mg, 30%). ¹H NMR (300 MHz, CDCl₃) δ 8.56 (d, *J* = 5.2 Hz, 2H), 7.85 (d, *J* = 8.2 Hz, 2H), 7.52 – 7.41 (m, 3H), 7.31 (m, 4H), 7.19 – 7.00 (m, 6H), 5.65 (s, 2H), 5.17 (s, 2H), 3.89 (s, 3H); ¹³C NMR (75 MHz, CDCl₃) δ 159.8, 159.1, 150.0, 149.1, 143.7, 141.6, 137.9, 136.7, 135.9, 129.6, 129.3, 129.0, 128.9, 128.3, 127.5, 126.9, 126.6, 123.3, 122.8, 120.6, 115.2, 73.1, 52.1, 46.5; ESI-MS *m/z*: [M + H]⁺ 477.0; mp 147.5-150.1 °C. Starting from this intermediate (10 mg, 0.02 mmol) the title compound was obtained following the procedure previously described for compound **7a**. The crude was purified by chromatography on silica gel (0.1% NH₄OH, 10% MeOH in DCM) giving **7e** (8 mg, 90%). ¹H NMR (300 MHz, MeOD) δ 8.48 (d, *J* = 5.2 Hz, 2H), 7.63 – 7.23 (m, 12H), 7.21 – 7.01 (m, 3H), 5.77 (s, 2H), 5.07 (s, 2H); ¹³C NMR (75 MHz, MeOD) δ 168.6, 159.8, 148.9, 147.4, 142.9, 140.6, 139.9, 136.2, 133.1, 131.6, 129.4, 129.3, 129.1, 128.1, 128.0, 127.7, 127.3, 126.5, 122.8, 121.3, 114.7, 73.0, 45.0. ESI-MS *m/z*: [M + H]⁺ 478.0; HRMS-ESI *m/z*: calcd for C₂₉H₂₄N₃O₄⁺ [M+H]⁺: 478,1761; found: 478.1749. FT-IR (neat) *v*_{max} 3479, 3197, 2960, 2855, 1632, 1599, 1377, 1260, 1088, 1009 cm⁻¹; mp decomposition; Anal. (C₂₉H₂₃N₃O₄) C, H, N.

5.2.33. 4-(((1-Benzyl-2-oxo-4-(pyridin-3-yl)-1,2-dihydroquinolin-3-yl)oxy)methyl)-*N*-hydroxybenzamide (**7i**). Starting from **24c** (56 mg, 0.17 mmol) methyl 4-(((1-benzyl-2-oxo-4-(pyridin-3-yl)-1,2-dihydroquinolin-3-yl)oxy)methyl)benzoate was obtained following the procedure previously described for compound **14a**. The crude was purified by chromatography on silica gel (2% MeOH in DCM) giving the intermediate (53 mg, 65%). ¹H NMR (300 MHz, CDCl₃) δ 8.69 (s, 1H), 8.51 (s, 1H), 7.86 (d, *J* = 8.2 Hz, 2H), 7.53 (t, *J* = 10.4 Hz, 1H), 7.46 – 7.20 (m, 8H), 7.20 – 7.01 (m, 4H), 5.67 (s, 2H), 5.37 – 5.12 (m, 2H), 3.89 (s, 3H); ESI-MS *m/z*: [M + H]⁺ 477.0. Starting from this intermediate (53 mg, 0.11 mmol) the title compound was obtained following the procedure previously described for compound **7a**. The crude was purified by chromatography on silica gel (0.1% NH₄OH, 10% MeOH in DCM) giving **7i** (33 mg, 62%). ¹H NMR (300 MHz, DMSO-*d*₆) δ 11.15 (s, 1H), 8.98 (s, 1H), 8.67 (d, *J* = 3.6 Hz, 1H), 8.49 (s, 1H), 7.79 – 7.65 (m, 1H), 7.59 (d, *J* = 8.2 Hz, 2H), 7.54 – 7.38 (m, 3H), 7.38 – 7.20 (m, 5H), 7.20 – 6.96 (m, 4H), 5.66 (s, 2H), 5.18 (s, 2H) ¹³C NMR (75 MHz, DMSO-*d*₆) δ 164.3, 158.8, 150.1, 149.7, 143.9, 140.2, 137.7, 137.0, 136.6, 134.8, 132.7, 129.8, 129.6, 129.2, 128.2, 127.6, 127.2, 127.1, 126.9, 123.9, 123.2, 120.7, 115.9, 73.0, 45.8; ESI-MS *m/z*: [M + H]⁺ 477.0 Anal; (C₂₉H₂₃N₃O₄) C, H, N.

5.2.34. *N*-Hydroxy-4-(((2-oxo-4-(pyridin-3-yl)-1-(pyridin-4-ylmethyl)-1,2-dihydroquinolin-3-yl)oxy)methyl)benzamide (**7j**).

Starting from **24d** (67 mg, 0.20 mmol) methyl 4-(((2-oxo-4-(pyridin-3-yl)-1-(pyridin-4-ylmethyl)-1,2-dihydroquinolin-3-yl)oxy)methyl)benzoate was obtained following the procedure previously described for compound **14a**. The crude was purified by chromatography on silica gel (2% MeOH in DCM) giving the intermediate (31 mg, 32%). ¹H NMR (300 MHz, CDCl₃) δ 8.70 (dt, *J* = 8.3, 4.1 Hz, 1H), 8.63 – 8.42 (m, 2H), 8.11 – 7.94 (m, 1H), 7.85 (d, *J* = 8.2 Hz, 2H), 7.61 – 7.45 (m, 2H), 7.46 – 7.29 (m, 1H), 7.29 – 6.97 (m, 7H), 5.65 (s, 2H), 5.35 – 5.08 (m, 2H), 3.89 (s, 3H). ESI-MS *m/z*: [M + H]⁺ 478.0. Starting from this

intermediate (30 mg, 0.06 mmol) the title compound was obtained following the procedure previously described for compound **7a**. The crude was purified by chromatography on silica gel (0.1% NH₄OH, 10% MeOH in DCM) giving **7j** (18 mg, 60%). ¹H NMR (300 MHz, MeOD) δ 8.63 (d, *J* = 4.1 Hz, 1H), 8.49 (d, *J* = 5.5 Hz, 2H), 8.38 (s, 1H), 7.72 (d, *J* = 7.8 Hz, 1H), 7.62 – 7.34 (m, 5H), 7.30 (d, *J* = 5.6 Hz, 2H), 7.19 (dd, *J* = 8.4, 5.4 Hz, 2H), 7.10 (d, *J* = 8.1 Hz, 2H), 5.78 (s, 2H), 5.25 – 5.03 (m, 2H); ¹³C NMR (75 MHz, MeOD) δ 166.3, 159.3, 149.3, 149.0, 148.5, 148.1, 147.1, 143.3, 140.2, 138.4, 136.2, 135.5, 131.9, 130.0, 129.6, 128.3, 126.7, 123.7, 123.1, 122.0, 120.6, 115.0, 72.9, 45.0; ESI-MS *m/z*: [M + H]⁺ 479.0; Anal. (C₂₈H₂₂N₄O₄) C, H, N.

5.2.36. 1-Benzyl-N-phenylpiperidin-4-amine (**27**) [28].

To a solution of aniline (303 μL, 3.35 mmol) in DCM (10 mL) **26** (800 mg, 4.02 mmol) and AcOH (19 μL, 0.34 mmol) were added. The mixture was stirred at 20 °C for 4 h, then NaBH(OAc)₃ (1.07 g, 5.03 mmol) was added and the reaction stirred at 25 °C for 12 h. After this time a saturated solution of NaHCO₃ (10 mL) was added and the mixture was extracted with DCM (3 x 10 mL). The combined organic layers were dried over Na₂SO₄ and concentrated in vacuo. The residue was purified by chromatography on silica gel (10% EtOAc in petroleum ether) affording **27** (950 mg, 89%) as a white solid. ¹H NMR (300 MHz, CDCl₃) δ 7.58 – 7.30 (m, 5H), 7.30 – 7.15 (m, 2H), 6.84 – 6.71 (m, 1H), 6.71 – 6.58 (m, 2H), 3.60 (s, 2H), 3.36 (m, 1H), 2.92 (m, 2H), 2.36 – 1.99 (m, 4H), 1.68 – 1.42 (m, 2H); ESI-MS *m/z*: [M + H]⁺ 267.1. The spectroscopic data are consistent with those reported in literature [28].

5.2.37. 1-(1-Benzylpiperidin-4-yl)indoline-2,3-dione (**28**) [28].

To a solution of oxalyl chloride (316 μL, 7.14 mmol) in dry DCM (6 mL) cooled at 0 °C, a solution of **27** (950 mg, 3.57 mmol) in DCM (4 mL) was slowly added. The reaction was allowed to reach 25 °C and stirred for 2 h, then the solvent was evaporated. The residue was dissolved in DCM (5 mL), cooled at 0 °C and AlCl₃ (952 mg, 7.14 mmol) was added. The new mixture was stirred at 40 °C for 2 h, then poured on ice and neutralized with a saturated solution of NaHCO₃ (15 mL). The mixture was filtered through paper and extracted with DCM (3 x 10 mL). The combined organic layers were dried over Na₂SO₄ and concentrated in vacuo. The residue was purified by chromatography on silica gel (3% MeOH in DCM) affording **28** (600 mg, 52%) as a red solid. ¹H NMR (300 MHz, CDCl₃) δ 7.72 – 7.48 (m, 2H), 7.46 – 7.15 (m, 6H), 7.09 (m, 1H), 4.34 – 4.05 (m, 1H), 3.57 (s, 2H), 3.04 (d, *J* = 11.3 Hz, 2H), 2.58 – 2.27 (m, 2H), 2.27 – 2.00 (m, 2H), 1.75 (d, *J* = 12.3 Hz, 2H); ¹³C NMR (75 MHz, CDCl₃) δ 183.5, 158.0, 150.3, 138.2, 130.7, 129.1, 128.3, 127.3, 125.6, 123.4, 117.9, 112.0, 62.7, 52.8, 50.9 (2C), 28.1; ESI-MS *m/z*: [M + H]⁺ 321.1; mp 158.1-161.6 °C. The spectroscopic data are consistent with those reported in literature [28].

5.2.38. 4-(((1-(1-Benzylpiperidin-4-yl)-2-oxo-4-phenyl-1,2-dihydroquinolin-3-yl)oxy)methyl)-N-hydroxybenzamide (**7f**).

Compound **28** (200 mg, 0.62 mmol) was submitted to the ring expansion reaction with benzaldehyde (63 μ L, 0.62 mmol) following the same condition described for the synthesis of compound **13a**. The purification of the crude by chromatography on silica gel (5% MeOH in DCM) afforded *1-(1-benzylpiperidin-4-yl)-3-hydroxy-4-phenylquinolin-2(1H)-one* (140 mg, 55%) as a red solid. $^1\text{H NMR}$ (300 MHz, CDCl_3) δ 7.81 (s, 1H), 7.62 – 7.21 (m, 12H), 7.21 – 7.01 (m, 2H), 3.77 – 3.46 (m, 3H), 3.26 – 2.82 (m, 4H), 2.41 – 2.19 (m, 2H), 1.89 – 1.69 (m, 2H); ESI-MS m/z : $[\text{M} + \text{H}]^+$ 411.1. This intermediate (140 mg, 0.59 mmol) was subjected to the alkylation procedure with methyl 4-(bromomethyl)benzoate (263 mg, 0.88 mmol) previously described for compound **14a**. Purification of the crude by chromatography on silica gel (3% MeOH in DCM) afforded *methyl 4-(((1-(1-benzylpiperidin-4-yl)-2-oxo-4-phenyl-1,2-dihydroquinolin-3-yl)oxy)methyl)benzoate* (50 mg, 15%) as a pale red solid. $^1\text{H NMR}$ (300 MHz, CDCl_3) δ 7.84 (d, $J = 8.3$ Hz, 3H), 7.57 – 7.16 (m, 12H), 7.16 – 6.99 (m, 3H), 5.10 (s, 2H), 3.88 (s, 3H), 3.65 (s, 2H), 3.13 (s, 5H), 2.31 (s, 2H), 1.81 (d, $J = 12.3$ Hz, 2H); ESI-MS m/z : $[\text{M} + \text{H}]^+$ 559.2. This latter intermediate (16 mg, 0.03 mmol) was submitted to the reaction with a 50% solution of NH_2OH in water (190 μ L, 2.87 mmol) previously described for compound **7a**. Purification of the crude by chromatography on silica gel (0.1% NH_4OH , 10% MeOH in DCM) affording **7f** (10 mg, 62%) as a brown solid. $^1\text{H NMR}$ (300 MHz, MeOD) δ 7.89 (s, 1H), 7.69 – 7.26 (m, 11H), 7.26 – 6.91 (m, 6H), 4.97 (s, 2H), 3.72 (s, 2H), 3.17 (d, $J = 12.1$ Hz, 5H), 2.43 (s, 2H), 1.77 (d, $J = 11.7$ Hz, 2H); $^{13}\text{C NMR}$ (75 MHz, MeOD) δ 166.4, 160.2, 143.2, 140.7, 138.9, 136.3, 133.3, 131.5, 129.5, 129.4, 128.7, 128.1, 128.0 (2C), 127.4, 126.5, 122.2, 121.7, 72.8, 62.0, 53.0, 29.3, 26.8; ESI-MS m/z : $[\text{M} + \text{H}]^+$ 560.1; FT-IR (neat) ν_{max} 3209, 2922, 2853, 1722, 1632, 1595, 1455, 1262, 1117, 1011 cm^{-1} ; mp decomposition; Anal. ($\text{C}_{35}\text{H}_{33}\text{N}_3\text{O}_4$) C, H, N.

5.2.39. *1-(4-(1,3-Dioxolan-2-yl)benzyl)indoline-2,3-dione (29)*.

Starting from isatin (500 mg, 3.40 mmol) and **22** (1.24 g, 5.10 mmol) the title compound was synthesized following the same procedure to obtain compound **23a**. The residue was used in the next step without further purifications and affording **29** (1.36 g, quantitative yield) as a red solid. $^1\text{H NMR}$ (300 MHz, CDCl_3) δ 7.68 – 7.56 (m, 1H), 7.56 – 7.30 (m, 5H), 7.09 (td, $J = 7.5, 0.8$ Hz, 1H), 6.80 – 6.66 (m, 1H), 5.78 (s, 1H), 4.94 (s, 2H), 4.22 – 3.91 (m, 4H).

5.2.40. *1-(4-(1,3-Dioxolan-2-yl)benzyl)-3-hydroxy-4-phenylquinolin-2(1H)-one (30a)*.

Starting from **29** (500 mg, 1.62 mmol) the title compound was obtained following the procedure described to get **13a**. The residue was purified by chromatography on silica gel (33% EtOAc in petroleum ether) affording **30a** (310 mg, 48%) as a brown solid. $^1\text{H NMR}$ (300 MHz, CDCl_3) δ 7.70 – 7.46 (m, 6H), 7.46 – 7.26 (m, 5H), 7.26 – 7.02 (m, 2H), 5.81 (s, 1H), 5.72 (s, 2H), 4.25 – 3.94 (m, 4H); ESI-MS m/z : $[\text{M} + \text{H}]^+$ 400.0.

5.2.41. *1-(4-(1,3-Dioxolan-2-yl)benzyl)-3-hydroxy-4-(pyridin-3-yl)quinolin-2(1H)-one (30b)*.

Starting from **29** (500 mg, 1.62 mmol) the title compound was obtained following the procedure described to get **13b**. The residue was purified by chromatography on silica gel (3% MeOH in DCM) affording **30b** (310 mg, 48%) as a brown solid. ¹H NMR (300 MHz, CDCl₃) δ 8.75 (d, *J* = 2.0 Hz, 2H), 8.10 (s, 1H), 7.84 (d, *J* = 7.8 Hz, 1H), 7.60 – 7.42 (m, 3H), 7.40 – 7.25 (m, 5H), 7.25 – 7.06 (m, 1H), 5.80 (s, 1H), 5.72 (s, 2H), 4.23 – 3.92 (m, 4H); ESI-MS *m/z*: [M + H]⁺ 401.0.

5.2.42. *Methyl 4-(((1-(4-(1,3-dioxolan-2-yl)benzyl)-2-oxo-4-phenyl-1,2-dihydroquinolin-3-yl)oxy)methyl)benzoate (31a)*.

Starting from **30a** (310 mg, 0.78 mmol) the title compound was obtained following the procedure described to get **14a**. The residue was purified by chromatography on silica gel (50% EtOAc in petroleum ether) affording **31a** (340 mg, 80%) as a yellow oil. ¹H NMR (300 MHz, CDCl₃) δ 7.85 (d, *J* = 8.3 Hz, 2H), 7.55 – 7.38 (m, 5H), 7.38 – 7.17 (m, 7H), 7.17 – 6.94 (m, 3H), 5.77 (s, 1H), 5.67 (s, 2H), 5.19 (s, 2H), 4.20 – 3.92 (m, 4H), 3.87 (s, 3H); ESI-MS *m/z*: [M + H]⁺ 548.0.

5.2.43. *Methyl 4-(((1-(4-(1,3-dioxolan-2-yl)benzyl)-2-oxo-4-(pyridin-3-yl)-1,2-dihydroquinolin-3-yl)oxy)methyl)benzoate (31b)*.

Starting from **30b** (310 mg, 0.77 mmol) the title compound was obtained following the procedure described to get **14a**. The residue was purified by chromatography on silica gel (33% Petroleum ether in EtOAc) affording **31b** (231 mg, 55%) as a red oil. ¹H NMR (300 MHz, CDCl₃) δ 8.68 (dd, *J* = 5.0, 1.7 Hz, 1H), 8.49 (d, *J* = 2.1 Hz, 1H), 7.85 (d, *J* = 8.3 Hz, 2H), 7.63 – 7.20 (m, 8H), 7.20 – 6.91 (m, 4H), 5.76 (s, 1H), 5.66 (s, 2H), 5.37 – 5.08 (m, 2H), 4.19 – 3.93 (m, 4H), 3.86 (s, 3H); ESI-MS *m/z*: [M + H]⁺ 549.0.

5.2.44. *4-(((1-(4-((Diethylamino)methyl)benzyl)-2-oxo-4-phenyl-1,2-dihydroquinolin-3-yl)oxy)methyl)-N-hydroxybenzamide (7g)*.

To a solution of **31a** (230 mg, 0.62 mmol) in THF (5 mL) a 1 N solution of HCl in water (5 mL) was added. The reaction was stirred at 25 °C for 1 h, then a saturated solution of NaHCO₃ (10 mL) was added and the mixture was extracted with EtOAc (3 x 10 mL). The combined organic layers were dried over Na₂SO₄ and concentrated in vacuo. The residue was used in the next step without further purifications. *Methyl 4-(((1-(4-formylbenzyl)-2-oxo-4-phenyl-1,2-dihydroquinolin-3-yl)oxy)methyl)benzoate* (310 mg, quantitative yield) was obtained as a yellow oil. ¹H NMR (300 MHz, CDCl₃) δ 9.99 (s, 1H), 7.98 – 7.72 (m, 4H), 7.60 – 6.91 (m, 13H), 5.74 (s, 2H), 5.19 (s, 2H), 3.90 (s, 3H). This intermediated was dissolved in DCM (5 mL) and dimethylamine (96 μL, 0.93 mmol) and AcOH (4 μL, 0.06 mmol) were added. This mixture was stirred at 25 °C for 2 h then a NaBH(OAc)₃ (197 mg, 0.93 mmol) was added and the reaction was stirred at 25 °C for 12 h. After this time, a saturated solution of NaHCO₃ (5 mL) was added and the mixture was extracted with DCM (3 x 5 mL). The combined organic layers were dried over Na₂SO₄ and concentrated in vacuo. The residue was purified by chromatography on silica gel (5% MeOH in DCM) affording *methyl 4-(((1-(4-((diethylamino)methyl)benzyl)-2-oxo-4-phenyl-1,2-dihydroquinolin-3-yl)oxy)methyl)benzoate* (204 mg,

59%) as a colorless oil. ^1H NMR (300 MHz, CDCl_3) δ 7.86 (d, $J = 8.3$ Hz, 2H), 7.57 – 7.42 (m, 3H), 7.42 – 7.18 (m, 9H), 7.18 – 6.95 (m, 3H), 5.84 – 5.48 (m, 2H), 5.21 (s, 2H), 3.88 (s, 3H), 3.56 (s, 2H), 2.53 (q, $J = 7.1$ Hz, 4H), 1.04 (t, $J = 7.1$ Hz, 6H); ESI-MS m/z : $[\text{M} + \text{H}]^+$ 561.2. Starting from this intermediate (100 mg, 0.18 mmol) the title compound was obtained following the procedure described to get **7a**. The residue was purified by chromatography on silica gel (0.1% NH_4OH , 10% MeOH in DCM) affording **7g** (75 mg, 74%) as a white solid. ^1H NMR (300 MHz, MeOD) δ 7.65 – 7.48 (m, 5H), 7.48 – 7.35 (m, 4H), 7.34 – 7.20 (m, 5H), 7.19 – 6.97 (m, 3H), 5.74 (s, 2H), 5.08 (s, 2H), 3.86 (s, 2H), 2.78 (q, $J = 7.2$ Hz, 4H), 1.16 (t, $J = 7.2$ Hz, 6H); ^{13}C NMR (75 MHz, $\text{DMSO}-d_6$) δ 164.2, 159.0, 143.5, 140.5, 139.4, 138.2, 136.6, 135.3, 133.6, 132.5, 129.8, 129.6, 129.2, 128.8, 128.6, 128.1, 127.2, 127.1, 126.9, 122.9, 121.1, 115.7, 73.0, 57.0, 46.5, 45.6, 12.0; ESI-MS m/z : $[\text{M} + \text{H}]^+$ 562.2. HRMS-ESI m/z : calcd for $\text{C}_{35}\text{H}_{36}\text{N}_3\text{O}_4^+$ $[\text{M}+\text{H}]^+$: 562,2700; found: 562.2678; FT-IR (neat) ν_{max} 3222, 2963, 2925, 1799, 1719, 1636, 1596, 1454, 1287, 1172, 1121, 1016 cm^{-1} ; mp 180.8-182.9 $^\circ\text{C}$, decomposition; Anal. ($\text{C}_{35}\text{H}_{35}\text{N}_3\text{O}_4$) C, H, N.

5.2.45. *4-(((1-(4-((Diethylamino)methyl)benzyl)-2-oxo-4-(pyridin-3-yl)-1,2-dihydroquinolin-3-yl)oxy)methyl)-N-hydroxybenzamide (7k)*.

Starting from **31b** (230 mg, 0.42 mmol) *methyl 4-(((1-(4-((diethylamino)methyl)benzyl)-2-oxo-4-(pyridin-3-yl)-1,2-dihydroquinolin-3-yl)oxy)-methyl)benzoate* was obtained following the procedure described for **7g**. The residue was purified by chromatography on silica gel (10% MeOH in DCM) affording *methyl 4-(((1-(4-((diethylamino)methyl)benzyl)-2-oxo-4-(pyridin-3-yl)-1,2-dihydroquinolin-3-yl)oxy)-methyl)benzoate* (110 mg, 47% (over two steps)) as a brown oil. ^1H NMR (300 MHz, CDCl_3) δ 8.69 (dd, $J = 4.7, 1.7$ Hz, 1H), 8.50 (s, 1H), 7.96 – 7.75 (m, 2H), 7.62 – 7.45 (m, 1H), 7.45 – 6.95 (m, 11H), 5.64 (s, 2H), 5.37 – 5.12 (m, 2H), 3.87 (s, 3H), 3.55 (s, 2H), 2.63 – 2.35 (m, 4H), 1.15 – 0.86 (m, 6H); ESI-MS m/z : $[\text{M} + \text{H}]^+$ 562.2. Starting from this intermediate (55 mg, 0.10 mmol) the title compound was obtained following the procedure described to get **7a**. The residue was purified by chromatography on silica gel (0.1% NH_4OH , 10% MeOH in DCM) affording **7k** (45 mg, 80%) as a white solid. ^1H NMR (300 MHz, MeOD) δ 8.63 (dd, $J = 4.9, 1.7$ Hz, 1H), 8.36 (dd, $J = 2.2, 0.9$ Hz, 1H), 7.71 (m, 1H), 7.65 – 7.41 (m, 5H), 7.34 (d, $J = 8.1$ Hz, 2H), 7.25 (d, $J = 8.1$ Hz, 2H), 7.21 – 7.00 (m, 4H), 5.90 – 5.59 (m, 2H), 5.27 – 5.11 (m, 2H), 3.64 (s, 2H), 2.58 (q, $J = 7.1$ Hz, 4H), 1.08 (t, $J = 7.2$ Hz, 6H); ^{13}C NMR: (75 MHz, $\text{DMSO}-d_6$) δ 164.3, 158.8, 150.0 (2C), 149.7, 143.9, 140.2, 139.0, 137.7, 136.6, 135.3, 134.8, 132.6, 129.8, 129.5, 129.4, 128.2, 127.2, 127.0, 123.9, 123.2, 120.6, 115.9, 73.0, 56.8, 46.4, 45.7, 11.8; ESI-MS m/z : $[\text{M} + \text{H}]^+$ 563.2. FT-IR (neat) ν_{max} 3228, 2958, 2922, 2818, 1638, 1597, 1456, 1307, 1182, 1123, 1019 cm^{-1} ; mp 184.5-188.5 $^\circ\text{C}$, decomposition; Anal. ($\text{C}_{34}\text{H}_{34}\text{N}_4\text{O}_4$) C, H, N.

5.3. Molecular Modeling

5.3.1. Proteins and Ligands Preparation

The crystal structures of *hHDAC6*, ~~and~~ *hHDAC1* and *zHDAC6* were downloaded from the Protein Data Bank (PDB) with the codes 5EDU, ~~and~~ 4BKX and 6THV respectively, and accurately prepared as previously

reported [4,15,38]. The proteins were exploited in the molecular docking calculation. The 3D structures of ligands were built in Maestro 10.1 (Schrödinger, LLC, New York, NY, 2015), and then minimized by means of MacroModel software employing the OPLS-2005 force field. The Generalized-Born/Surface-Area model was employed to simulate the solvent effects using the analytical [39], and no cutoff for nonbonded interactions was selected. Polak-Ribiere conjugate gradient (PRCG) method with 1000 maximum iterations and 0.001 gradient convergence threshold was employed. The quinolone derivatives were treated by LigPrep application (LigPrep version 3.3, Schrödinger, LLC, New York, NY, 2015) in order to generate the most probable ionization state at cellular pH (7.4 ± 0.2) as reported by us previously [40,41]. We used a neutral hydroxamic acid moiety of the quinolone compounds, since the hydroxamic acid proton should not be transferred in HDAC isoforms containing histidines in the binding site close to the reactive metal center, as in the case of HDAC1 and HDAC6.

5.3.2. Molecular Docking and Molecular Properties Prediction

Using the ligands and proteins prepared as above-mentioned we employed Glide software (Glide, version 6.6, Schrödinger, LLC, New York, NY, 2015) to perform the docking studies presented in this paper, applying Glide standard precision (SP) scoring function. Energy grids were prepared using default value of protein atom scaling factor (1.0 \AA) within a cubic box centered on the zinc ion which roughly represents the center of the active sites [14,15]. The ligands were docked into the enzymes after grid generation introducing the metal constraints. The number of poses entered to post-docking minimization was set to 50. Glide SP score was evaluated. Molecular properties were evaluated by means of QikProp (QikProp, version 4.3, Schrödinger, LLC, New York, NY, 2015).

5.2. Solubility and chemical stability studies

*5.2.1. HPLC analysis of compounds **6b** and **7e,k***

For the HPLC analysis a Chromolith HPLC column RP-18 was employed. The runs were performed by a gradient elution starting from a mixture 20% MeCN (0.1% TFA as phase modifier) in H₂O (0.1% TFA as phase modifier) to 90% MeCN (0.1% TFA) in H₂O (0.1% TFA) in 15 min. The flow speed was settled at 1.0 mL/min and the temperature was maintained at 25 °C. The volume of injection of the sample was 10 mL and the wavelength selected for the detection was 254 nm. The retention times obtained following this protocol for compounds **6b** and **7e,k** were 7.3 min, 5.6 min and 3.7 min, respectively.

5.2.2. Solubility assay and chemical stability at 25 °C

A stock solution for each tested compound was prepared dissolving the sample in DMSO to a final concentration of 10 mM. From the stock solution, three samples were prepared: one was used as the standard solution and the other two as the test solutions at pH 3.0 and pH 7.4. The sample concentration of these solutions was 250 μM with a DMSO content of 2.5% (v/v). The standard solution was prepared by dilution of the stock solution in PBS-buffer solution (MeCN/water, 60:40); the dilution of the stock solution in 50

mM acetic acid afforded the samples solution at pH 3.0; and the dilution of the stock solution in 50 mM aqueous PBS-buffer afforded the sample' solution at pH 7.4. These suspension/solutions were sealed and left for 24 h at 25 °C under orbital shaking to achieve “pseudothermodynamic equilibrium”. After that time, the solutions were filtered using PTFE filters and successively diluted 1:2 with the buffer solution used for the preparation of the samples. Then they were analyzed by HPLC/UV/ DAD, using UV detection at 254 nm for quantitation. Solubility was calculated by comparing areas of the sample and of the standard:

$$S = \frac{A_{smp} \times FD \times C_{st}}{A_{st}}$$

S = solubility of the compound (μM); A_{smp} = UV area of the sample solution; FD = dilution factor (2); C_{st} = standard concentration (250 μM); A_{st} = UV area of the standard solution.

For each sample the analysis was performed in triplicate and the solubility result reported was obtained from the average of the three values. The same sample solutions were prepared to evaluate the chemical stability of the compounds after 24 h at 25 °C and analyzed by HPLC/UV/DAD, using UV detection at 254 nm for quantitation. Stability was calculated by comparing the area of the peak at T₀ and the area of the peak of the same solution after 24 h. A stability percentage value was calculated by this method at pH 3.0 and pH 7.4 for each compound by applying the following formula:

$$\%_{remaining} = \frac{AC_{24}}{AC_{T_0}} \times 100$$

AC₂₄ = area of the sample after 24 h at 25 °C; AC_{T₀} = area of the sample at T₀. For each sample the analysis was performed in triplicate and the stability result reported was obtained from the average of the three values.

5.3. Biological data

5.3.1. In vitro testing of HDAC1 and HDAC6

OptiPlate-96 black microplates (PerkinElmer) were employed with an assay volume of 60 μL. Human recombinant HDAC1 (BPS Bioscience, Catalog #: 50051) or human recombinant HDAC6 (BPS Bioscience, Catalog #: 50006) were diluted in incubation buffer (50 mM Tris-HCl, pH 8.0, 137 mM NaCl, 2.7 mM KCl, 1 mM MgCl₂ and 1 mg/mL BSA). A total of 52 μL of this dilution were incubated with 3 μL of different concentrations of inhibitors in DMSO and 5 μL of the fluorogenic substrate ZMAL (Z-(Ac)Lys-AMC) [42,43] (126 μM) at 37 °C. After 90 min incubation time, 60 μL of the stop solution (33 μM Trichostatin A and 6 mg/mL trypsin in trypsin buffer [Tris-HCl 50 mM, pH 8.0, NaCl 100 mM]), were added. After a following incubation at 37 °C for 30 min, the fluorescence was measured on a BMG LABTECH POLARstar

OPTIMA plate reader (BMG Labtechnologies, Germany) with an excitation wavelength of 390 nm and an emission wavelength of 460 nm [43,44].

5.3.2. *In vitro* testing of HDAC8

Recombinant human HDAC8 was purchased as part of the Fluor-de-Lys HDAC8 fluorimetric drug discovery kit (Enzo Life Sciences, No. BMLAK518). Dose-response curves were built for each inhibitor in order to estimate the respective IC₅₀. DMSO concentration was kept constant to 0.5% and, for each compound, a control curve (enzymes incubated with DMSO only) was added. The Fluor-de-Lys substrate was used at 50 μM. A preincubation period of 15 min was chosen to keep safe from the possibility of a slow-binding inhibition. Hence, the compounds, substrate, and enzyme (266 nM) were incubated, and the reaction was allowed to proceed for 1 h at 30 °C; 2 μM TSA within 50 μL of 1× Enzo Developer II was added to quench the reaction and the mixture was further incubated for 1 h at 30 °C. Fluorescence was measured in a plate reader (Varioskan Lux, Thermo Fisher Scientific) with excitation wave length at 370 nm and emission at 450 nm. Data were analyzed by nonlinear regression fit using a generalized form of a dose-response curve:[45]

$$y_{res} = y_{min} + \frac{y_{max} - y_{min}}{\left(1 + \frac{[I]}{IC_{50}}\right)}$$

y_{res} = is the residual activity of the enzyme in the presence of inhibitor at concentration [I]; y_{max} = the maximum observed value for the enzyme at zero inhibitor concentration; y_{min} = the minimum observed value for the enzyme at the highest inhibitor concentration. The model did fit three parameters, namely: IC₅₀, y_{max} , and y_{min} .

In addition, since the total enzyme concentration used in the assay (266 nM) was in the same order of magnitude to the obtained IC_{50s} for two out of three inhibitors (namely, **7g** and **7k**), a more accurate model was chosen to fit the experimental data, ultimately to account for the possibility of a tight-binding interaction. The fit model was in the form of the Morrison equation as implemented in Copeland as reported below [45]:

$$\frac{v_i}{v_0} = 1 - \frac{\sqrt{([E] - [I] - K_i^{app})^2 - 4[E][I]}}{2[E]}$$

v_0 and v_i = were the rate observed in the absence or in the presence of the inhibitor at concentration [I], and [E] was kept fixed at 266 nM. It was assumed that the ratio v_i/v_0 was proportional to the signal (arbitrary fluorescence unit) as obtained by using Fluor-de-Lys kit. This model yields apparent inhibitor constant which should be regarded as a better estimate of interaction with respect to IC₅₀.

5.4. Cell-based Assays

5.4.1 Cell lines

HCT-116, colon cancer cells were propagated in Dulbecco's Modified Eagle's Medium (Euroclone) with 10% fetal bovine serum (FBS; Euroclone), 2 mM L-glutamine (Euroclone), and antibiotics (100 U/ml penicillin, 100 mg/ml streptomycin; Euroclone). U937, histiocytic lymphoma cells were grown in RPMI-

1640 Medium (Euroclone) containing 4.5 g/L glucose (Euroclone) supplemented with 10% FBS (Euroclone), 100 U/mL penicillin-streptomycin (Euroclone), and 2 mM L-glutamine (Euroclone). The cell lines were purchased from ATCC.

5.4.2 MTT assay

Cell viability was determined using the standard Thiazolyl Blue Tetrazolium Bromide [3-(4,5-dimethylthiazol-2-yl)-2,5-diphenyltetrazolium bromide] (MTT; Sigma) assay. A total of 2.5×10^4 cells/well, plated in a 48-well, were treated, in triplicate, with the compounds **7a**, **7k** and **7g** at 50, 25, 10, 5 and 1 μ M for 12, 24 and 48 h. After induction the MTT solution was added at 0.5 mg/ml for 3 h. For HCT-116, adhesion cells, the supernatant was simply removed, whereas for suspension cells, U937, the plate was first centrifuged for 5 min at 1200 rpm. The purple formazan crystals were dissolved in 100 μ l/well of isopropanol (Carlo Erba Reagents) and the absorbance was read at a wavelength of 570 nm with a TECAN M-200 reader (Tecan). The IC_{50} was analyzed using GraphPad Prism 7.0 software (GraphPad Software).

5.4.3 Total protein extraction

HCT-116 and U937 cells were treated with the compounds **7a**, **7k** and **7g** at 10 μ M for 12 and 24 h. The cells, after treatment, were harvested and washed twice with PBS (Euroclone), and then were lysed in protein extraction buffer containing H₂O with 50 mM Tris HCl pH 8.0 solution, 5 mM EDTA, 1% NP40, 150 mM NaCl, 0.5 % sodium deoxycholate, 0.1% SDS, and 1X protein inhibitor proteinase cocktail before use. The cells were then incubated with the extraction buffer for 15 min at 4°C, centrifuged at 13,000 rpm at 4°C for 30 min, and the supernatant was recovered. Total protein extract was determined using a Bradford assay (Bio-Rad).

5.4.4 Protein histone extraction

After treatment with the compounds **7a**, **7k** and **7g**, at the same conditions used for the total protein extract, HCT-116 and U937 cells were lysed in Triton extraction buffer (TEB) containing PBS with 0.5% Triton X-100 (v/v), 2 mM phenylmethylsulfonyl fluoride, and 0.02% (w/v) NaN₃ at a cell density of 10^7 cells/mL for 10 min on ice and centrifuged (2,000 rpm at 4 °C for 10 min). The supernatant was removed. Then, the pellet was washed with half the volume of TEB and centrifuged at 2000 rpm at 4 °C for 10 min, and, was suspended in 0.2 N HCl overnight at 4 °C on a rolling table. The samples were centrifuged at 2,000 rpm for 10 min at 4 °C and the supernatant was recovered. The histone protein was determined using a Bradford assay (Bio-Rad).

5.4.5 Western blotting

Western blotting analysis was performed by loading 40 μ g of total protein and 5 μ g for histone protein extract at different concentrations of polyacrylamide gels, depending on the antibodies band. Antibodies used were: PARP (46D11, Cell Signaling), Anti-Acetylated Tubulin (T7451, Sigma), Hsp90(AcLys294) (NBP1-

77944, Bio-Techne SRL), H3K9/14ac (ab232952, Abcam), GAPDH (sc-47724; Santa Cruz Biotechnology), H4 (ab10158, Abcam) Semi-quantitative analysis was performed using ImageJ software.

5.4.6 Statistical Analysis

Graphs represent the mean of three independent experiments with an error bar indicating standard deviation. Differences between the treated cells versus control cells were analyzed using GraphPad Prism 7.0 software (GraphPad Software). Statistical analysis was performed by applying one-way analysis of variance (ANOVA) and Dunnett's multiple-comparison test. Differences between groups were considered to be significant at a p-value of < 0.05. **** p-value \leq 0.0001, *** p-value \leq 0.001, ** p-value \leq 0.01, * p-value \leq 0.05, ns p-value > 0.05 vs control cells.

5.5. Mutagenicity assay: Ames test

The TA100 and TA98 strains of *Salmonella typhimurium* were utilized for mutagenicity assay in absence and presence of metabolic activation, i.e. with and without S9 fraction. The tester strains used were selected because they are sensitive and detect a large proportion of known bacterial mutagens and are most commonly used routinely within the pharmaceutical industry [46,47]. The following specific positive controls were used, respectively, with and without S9 fraction: 2-Nitrofluorene (2-NF) 2 μ g/mL + 4-Nitroquinoline *N*-oxide (4-NQO) 0,1 μ g/mL, and 2-aminoanthracene (2-AA) 5 μ g/mL. Approximately 10^7 bacteria were exposed to 6 concentrations of each test sample ranging from ranging from 8 to 160 μ M, as well as to positive and negative controls, for 90 minutes in medium containing sufficient histidine to support approximately two cell divisions. After 90 minutes, the exposure cultures were diluted in pH indicator medium lacking histidine, and aliquoted into 48 wells of a 384-well plate. Within two days, cells which had undergone the reversion to His grew into colonies. Metabolism by the bacterial colonies reduced the pH of the medium, changing the color of that well. This color change can be detected visually. The number of wells containing revertant colonies were counted for each dose and compared to a zero-dose control. Each dose was tested in six replicates. The material was regarded mutagenic if the number of histidine revertant colonies was twice or more than the spontaneous revertant colonies.

5.6. Cytotoxicity assay on NIH3T3 cell line

Cells (5×10^4) suspended in 1 mL of complete medium were seeded in each well of a 24 well round multidish and incubated at 37 °C in an atmosphere of 5% CO₂. After 24 hours of culture, the culture medium was discharged and test samples, solubilized in DMSO, were added to each well at different concentration values. For the evaluation of cytotoxicity, three experiment repeated in six replicates were performed and all compounds were tested at increasing concentrations ranging from 8 to 160 μ M. The samples were set up in six replicates for each tested concentration. Complete medium was used as negative control. Cell viability and proliferation was evaluated by Neutral Red uptake after 24 hours of incubation with NIH3T3 as follows. First, the following solutions were prepared in order to determine the percentage of viable cells:

1. Neutral Red (NR) stock solution: 0.33 g NR dye powder in 100 ml sterile H₂O
2. NR medium: 1.0 mL NR stock solution + 99.0 routine culture medium pre-warmed to 37 °C
3. NR desorb solution: 1% glacial acetic acid solution + 50% ethanol + 49% H₂O

At the end of incubation, the routine culture medium was removed from each plate and the cells were carefully rinsed with 1 ml pre-warmed D-PBS 0.1 M. Plates were then gently blotted with paper towels. 1.0 ml NR medium was added to each dish and further incubated at 37 °C, 95% humidity, 5.0% CO₂ for 3 hours. The cells were checked during incubation for NR crystal formation. After incubation, the NR medium was removed, and the cells were carefully rinsed with 1 mL pre-warmed D-PBS 0.1 M. PBS was decanted and blotted from the dishes and exactly 1 mL NR desorb solution was added to each sample. Plates were placed on a shaker for 20-45 minutes to extract NR from the cells and form a homogeneous solution. During this step the samples were covered to protect them from light. Five minutes after removal from the shaker, absorbance was read at 540 nm with a UV/visible spectrophotometer (Varian Cary 1E).

5.7. Cytotoxicity assay on human PBMC cell line

Cell viability on human PBMC was determined by using the Guava® ViaCount™ Reagent (Luminex Corporation, US). PBMCs were seeded 1.5 x10⁶/mL in complete medium and treated with 15 μM, 45 μM and 90 μM 7G and 7K compounds or vehicle (DMSO) for 24 h and 48 h. The percentage of viable cells was measured by flow cytometry carried out using GUAVA easyCyte cytometer (Luminex Corporation, US). Analysis was conducted with Guava® ViaCount™ software module (Luminex Corporation, US).

Author contributions

The manuscript was written through contribution of all authors. All authors have given approval to the final version of the manuscript.

Declaration of competing interest

The authors declare that they have no known competing financial interests or personal relationships that could have appeared to influence the work reported in this paper.

Acknowledgement

Authors thank Progetto Dipartimento di Eccellenza DBCF-UNISI 2018-2022. A.P.S. Support from the European Union's Horizon 2020 (EU) Research and Innovation Programme under the Marie Skłodowska-Curie grant agreement No. 721906-TRACT is acknowledged. N.R. Tuscany strategic project POR-FSE 2014-2020, 'Medicina di Precisione e Malattie Rare'(MePreMaRe), (ACE-ESCC). G.R. acknowledges the CNR-CNCCS "Rare, Neglected and Poverty Related Diseases - Schistodiscovery Project" (DSB.AD011.001.003). L.A. Support from the MIUR20152TE5PK; EPICHEMPIO CM1406; VALERE: Vanvitelli per la Ricerca; Campania Regional Government Technology Platform Lotta alle Patologie

Oncologiche: iCURE; Campania Regional Government FASE2: IDEAL. MIUR, Proof of Concept POC01_00043.

Appendix A. Supplementary data

Supplementary data to this article can be found online at [xxxx](#)

References

- [1] T. Li, C. Zhang, S. Hassan, X. Liu, F. Song, K. Chen, W. Zhang, J. Yang, Histone deacetylase 6 in cancer, *J. Hematol. Oncol.* 11 (2018) 111. <https://doi.org/10.1186/s13045-018-0654-9>.
- [2] F. Saccoccia, M. Brindisi, R. Gimmelli, N. Relitti, A. Guidi, A. Prasanth, C. Cavella, S. Brogi, G. Chemi, G. Papoff, D. Herp, M. Jung, G. Campiani, S. Gemma, G. Ruberti, Screening and phenotypical characterization of *Schistosoma mansoni* histone deacetylase 8 (SmHDAC8) inhibitors as multi-stage antischistosomal agents histone deacetylase 8 (Sm HDAC8) inhibitors as multi-stage anti- a Institute b Department c Department, *ACS Infect. Dis.* 6 (2020) 100–113. <https://doi.org/10.1021/acsinfecdis.9b00224>.
- [3] M. Brindisi, A.P. Saraswati, S. Brogi, S. Gemma, S. Butini, G. Campiani, Old but Gold: Tracking the New Guise of Histone Deacetylase 6 (HDAC6) Enzyme as a Biomarker and Therapeutic Target in Rare Diseases, *J. Med. Chem.* 63 (2020) 23–39. <https://doi.org/10.1021/acs.jmedchem.9b00924>.
- [4] Y. Hai, D.W. Christianson, Histone deacetylase 6 structure and molecular basis of catalysis and inhibition, *Nat. Chem. Biol.* 12 (2016) 741–747. <https://doi.org/10.1038/nchembio.2134>.
- [5] E. Landucci, M. Brindisi, L. Bianciardi, L.M. Catania, S. Daga, S. Croci, E. Frullanti, C. Fallerini, S. Butini, S. Brogi, S. Furini, R. Melani, A. Molinaro, F.C. Lorenzetti, V. Imperatore, S. Amabile, J. Mariani, F. Mari, F. Ariani, T. Pizzorusso, A.M. Pinto, F.M. Vaccarino, A. Renieri, G. Campiani, I. Meloni, iPSC-derived neurons profiling reveals GABAergic circuit disruption and acetylated α -tubulin defect which improves after iHDAC6 treatment in Rett syndrome, *Exp. Cell Res.* 368 (2018) 225–235. <https://doi.org/https://doi.org/10.1016/j.yexcr.2018.05.001>.
- [6] Y. Hai, S.A. Shinsky, N.J. Porter, D.W. Christianson, Histone deacetylase 10 structure and molecular function as a polyamine deacetylase, *Nat. Commun.* 8 (2017) 15368. <https://doi.org/10.1038/ncomms15368>.
- [7] M. Duvic, J. Vu, Vorinostat: a new oral histone deacetylase inhibitor approved for cutaneous T-cell lymphoma, *Expert Opin. Investig. Drugs.* 16 (2007) 1111–1120. <https://doi.org/10.1517/13543784.16.7.1111>.
- [8] C. Grant, F. Rahman, R. Piekarz, C. Peer, R. Frye, R.W. Robey, E.R. Gardner, W.D. Figg, S.E. Bates, Romidepsin: a new therapy for cutaneous T-cell lymphoma and a potential therapy for solid tumors, *Expert Rev. Anticancer Ther.* 10 (2010) 997–1008. <https://doi.org/10.1586/era.10.88>.
- [9] M.P. Fenichel, FDA approves new agent for multiple myeloma, *J. Natl. Cancer Inst.* 107 (2015) djv165. <https://doi.org/10.1093/jnci/djv165>.
- [10] R.M. Poole, Belinostat: First Global Approval, *Drugs.* 74 (2014) 1543–1554. <https://doi.org/10.1007/s40265-014-0275-8>.
- [11] K. V Butler, J. Kalin, C. Brochier, G. Vistoli, B. Langley, A.P. Kozikowski, Rational Design and Simple Chemistry Yield a Superior, Neuroprotective HDAC6 Inhibitor, Tubastatin A, *J. Am. Chem. Soc.* 132 (2010) 10842–10846. <https://doi.org/10.1021/ja102758v>.
- [12] M. Morgen, R.R. Steimbach, M. Géraldy, L. Hellweg, P. Sehr, J. Ridinger, O. Witt, I. Oehme, C.J.

- Herbst-Gervasoni, J.D. Osko, N.J. Porter, D.W. Christianson, N. Gunkel, A.K. Miller, Design and Synthesis of Dihydroxamic Acids as HDAC6/8/10 Inhibitors, *ChemMedChem*. 15 (2020) 1163–1174. <https://doi.org/10.1002/cmdc.202000149>.
- [13] M. Géraldy, M. Morgen, P. Sehr, R.R. Steimbach, D. Moi, J. Ridinger, I. Oehme, O. Witt, M. Malz, M.S. Nogueira, O. Koch, N. Gunkel, A.K. Miller, Selective Inhibition of Histone Deacetylase 10: Hydrogen Bonding to the Gatekeeper Residue is Implicated, *J. Med. Chem.* 62 (2019) 4426–4443. <https://doi.org/10.1021/acs.jmedchem.8b01936>.
- [14] M. Brindisi, C. Cavella, S. Brogi, A. Nebbioso, J. Senger, S. Maramai, A. Ciotta, C. Iside, S. Butini, S. Lamponi, E. Novellino, L. Altucci, M. Jung, G. Campiani, S. Gemma, Phenylpyrrole-based HDAC inhibitors: synthesis, molecular modeling and biological studies, *Future Med. Chem.* 8 (2016) 1573–1587. <https://doi.org/10.4155/fmc-2016-0068>.
- [15] M. Brindisi, J. Senger, C. Cavella, A. Grillo, G. Chemi, S. Gemma, D.M. Cucinella, S. Lamponi, F. Sarno, C. Iside, A. Nebbioso, E. Novellino, T.B. Shaik, C. Romier, D. Herp, M. Jung, S. Butini, G. Campiani, L. Altucci, S. Brogi, Novel spiroindoline HDAC inhibitors: Synthesis, molecular modelling and biological studies, *Eur. J. Med. Chem.* 157 (2018) 127–138. <https://doi.org/https://doi.org/10.1016/j.ejmech.2018.07.069>.
- [16] A.K. Ghosh, A.M. Veitschegger, S. Nie, N. Relitti, A.J. Macrae, M.S. Jurica, Enantioselective Synthesis of Thailanstatin A Methyl Ester and Evaluation of in Vitro Splicing Inhibition, *J. Org. Chem.* 83 (2018) 5187–5198. <https://doi.org/10.1021/acs.joc.8b00593>.
- [17] J. Szychowski, J.-F. Truchon, Y.L. Bennani, Natural Products in Medicine: Transformational Outcome of Synthetic Chemistry, *J. Med. Chem.* 57 (2014) 9292–9308. <https://doi.org/10.1021/jm500941m>.
- [18] D. Zhang, A. Kanakkanthara, Beyond the Paclitaxel and Vinca Alkaloids: Next Generation of Plant-Derived Microtubule-Targeting Agents with Potential Anticancer Activity, *Cancers (Basel)*. 12 (2020) 1721.
- [19] S. Yuan, J.V. Gopal, S. Ren, L. Chen, L. Liu, Z. Gao, Anticancer fungal natural products: Mechanisms of action and biosynthesis, *Eur. J. Med. Chem.* 202 (2020) 112502. <https://doi.org/https://doi.org/10.1016/j.ejmech.2020.112502>.
- [20] J.M. Kraus, H.B. Tatipaka, S.A. McGuffin, N.K. Chennamaneni, M. Karimi, J. Arif, C.L.M.J. Verlinde, F.S. Buckner, M.H. Gelb, Second Generation Analogues of the Cancer Drug Clinical Candidate Tipifarnib for Anti-Chagas Disease Drug Discovery, *J. Med. Chem.* 53 (2010) 3887–3898. <https://doi.org/10.1021/jm9013136>.
- [21] G. Balasubramanian, N. Kilambi, S. Rathinasamy, P. Rajendran, S. Narayanan, S. Rajagopal, Quinolone-based HDAC inhibitors, *J. Enzyme Inhib. Med. Chem.* 29 (2014) 555–562. <https://doi.org/10.3109/14756366.2013.827675>.
- [22] R.E. Hawtin, D.E. Stockett, J.A.W. Byl, R.S. McDowell, N. Tan, M.R. Arkin, A. Conroy, W. Yang, N. Osheroff, J.A. Fox, Voreloxin Is an Anticancer Quinolone Derivative that Intercalates DNA and

Poisons Topoisomerase II, *PLoS One*. 5 (2010) e10186.

<https://doi.org/10.1371/journal.pone.0010186>.

- [23] X. Wang, X. Jiang, S. Sun, Y. Liu, Synthesis and biological evaluation of novel quinolone derivatives dual targeting histone deacetylase and tubulin polymerization as antiproliferative agents, *RSC Adv.* 8 (2018) 16494–16502. <https://doi.org/10.1039/C8RA02578A>.
- [24] A.P. Saraswati, N. Relitti, M. Brindisi, J.D. Osko, G. Chemi, S. Federico, A. Grillo, S. Brogi, N.H. McCabe, R.C. Turkington, O. Ibrahim, J. O’Sullivan, S. Lamponi, M. Ghanim, V.P. Kelly, D. Zisterer, R. Amet, P. Hannon, F. Vanni, C. Ulivieri, D. Herp, F. Sarno, A. Di Costanzo, F. Saccoccia, G. Ruberti, M. Jung, L. Altucci, S. Gemma, S. Butini, D.W. Christianson, G. Campiani, Spiroindoline-Capped Selective HDAC6 Inhibitors: Design, Synthesis, Structural Analysis and Biological Evaluation, *ACS Med. Chem. Lett.* (2020) Just Accepted. <https://doi.org/10.1021/acsmchemlett.0c00395>.
- [25] Y. Tangella, K.L. Manasa, N.H. Krishna, B. Sridhar, A. Kamal, B. Nagendra Babu, Regioselective Ring Expansion of Isatins with in Situ Generated α -Aryldiazomethanes: Direct Access to Viridicatin Alkaloids, *Org. Lett.* 20 (2018) 3639–3642. <https://doi.org/10.1021/acs.orglett.8b01417>.
- [26] M.D. Greenhalgh, S.M. Smith, D.M. Walden, J.E. Taylor, Z. Brice, E.R.T. Robinson, C. Fallan, D.B. Cordes, A.M.Z. Slawin, H.C. Richardson, M.A. Grove, P.H.-Y. Cheong, A.D. Smith, A C=O \cdots Isothiuronium Interaction Dictates Enantiodiscrimination in Acylative Kinetic Resolutions of Tertiary Heterocyclic Alcohols, *Angew. Chemie Int. Ed.* 57 (2018) 3200–3206. <https://doi.org/10.1002/anie.201712456>.
- [27] Z. Liu, Q. Lin, Q. Huang, H. Liu, C. Bao, W. Zhang, X. Zhong, L. Zhu, Semiconductor quantum dots photosensitizing release of anticancer drug, *Chem. Commun.* 47 (2011) 1482–1484. <https://doi.org/10.1039/C0CC04676K>.
- [28] L. Spear, Kerry, U. Campbell, *Heterocyclic Compounds and Methods of Use Thereof*, 2014.
- [29] A.H. Boulares, A.G. Yakovlev, V. Ivanova, B.A. Stoica, G. Wang, S. Iyer, M. Smulson, Role of Poly(ADP-ribose) Polymerase (PARP) Cleavage in Apoptosis: Caspase 3-Resistant PARP Mutant Increases Rates of Apoptosis in Transfected Cells, *J. Biol. Chem.* 274 (1999) 22932–22940. <https://doi.org/10.1074/jbc.274.33.22932>.
- [30] J.J. Kovacs, P.J.M. Murphy, S. Gaillard, X. Zhao, J.-T. Wu, C. V Nicchitta, M. Yoshida, D.O. Toft, W.B. Pratt, T.-P. Yao, HDAC6 Regulates Hsp90 Acetylation and Chaperone-Dependent Activation of Glucocorticoid Receptor, *Mol. Cell.* 18 (2005) 601–607. <https://doi.org/https://doi.org/10.1016/j.molcel.2005.04.021>.
- [31] S. Gemma, C. Camodeca, M. Brindisi, S. Brogi, G. Kukreja, S. Kunjir, E. Gabellieri, L. Lucantoni, A. Habluetzel, D. Taramelli, N. Basilico, R. Gualdani, F. Tadini-Buoninsegni, G. Bartolommei, M.R. Moncelli, R.E. Martin, R.L. Summers, S. Lamponi, L. Savini, I. Fiorini, M. Valoti, E. Novellino, G. Campiani, S. Butini, Mimicking the Intramolecular Hydrogen Bond: Synthesis, Biological Evaluation, and Molecular Modeling of Benzoxazines and Quinazolines as Potential Antimalarial

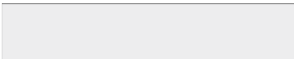
- Agents, *J. Med. Chem.* 55 (2012) 10387–10404. <https://doi.org/10.1021/jm300831b>.
- [32] A. Grillo, G. Chemi, S. Brogi, M. Brindisi, N. Relitti, F. Fezza, D. Fazio, L. Castelletti, E. Perdona, A. Wong, S. Lamponi, A. Pecorelli, M. Benedusi, M. Fantacci, M. Valoti, G. Valacchi, F. Micheli, E. Novellino, G. Campiani, S. Butini, M. Maccarrone, S. Gemma, Development of novel multipotent compounds modulating endocannabinoid and dopaminergic systems, *Eur. J. Med. Chem.* 183 (2019) 111674. <https://doi.org/10.1016/j.ejmech.2019.111674>.
- [33] P.L. Skipper, S.R. Tannenbaum, W.G. Thilly, E.E. Furth, W.W. Bishop, Mutagenicity of Hydroxamic Acids and the Probable Involvement of Carbamoylation, *Cancer Res.* 40 (1980) 4704 LP – 4708. <http://cancerres.aacrjournals.org/content/40/12/4704.abstract>.
- [34] S. Shen, A.P. Kozikowski, Why Hydroxamates May Not Be the Best Histone Deacetylase Inhibitors—What Some May Have Forgotten or Would Rather Forget?, *ChemMedChem.* 11 (2016) 15–21. <https://doi.org/10.1002/cmdc.201500486>.
- [35] M.S. Lee, M. Isobe, Metabolic Activation of the Potent Mutagen, 2-Naphthohydroxamic Acid, in *Salmonella typhimurium* TA98, *Cancer Res.* 50 (1990) 4300–4307.
- [36] L. Jašíková, E. Hanikýřová, A. Škríba, J. Jašík, J. Roithová, Metal-assisted lossen rearrangement, *J. Org. Chem.* 77 (2012) 2829–2836. <https://doi.org/10.1021/jo300031f>.
- [37] V. Hoffmann, N. Jenny, D. Häussinger, M. Neuburger, M. Mayor, Rotationally Restricted 1,1'-Bis-(phenylethynyl)ferrocene Subunits in Macrocycles, *European J. Org. Chem.* 2016 (2016) 2187–2199. <https://doi.org/10.1002/ejoc.201600158>.
- [38] C.J. Millard, P.J. Watson, I. Celardo, Y. Gordiyenko, S.M. Cowley, C.V. Robinson, L. Fairall, J.W.R. Schwabe, Class I HDACs Share a Common Mechanism of Regulation by Inositol Phosphates, *Mol. Cell.* 51 (2013) 57–67. <https://doi.org/https://doi.org/10.1016/j.molcel.2013.05.020>.
- [39] W.C. Still, A. Tempezyk, R.C. Hawley, T. Hendrickson, Semianalytical treatment of solvation for molecular mechanics and dynamics, *J. Am. Chem. Soc.* 112 (1990) 6127–6129. <https://doi.org/10.1021/ja00172a038>.
- [40] A. Vallone, S. D'Alessandro, S. Brogi, M. Brindisi, G. Chemi, G. Alfano, S. Lamponi, S.G. Lee, J.M. Jez, K.J.M. Koolen, K.J. Dechering, S. Saponara, F. Fusi, B. Gorelli, D. Taramelli, S. Parapini, R. Caldelari, G. Campiani, S. Gemma, S. Butini, Antimalarial agents against both sexual and asexual parasites stages: structure-activity relationships and biological studies of the Malaria Box compound 1-[5-(4-bromo-2-chlorophenyl)furan-2-yl]-N-[(piperidin-4-yl)methyl]methanamine (MMV019918) and analog, *Eur. J. Med. Chem.* 150 (2018) 698–718. <https://doi.org/https://doi.org/10.1016/j.ejmech.2018.03.024>.
- [41] S. Brogi, A. Ramunno, L. Savi, G. Chemi, G. Alfano, A. Pecorelli, E. Pambianchi, P. Galatello, G. Compagnoni, F. Foche, G. Biamonti, G. Valacchi, S. Butini, S. Gemma, G. Campiani, M. Brindisi, First dual AK/GSK-3 β inhibitors endowed with antioxidant properties as multifunctional, potential neuroprotective agents, *Eur. J. Med. Chem.* 138 (2017) 438–457. <https://doi.org/https://doi.org/10.1016/j.ejmech.2017.06.017>.

- [42] B. Heltweg, F. Dequiedt, E. Verdin, M. Jung, Nonisotopic substrate for assaying both human zinc and NAD⁺-dependent histone deacetylases, *Anal. Biochem.* 319 (2003) 42–48. [https://doi.org/https://doi.org/10.1016/S0003-2697\(03\)00276-8](https://doi.org/https://doi.org/10.1016/S0003-2697(03)00276-8).
- [43] D. Wegener, F. Wirsching, D. Riester, A. Schwienhorst, A Fluorogenic Histone Deacetylase Assay Well Suited for High-Throughput Activity Screening, *Chem. Biol.* 10 (2003) 61–68. [https://doi.org/https://doi.org/10.1016/S1074-5521\(02\)00305-8](https://doi.org/https://doi.org/10.1016/S1074-5521(02)00305-8).
- [44] B. Heltweg, J. Trapp, M. Jung, In vitro assays for the determination of histone deacetylase activity, *Methods.* 36 (2005) 332–337. <https://doi.org/https://doi.org/10.1016/j.ymeth.2005.03.003>.
- [45] R.A. Copeland, *Reversible Inhibitors*, 2000. <https://doi.org/doi:10.1002/0471220639.ch8>.
- [46] D. Purves, C. Harvey, D. Tweats, C.E. Lumley, Genotoxicity testing: current practices and strategies used by the pharmaceutical industry, *Mutagenesis.* 10 (1995) 297–312. <https://doi.org/10.1093/mutage/10.4.297>.
- [47] T.J. Makhafola, E.E. Elgorashi, L.J. McGaw, L. Verschaeve, J.N. Eloff, The correlation between antimutagenic activity and total phenolic content of extracts of 31 plant species with high antioxidant activity, *BMC Complement. Altern. Med.* 16 (2016) 490. <https://doi.org/10.1186/s12906-016-1437-x>.



Click here to access/download

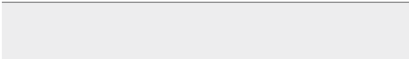
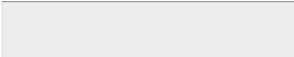
Supplementary Material - For Publication Online
Supplementary material_Viridicatin.docx





Click here to access/download

Supplementary Material - For Review Purposes Only
Supplementary material_Viridicatin Tracked.docx



Declaration of interests

The authors declare that they have no known competing financial interests or personal relationships that could have appeared to influence the work reported in this paper.

The authors declare the following financial interests/personal relationships which may be considered as potential competing interests:

Novel quinolone-based potent and selective HDAC6 inhibitors: synthesis, molecular modelling studies and biological investigation

Nicola Relitti ^{a,1}, A. Prasanth Saraswati ^{a,1}, Giulia Chemi ^{a,2}, Margherita Brindisi ^{a,3}, Simone Brogi ^b, Daniel Herp ^c, Karin Schmidtkunz ^c, Fulvio Saccoccia ^d, Giovina Ruberti ^d, Cristina Ulivieri ^e, Francesca Vanni ^e, Federica Sarno^f, Lucia Altucci^f, Stefania Lamponi ^a, Manfred Jung ^c, Sandra Gemma ^a, Stefania Butini ^a, Giuseppe Campiani ^{a,*}

^a *Department of Biotechnology, Chemistry and Pharmacy, DoE Department of Excellence 2018-2022, University of Siena, via Aldo Moro 2, 53100, Siena, Italy*

^b *Department of Pharmacy, University of Pisa, via Bonanno 6, 56126, Pisa, Italy*

^c *Institute of Pharmaceutical Sciences, Albert-Ludwigs-Universität Freiburg, Albertstraße 25, 79104, Freiburg, Germany*

^d *Institute of Biochemistry and Cell Biology, CNR, Campus A. Buzzati-Traverso. Via E. Ramarini 32, 00015 Monterotondo (Rome) Italy*

^e *Department of Life Sciences, University of Siena, via Aldo Moro 2, 53100, Siena, Italy*

^f *Department of Precision Medicine, University of Campania Luigi Vanvitelli, Vico L. de Crecchio 7, 80138, Naples, Italy*

Corresponding author.

E-mail address: campiani@unisi.it (G. Campiani)

¹ These authors equally contributed.

² Present address: Wellcome Centre for Anti-Infectives Research, Drug Discovery Unit, Division of Biological Chemistry and Drug Discovery, University of Dundee, DD1 5EH Dundee, United Kingdom

³ Present address: Department of Pharmacy, University of Napoli Federico II, DoE Department of Excellence 2018-2022, Via D. Montesano 49, 80131, Napoli, Italy

Abstract

In this work we describe the synthesis of potent and selective quinolone-based histone deacetylase 6 (HDAC6) inhibitors. The quinolone moiety has been exploited as an innovative bioactive cap-group for HDAC6 inhibition; its synthesis was achieved by applying a multicomponent reaction. The optimization of potency and selectivity of these products was performed by employing computational studies which led to the discovery of the diethylaminomethyl derivatives **7g** and **7k** as the most promising hit molecules. These compounds were investigated in cellular studies to evaluate their anticancer effect against colon (HCT-116) and histiocytic lymphoma (U937) cancer cells, showing good to excellent potency, leading to tumor cell death by apoptosis induction. The small molecules **7a**, **7g** and **7k** were able to strongly inhibit the cytoplasmic and slightly the nuclear HDAC enzymes, increasing the acetylation of tubulin and of the lysine 9 and 14 of histone 3, respectively. Compound **7g** was also able to increase Hsp90 acetylation levels in HCT-116 cells, thus further supporting its HDAC6 inhibitory profile. Cytotoxicity and mutagenicity assays of

these molecules showed a safe profile; moreover, the HPLC analysis of compound **7k** revealed good solubility and stability profile.

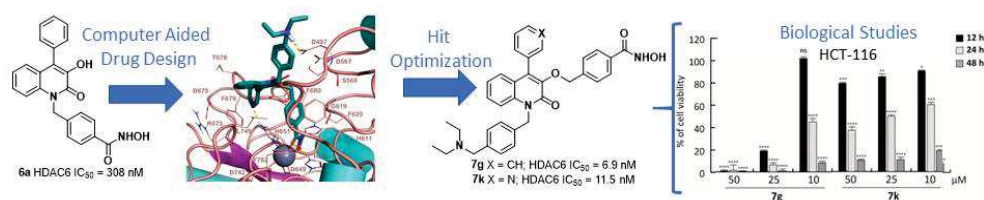
Keywords

HDAC6 inhibitors, HDAC, quinolone synthesis, cancer, structure-activity relationships, molecular modeling

Highlights

- Rational design and synthesis of novel quinolone-based selective HDAC6 inhibitors
- Compounds **7g** and **7k** were the most potent compounds against HDAC6
- These compounds possess a good selectivity towards HDAC6 over the 1 and 8 isoforms
- Compound **7g** showed a strong reduction in cell viability against HCT-116 cells
- Induction of apoptosis was observed after the treatment with **7g** and **7k**

Graphical abstract



Abbreviations

AcHsp90 (AcLys294), acetylated Hsp90 in lysine 294; AcTub, acetylated α -tubulin; DCM, dichloromethane; DIBAL, diisobutylaluminum hydride; DMF, dimethylformamide; DMSO, dimethyl sulfoxide; H3K9/14ac, acetylated histone H3 in lysine 9 and 14; HCT-116, colon cancer cells; HDAC, histone deacetylase; HDACi, HDAC inhibitors; Hsp90, heat-shock protein 90; PARP, Poly(ADP-ribose) polymerase; PTSA, *p*-toluenesulfonic acid; PTSH, *p*-toluenesulfonyl hydrazide; SAR, structure-activity relationship; SP, standard precision; TFA, trifluoroacetic acid; THF, tetrahydrofuran; U937, histiocytic lymphoma; ZBG, zinc binding group.

1. Introduction

Histone deacetylases (HDACs) are enzymes involved in the removal of acetyl groups from histones, thus modulating gene transcription. Their over-expression has been ascertained in solid cancers, hematological malignancies, and parasitic disorders, making them a viable target for developing novel chemotherapeutic agents [1,2], as well as in rare diseases [3]. Of the 18 identified HDAC isoforms (subdivided into 4 classes, I-IV), HDAC6 is unique owing to the presence of a zinc finger ubiquitin binding domain and its localization. Structurally, it contains two catalytic domains, DD1 and DD2, present at the *N*-terminal and the central region, respectively. With regard to its localization, HDAC6 is a cytoplasmic enzyme (unlike HDAC1, 2 and 3, that are nuclear localized and HDAC8, that can show both nuclear and cytoplasmic spreading) which can shuttle between cytoplasm and the nucleus in response to cellular signaling [4]. Apart from its action on

histones it also exerts deacetylase activity on non-histone substrates such as α -tubulin, heat-shock protein 90 (Hsp90), peroxiredoxin, cortactin, and tau [3]. This specific feature of HDAC6 is responsible for its unique role in the pathogenesis of cancer and a number of rare diseases such as idiopathic pulmonary fibrosis, inherited retinal disorders, Rett syndrome, and Charcot-Marie-Tooth disease [3,5]. Comparatively, HDAC10 that has a closer structural correlation with HDAC6 has a very weak activity as a lysine deacetylase and its role has so far been described mostly for autophagy promotion [6].

Several HDAC inhibitors (HDACi) have successfully reached the clinic and are being used as therapeutic tools to treat different malignancies. Representative HDACi include: vorinostat (**1**, SAHA, 1) [7] and romidepsin (**2**) [8] for the treatment of cutaneous T-cell lymphomas, panobinostat (**3**) [9] for multiple myeloma, and belinostat (**4**) [10] for relapsed or refractory peripheral T-cell lymphoma. These compounds behave as pan-HDACi since they inhibit several HDAC isoforms, thus causing many side effects. The discovery of Tubastatin A (**5**) a tetrahydropyrido[4,3-*b*]indole hydroxamic acid, as a selective HDAC6i has paved the way for the development of isoform-selective HDACi. However, a potent inhibition of HDAC10 isoform has been reported after exposure with **5** [11–13]. Identification of isoform-selective compounds is vital for dissecting the biological roles of specific HDACs and for developing safer therapeutic tools. The general pharmacophoric model of HDACi encompasses three key components namely: the surface recognition group (cap), the zinc binding group (ZBG) and a linker bridging the two portions. Based on this model several selective HDAC6 inhibitors have been developed mainly by modifying the cap and the linker portions, while retaining hydroxamate as the ZBG [2,14,15].

Many natural products have been identified possessing potent anticancer properties, which have inspired chemists to use them as building blocks in the synthesis of novel chemotherapeutics [16–19]. In this context, functionalized 4-arylquinolin-2(1*H*)-ones represent an attractive scaffold for developing biologically active molecules, including the orally active anticancer agent tipifarnib, that is currently undergoing clinical investigation [20].

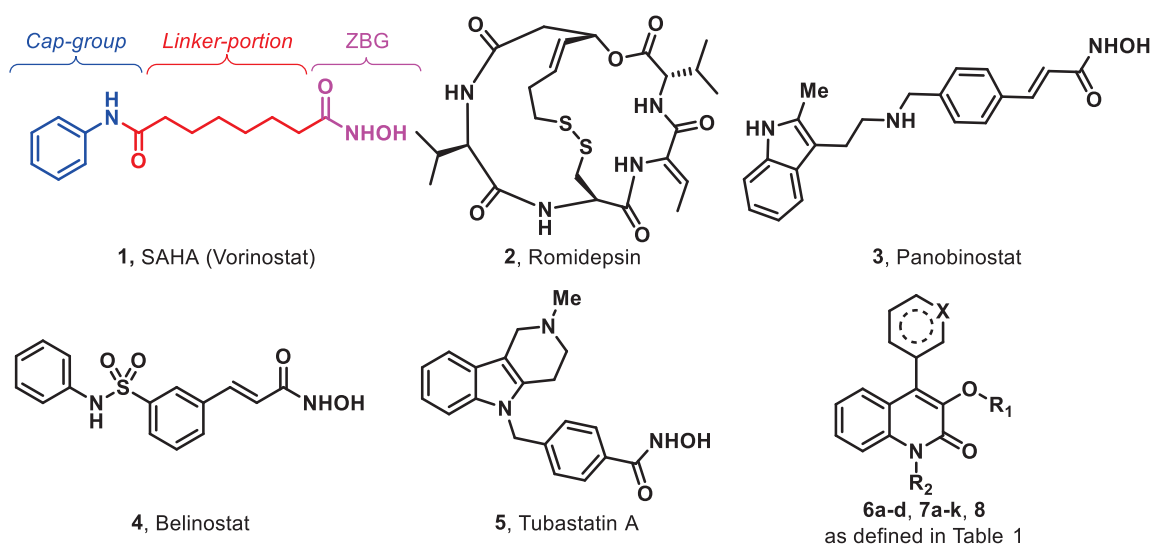


Figure 1. Representative structures of HDAC inhibitors (**1-5**) and general structure of the title compounds **6-8**.

In our pursuit to identify novel cap groups for potent and selective HDAC6i [14,15,24], we exploited the potential of a naturally occurring compound containing the quinolone skeleton as an effective versatile and hindered cap-group suitable for a broad variety of scaffold decorations (as shown in the general structure of Figure 1). By a virtual screening approach, we identified several cap-groups; a preliminary computational investigation, using compound **6a**, characterized by a viridicatin-based cap-group, showed that it perfectly fits into the hydrophobic sub-pocket delimited by L712 and F642 (*Danio rerio* HDAC6 numbering, corresponding to residues L749 and F679 in *h*HDAC6). Moreover, by our computational approach, we observed that the cap-group of Tubastatin A and **6a** into *z*/HDAC6 (PDB ID: 6THV) target the same region of the enzyme as highlighted in Figure 2. Therefore, we selected this interesting quinolone-based cap-group to rationally design and synthesize a new focused library of HDAC6 selective inhibitors as described below. According to our preliminary *in silico* analysis and aiming at obtaining compounds with high selectivity index towards HDAC6 (over HDAC1) to be screened against different cancer cell lines we synthesized a library of quinolone-based hydroxamates. The synthesis of the 3-hydroxy-4-arylquinolin-2(1*H*)-ones moiety was carried out by the application of a multicomponent ring-expansion recently reported by Tangella *et al.* This protocol permits the conversion of isatin to viridicatin alkaloids after the *in situ* generation of α -aryldiazomethanes in presence of an aldehyde [25]. This protocol enabled us to develop novel HDAC6i (compounds **6a-d**, **7a-k** and **8**, Table 1) bearing *N*- or *O*-appended linker moieties, and a variety of focused modifications at both their heterocyclic core and the aromatic portions.

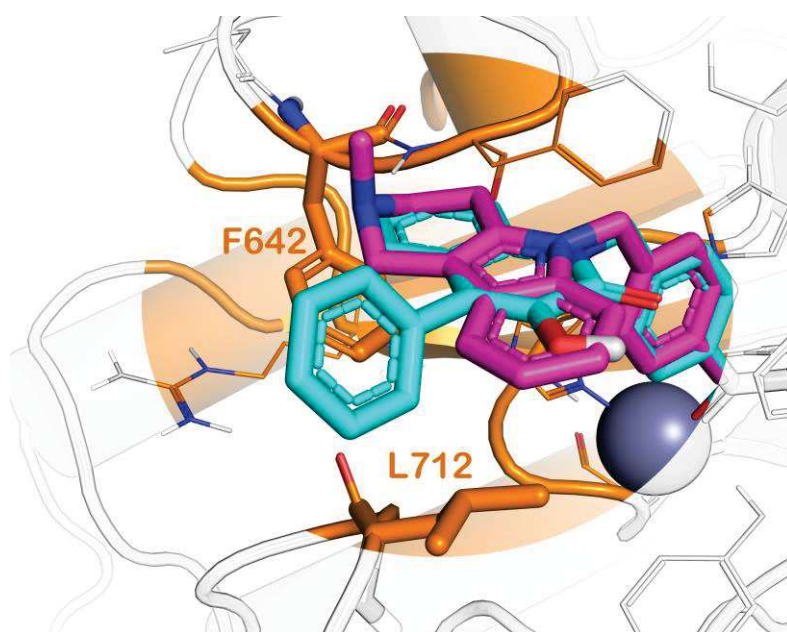
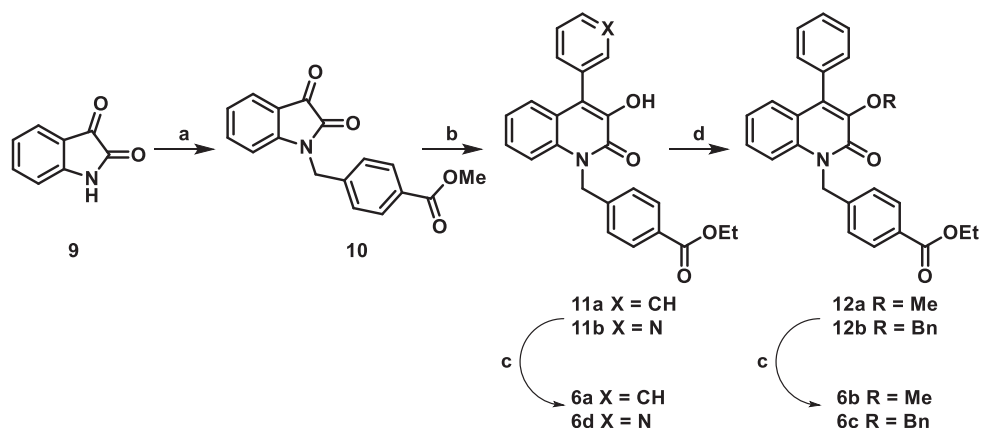


Figure 2. Docked pose of **6a** into *z*/HDAC6 (PDB ID: 6THV), superposed to the crystallized inhibitor Tubastatin A belonging to 6THV. Focus on residues in sticks that are the constituents of the hydrophobic sub-pocket explored by the viridicatin cap-group (residues L712 and F642 in *z*/HDAC6 correspond to L749 and F679 in *h*HDAC6) is presented. The picture was generated by means of PyMOL.

2. Chemistry

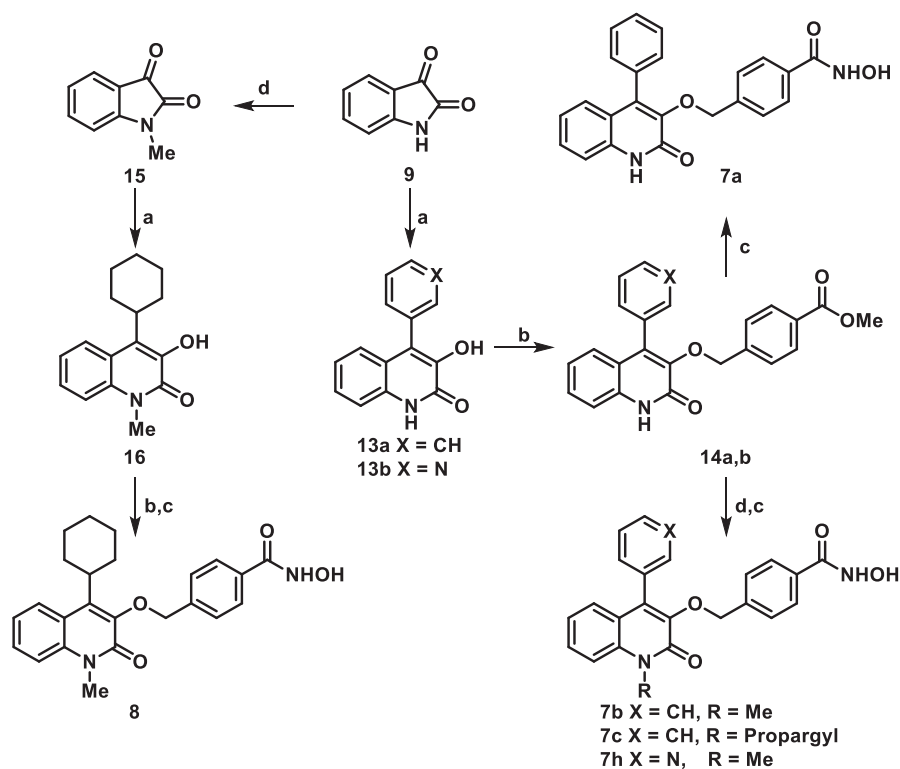
The structures of final compounds **6a-d**, **7a-k** and **8** are shown in Table 1. In order to achieve the synthesis of the quinolone core of the compounds, the ring expansion procedure described by Tangella *et al* was applied [25]. It is a multicomponent reaction involving: an aldehyde, activated with *p*-toluenesulfonyl hydrazide (PTSH), and a *N*-substituted isatin in the presence of K_2CO_3 as base.

In Scheme 1 the synthesis of the final compounds **6a-d** is described. Isatin (**9**) was alkylated with methyl 4-(bromomethyl)benzoate and the resulting product **10** was subjected to the ring expansion procedure with benzaldehyde or 3-pyridinecarboxaldehyde obtaining compounds **11a,b**, respectively. As expected, a transesterification with EtOH occurred in this step. Intermediates **11a,b** were converted to their corresponding hydroxamic acid derivatives **6a,d** after treatment with a strong excess of aqueous NH_2OH in the presence of KOH. Intermediate **11a** was also submitted to *O*-alkylation with MeI or benzyl bromide providing derivatives **12a,b**, respectively. These latter were converted into final compounds **6b,c** upon reaction with NH_2OH and KOH.



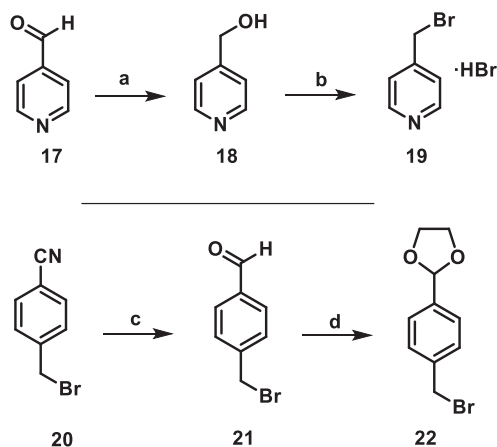
Scheme 1. Synthesis of compounds 6a-d. Reagents and conditions: (a) methyl 4-(bromomethyl)benzoate, NaH, DMF, 0 to 25 °C, 12 h, quantitative yield; (b) PTSH, benzaldehyde or 3-pyridinecarboxaldehyde, K_2CO_3 , EtOH, 80 °C, 12 h, 32-64%; (c) NH_2OH (50% water solution), KOH, DCM, MeOH, 25 °C, 3 h, 82-97%; (d) MeI, NaH, THF, 0 to 25 °C, 12 h; or BnBr, KI, K_2CO_3 , DMF, 80 °C, 12 h, 29-64%.

In Scheme 2 is reported the synthesis of compounds **7a-c,h** and **8**. The ring expansion performed on isatin (**9**) in the presence of benzaldehyde or 3-pyridinecarboxaldehyde provided quinolone derivatives **13a,b**, respectively. These latter were subjected to alkylation reaction with methyl 4-(bromomethyl)benzoate in the presence of K_2CO_3 as the base to furnish the *O*-alkylated intermediates **14a,b**. Treatment of **14a** with NH_2OH in the presence of KOH led to compound **7a**. Alternatively, alkylation of the lactam nitrogen of **14a,b** with MeI or propargyl bromide followed by reaction with NH_2OH , led to the *N*-alkyl derivatives **7b,c,h** [26]. For the synthesis of compound **8**, isatin was alkylated with MeI and successively subjected to the ring expansion reaction with cyclohexanecarboxaldehyde obtaining compound **16**. From this intermediate, compound **8** was obtained as previously described.



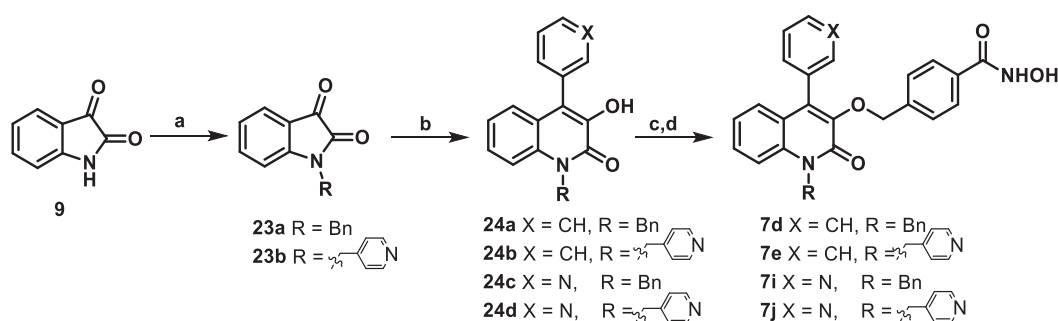
Scheme 2. Synthesis of compounds 7a-c,h and 8. Reagents and conditions: (a) PTSH, benzaldehyde or 3-pyridinecarboxaldehyde or cyclohexanecarboxaldehyde, K_2CO_3 , EtOH, 80 °C, 12 h, 30-45%; (b) methyl 4-(bromomethyl)benzoate, K_2CO_3 , KI, DMF, 80 °C, 12 h, 20-74%; (c) NH_2OH , KOH, DCM, MeOH, H_2O , 25 °C, 3 h, 50-98%; (d) MeI/ propargyl bromide, NaH, THF, 0 to 25 °C, 12 h, 56% to quantitative yield.

In Scheme 3 is reported the synthesis of bromides **19** and **22** used as alkylating agents for the synthesis of final compounds **7e**, **7g** and **7k**. Following the procedure described by Liu et al. 4-pyridinecarboxaldehyde (**17**) was reduced to alcohol **18** with $NaBH_4$ and then converted to the corresponding bromide **19** after treatment with PBr_3 [27]. For the synthesis of the intermediate **22**, 4-(bromomethyl)benzonitrile (**20**) was reduced with DIBAL to the corresponding benzaldehyde **21**, that was successively converted to dioxolane **22** with ethylene glycol in the presence of PTSA [28].



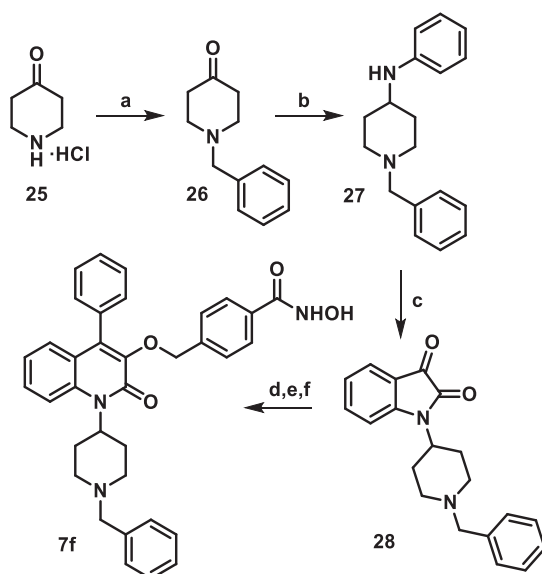
Scheme 3. Synthesis of bromo-derivatives 19 and 22. Reagents and conditions: (a) NaBH₄, MeOH, 0 to 25 to 25 °C, 2 h, 80%; (b) 48% HBr, 100 °C, 4 h then PBr₃, DCM, 45 °C, 4 h, 93%; (c) DIBAL, DCM, -78 to 0 °C, 1 h, quantitative yield; (d) ethylene glycol, PTSA, toluene, 110 °C, 12 h, 69%.

In Scheme 4 the synthesis of final compounds **7d,e,i,j** is described. Isatin was alkylated with benzyl bromide or bromide **19** using NaH as the base to generate intermediates **23a,b** [26]. These compounds were subjected to the previously described ring expansion procedure with benzaldehyde or 3-pyridinecarboxaldehyde to provide the desired 2-quinolones **24a-d** that were converted to the final compounds **7d,e,i,j** in the presence of NH₂OH.



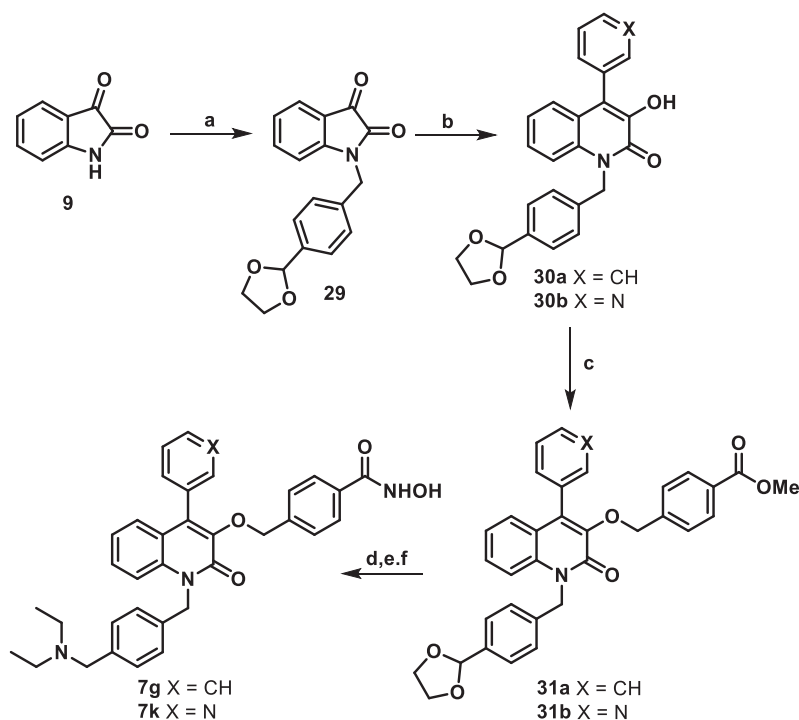
Scheme 4. Synthesis of compounds 7d,e,i,j. Reagents and conditions: (a) BnBr or **19**, NaH, DMF, 0 to 25 °C, 12 h, 38-74%; (b) PTSH, benzaldehyde or 3-pyridinecarboxaldehyde, K₂CO₃, EtOH, 80 °C, 12 h, 24-44%; (c) methyl 4-(bromomethyl)benzoate, K₂CO₃, KI, DMF, 80 °C, 12 h, 62-30%; (d) NH₂OH, KOH, DCM, MeOH, H₂O, 25 °C, 3 h, 45-90%.

The synthesis of compound **7f** is described in Scheme 5. Since alkylation of the isatin with 1-benzyl-4-bromo or iodopiperidine failed in all the attempted conditions, *N*-alkylated isatin **28** was prepared starting from piperidone (**25**) following a procedure described in a patent by Spear et al. [28]. **25** was first *N*-benzylated and then subjected to a reductive amination protocol with aniline in presence of NaBH(OAc)₃ providing intermediate **27**. This compound was treated with oxalyl chloride, obtaining an unstable intermediate that was immediately treated with AlCl₃ in DCM to afford isatin derivative **28** under Friedel-Craft conditions. Ring expansion, alkylation, and final reaction with NH₂OH were then performed as previously described, leading to the formation of compound **7f**.



Scheme 5. Synthesis of compound 7f. Reagents and Conditions: (a) Benzyl bromide, K_2CO_3 , DMF, 80 °C, 12 h, 70%; (b) aniline, $NaBH(OAc)_3$, DCM, AcOH, 0 to 25 °C, 12 h, 89%; (c) oxalyl chloride, DCM, 25 °C, 2 h; then $AlCl_3$, DCM, 40 °C, 2 h, 52%; (d) PTSH, benzaldehyde, K_2CO_3 , EtOH, 80 °C, 12 h, 55%; (e) methyl 4-(bromomethyl)benzoate, K_2CO_3 , KI, DMF, 80 °C, 12 h, 15%; (f) NH_2OH , KOH, DCM, MeOH, H_2O , 25 °C, 3 h, 62%.

In Scheme 6 the synthesis of the final compounds **7g,k** is described. Isatin was alkylated with bromide **22** affording intermediate **29**. This compound was subjected to the previously described ring expansion procedure to get the desired quinolones **30a,b**. These intermediates were alkylated with methyl 4-(bromomethyl)benzoate obtaining **31a,b** which were subsequently deprotected in acidic medium, and the corresponding free aldehydes were subjected to a reductive amination protocol with diethylamine in the presence $NaBH(OAc)_3$, affording the corresponding diethylamino derivatives, that were converted to the final compounds **7g,k** as previously described.



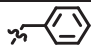
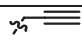
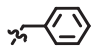
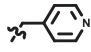
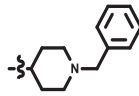
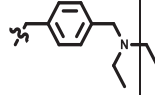
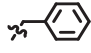
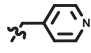
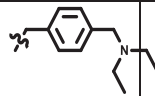
Scheme 6. Synthesis of compounds 7g,k. Reagents and conditions: (a) **22**, NaH, DMF, 0 to 25 °C, 12 h, quantitative yield; (b) PTSH, benzaldehyde or 3-pyridinecarboxaldehyde, K₂CO₃, EtOH, 80 °C, 12 h, 48%; (c) methyl 4-(bromomethyl)benzoate, K₂CO₃, KI, DMF, 80 °C, 12 h, 55-80%; (d) 6 N HCl, THF, 25 °C, 1 h, quantitative yield; (e) diethylamine, NaBH(OAc)₃, DCM, AcOH, 0 to 25 °C, 12 h, 47-59%; (f) NH₂OH, KOH, DCM, MeOH, H₂O, 25 °C, 3 h, 74-80%.

3. Results and Discussion

The compounds herein developed were firstly tested in enzymatic assay to evaluate their HDAC6 inhibitory profile compared with the HDAC1 and 8 isoforms. Successively, the ability of the best performing compounds to induce the acetylation of histone, tubulin and HSP90 was evaluated, followed by assessment of their anticancer properties in two cell lines (HCT-116 and U937). We have also determined key pharmacokinetic parameters (solubility and chemical stability), toxicity and mutagenicity of selected compounds.

Table 1. Novel HDAC6 inhibitors **6a-d**, **7a-k** and **8** against *h*HDAC1, as IC₅₀ (μM), and *h*HDAC6, as IC₅₀ (nM).^a

| Cpd | R | X | HDAC1 IC ₅₀ | HDAC6 IC ₅₀ | HDAC6/HDAC1 |
|------|---|---|------------------------|------------------------|-------------|
| 6a-d | | | | | |
| 7a-k | R | | | | |
| 8 | | | | | |

| | | | (μM) | (nM) | |
|----|---|----|---------------------------------------|------------------|------|
| 6a | H | CH | 11 ± 1 | 308 ± 51 | 3.6 |
| 6b | Me | CH | 4.5 ± 0.31 | 61.6 ± 7.5 | 73 |
| 6c |  | CH | 5.5 ± 0.3 | 84.5 ± 7.9 | 65 |
| 6d | H | N | 50 96% 25 82% 10 36% 1 < 10% | 295.6 ± 24.4 | n.d. |
| 7a | H | CH | 6.6 ± 0.4 | 146.9 ± 14.2 | 45 |
| 7b | Me | CH | 50 80% 25 46% 10 26% 1 < 10% | 518.9 ± 17.1 | n.d. |
| 7c |  | CH | 6.1 ± 0.9 | 82.3 ± 11.4 | 74 |
| 7d |  | CH | 50 97% 25 93% 10 76% 1 17% | 176.0 ± 14.7 | n.d. |
| 7e |  | CH | 1.2 ± 0.2 | 84.1 ± 9.9 | 14 |
| 7f |  | CH | 50 79% 25 67% 10 46% 1 < 10% | 870.4 ± 87.8 | n.d. |
| 7g |  | CH | 0.322 ± 0.073 | 6.9 ± 0.9 | 46 |
| 7h | Me | N | 5.01 ± 0.44 | 46 ± 5 | 109 |
| 7i |  | N | 2.5 ± 0.41 | 25.6 ± 3.1 | 96 |
| 7j |  | N | 1.7 ± 0.31 | 45.3 ± 5.6 | 38 |
| 7k |  | N | 0.319 ± 0.08 | 11.5 ± 1.5 | 29 |
| 8 | - | - | 3.0 ± 0.18 | 33.0 ± 2.6 | 91 |

^aEach value is the mean of at least three determinations; compounds were assayed at eight concentrations; results are expressed with SD.

3.1. Structure-activity relationships (SAR)

From the enzymatic assay emerged a significant affinity of the molecules for the HDAC6 with selectivity over HDAC1 and 8 isoforms (Tables 1 and 2). Starting from compound **6a** (HDAC6 IC₅₀ = 308 nM) we decided to explore the effect of the introduction of alkyl groups such as methyl or benzyl substituent on the oxygen at C3 (**6b,c**). These modifications led to a significant improvement in both the HDAC6 inhibition potency (HDAC6 IC₅₀ of 61 and 84 nM, for **6b** and **6c** respectively) and the selectivity over HDAC1 isoform. Successively we decided to explore the effect of replacing the 4-phenyl group with a more basic 3-pyridyl group (compound **6d**); this modification did not improve potency and led to a HDAC6 inhibition (295 nM) similar to **6a**. We then decided to interrogate the outcome of a switch of the acidic ZBG from the N1 to the oxygen atom at C3; thus, we developed a series of analogues typified by **7a**. This new prototypic compound led to improved potency at HDAC6 over **6a** (**7a** HDAC6 IC₅₀ = 147 nM). Following exploration of several substituents at N1 generated compounds **7b-g**. This focused series of derivatives demonstrated that the introduction of a basic lateral chain such as 4-pyridyl (**7e**) or *N,N*-diethylaminomethylbenzyl (**7g**) determined a strong increase in HDAC6 inhibition (**7e,g** HDAC6 IC₅₀ equal to 84 and 7 nM, respectively). Also, it was shown that the introduction of large and/or alkyl substituents generated analogues with weaker potency against HDAC6 (**7b-d,f** IC₅₀ ranging from 82 to 870 nM). The substitution of the phenyl ring at C4 with a 3-pyridyl group (compounds **7h-k**) resulted in a general increase of HDAC6 inhibition, when compared to **7a**, with IC₅₀ values ranging from 12 to 46 nM. As observed for **7g**, also compound **7k**, bearing a *N,N*-diethylaminomethylbenzyl at N1, showed the highest potency of this subgroup of analogues. From **7a**, the introduction of a methyl group at N1 and the replacement of the phenyl group at C4 with a cyclohexyl group led to compound **8**. This compound showed a good inhibitory profile for HDAC6 together with a significant selectivity over HDAC1 (IC₅₀ = 33 nM and selectivity index of 91).

In order to gain a full picture in terms of SAR analysis for the new series of compounds, we flanked *in vitro* data with computational studies. Starting from the molecular docking calculations using Glide employing Standard Precision (SP) as scoring function and visual inspection we were able to understand the general trend of the preferred binding modes of quinolone derivatives on HDAC1 and HDAC6 isoforms (for more details see the appropriate sections in the supplementary material file). Keeping on with the already described inhibitors, for our newly developed derivatives we retained the *para*-substituted phenylhydroxamic acid functionality, anchored to the benzyl linker, as the ZBG. Among the derivatives the polar contacts established by the hydroxamic acid of the ZBG were similar and represented by three H-bonds established between the carbonyl and Y782, the NH and G619, the OH and H610. Considering the specific contacts, we primarily focused our attention to the best positioning of the ZBG on the quinolone scaffold (heterocyclic nitrogen vs exocyclic hydroxyl group). Merging the results of the docking studies and the enzymatic tests we observed that: when the ZBG is placed on the nitrogen atom as for compounds **6a-d** the activity on HDAC6 slightly decreases when compared to the substitution on the oxygen atom (3-OH) (i.e. compounds **7a-k** and **8**). The binding mode of compounds is depicted in Figures 3 and Figures S1, S3. The whole orientation of the scaffolds of compound **6a,b** (Figures 3A,B), presented a similar binding mode, differing from that of the other analogues as represented in Figures 3C-F and Figures S1-S3 (see details in the Supplementary Material

sections). Compound **7a** (Figure 3C), with no substituents on *N1*, was able to establish two π - π stackings with F620, F680 through the phenyl ring of the ZBG, and an additional H-bond between H651 and the carbonyl of the quinolone core. The binding mode of compounds **7b-d,h,i,j** is discussed in the Supplementary Material section.

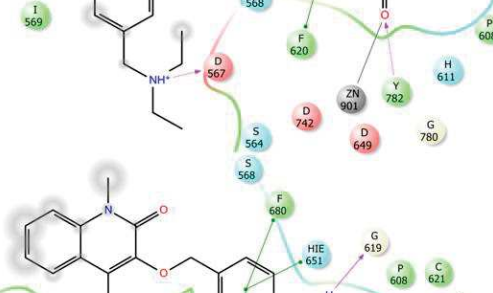
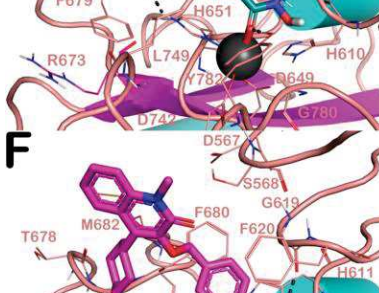
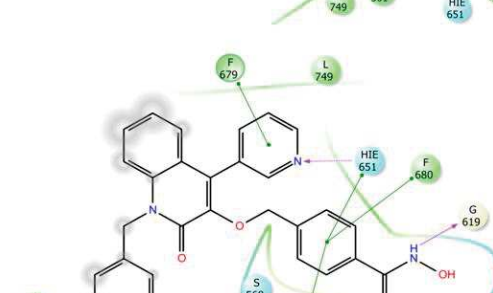
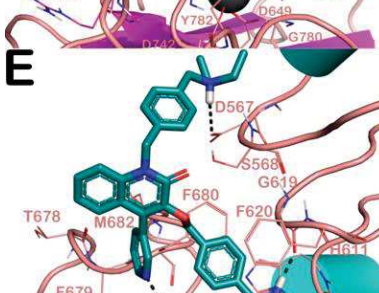
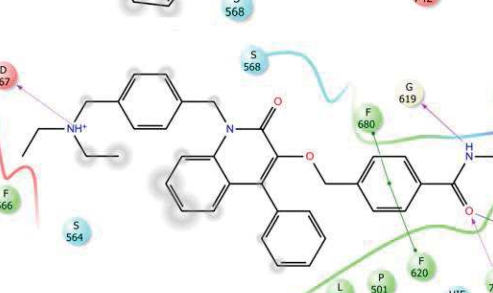
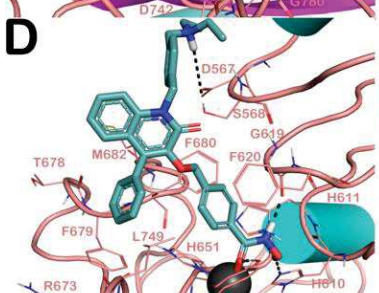
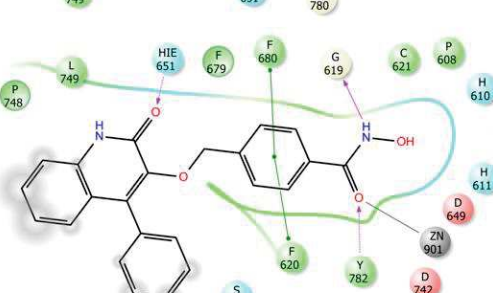
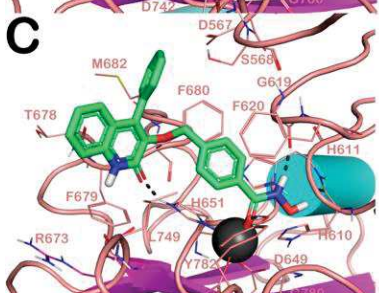
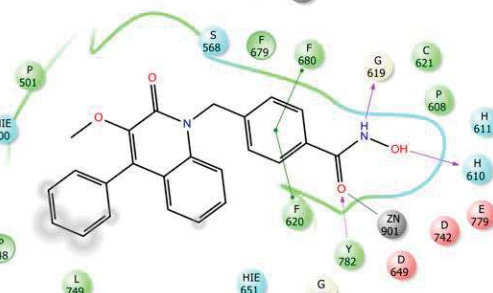
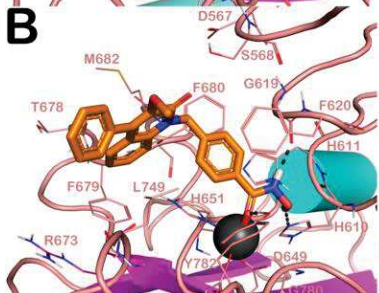
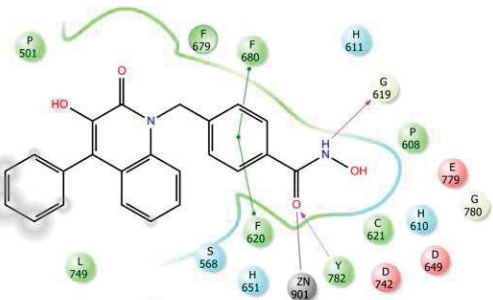
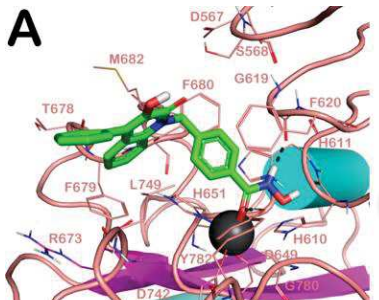


Figure 3. Docked poses into HDAC6 (PDB ID: 5EDU) of compounds **6a,b**, **7a**, **7g**, **7k** and **8** (panels A-F, respectively). Compounds are represented as sticks. The residues of the active sites are represented as lines and the whole protein is represented as cartoon. The Zn²⁺ ion is represented as a gray sphere. The polar contacts are depicted as dotted lines while the coordination bond as plain lines. The pictures were generated by means of PyMOL.

With the dual aim of increasing polar contacts within HDAC6 binding site while improving water solubility of these molecules, we introduced some functionalities on the quinolone scaffold leading to compounds **6d**, **7e-k** bearing pyridine at C4, benzylpiperidine and diethylaminomethylbenzyl groups at N1 (Figures 3D-E for compounds **7g** and **7k**). The introduction of a pyridin-3-yl instead of the phenyl ring at C4 (compound **6d**, Figure S1B), gave better results in terms of selectivity between the two investigated isoforms, compared to the parent compound **6a**. These findings prompted us to evaluate the introduction of the 4-methylenepyridine system at N1 on the series of compound **7**. Although establishing a polar contact through the nitrogen of the pyridine with the backbone of F680, compound **7e** (Figure S3A) did not show a satisfactory profile towards the HDAC6 isoform, since a similar set of contacts were also established with the HDAC1 isoform. The insertion of the different basic functionalities like the benzylpiperidine, as for compound **7f** (Figure S3B), resulted in an increase in the length of the molecule that precluded the formation of any relevant H-bond, decreasing the HDAC6 inhibitory potency. On the contrary, the insertion of a diethylaminomethylbenzyl portion at N1 as in compound **7g** (Figure 3D) provided the most potent HDAC6 inhibitor, with a potency in the low nanomolar range. As expected, the more flexible and protonatable diethylaminomethylbenzyl substituent allowed to form not only a new and not previously observed H-bond with the D567 residue, but also a strong salt bridge with the same residue. In summary, the introduction of a flexible and protonatable moiety, able to establish a salt bridge and a polar contact with D567 in HDAC6, is a preferred choice to improve the potency of enzyme inhibition. On the other hand, isoform selectivity was improved by introducing at C4 the pyridin-3-yl, retaining a significant potency (**7h-i**, Figure S3C,D) and with over 100-fold selectivity ratio towards HDAC6 over HDAC1. Compound **7k** (Figure 2E) showed a different binding mode compared to the other compounds of the series. With the introduction of the pyridine-4-yl, and additional bond with H651 was established, maintaining the same inhibitory profile. Furthermore, taking into consideration the hydrophobic residues present in the interaction site of HDAC6, we introduced a cyclohexyl ring at C4 in place of the aromatic system, obtaining **8**, the binding mode of which is shown in Figure 2F. Owing to ring flexibility and lower steric hindrance of the methyl at N1 of **8**, different residues were engaged through hydrophobic interactions, namely F679, F680 and L749.

In addition, we performed molecular docking calculation for assessing the putative binding mode of the developed compounds into HDAC1 enzyme. The output of this calculation is depicted in Figures S4-S6, and the binding mode of all molecules is reported in the Supplementary Material.

3.2. *hHDAC8 inhibition assays*

Binding affinity studies towards *h*HDAC8 isoform were conducted on the best HDAC6 inhibitors (**7g,k** and **8**) to have an indication of the potency and selectivity of these new quinolone-based derivatives also against this isoform. Among the three tested derivatives, compound **7g** demonstrated the highest selectivity with an IC₅₀ value of 0.55 μM (Table 2) and an index of 80 (HDAC8/HDAC6), while compound **8** was the least potent with an IC₅₀ value of 1.64 μM and a selectivity index of 50. These results highlighted a significant selectivity profile of these compounds towards HDAC6.

Table 2. Inhibitory activity of compounds **7g,k** and **8** as IC₅₀ (μM), and apparent inhibitor constant (K^{app}) against the *h*HDAC8 enzyme

| Cpd | 7g | 7k | 8 | TubA |
|------------------------------------|-------------|-------------|------------|-------------------|
| IC ₅₀ (μM) ^a | 0.55 ± 0.15 | 0.49 ± 0.20 | 1.64 ± 0.3 | 0.695 |
| K ^{app} (μM) ^a | 0.36 ± 0.1 | 0.40 ± 0.1 | 1.93 ± 0.2 | n.d. ^b |
| HDAC8/HDAC6 | 80 | 42 | 50 | 23 |

^aAll compounds were assayed at least two times, and the results are expressed with standard deviations.

^bn.d. Not determined

3.3. Cell-based studies

The anticancer effect of compounds **7g** and **7k**, the best performing small-molecules emerged from the HDAC6 *in vitro* experiments, and one of the starting hit **7a**, were evaluated in cell-based MTT assays against a colon cancer cell line (HCT-116) and a histiocytic lymphoma cell line (U937). All compounds showed a good cytotoxic activity in HCT-116 when used at 50 μM for 24 h and 48 h of induction (Table 3 and Table S1). However, **7g** resulted to be the best molecule tested, with an IC₅₀ of 3.6 μM after 48 h of induction, causing a strong block of cell proliferation already at 25 μM (80%), and at 10 μM, after 24 and 48 h 50% and 90% respectively. Compound **7k**, showed a potent cytotoxicity against HCT-116 cells after 48 h of induction at all concentrations, showing 10 to 20% of cell survival. In accordance with HDAC enzymatic results, compound **7a** resulted the least potent molecule, showing the best results only when tested at 50 μM for 48 h (10% cell viability). In U937 cells, these compounds were found to be less active, inducing the 60-70% of cell proliferation reduction after 48 h at 50 μM (Table 3 and Table S2). Compound **7a** was the most potent in this cell line with respect to the other compounds.

Table 3. IC₅₀ of **7a**, **7k** and **7g** in HCT-116 and U937 cell lines.

| | IC ₅₀ (μM) | | | | | | |
|-----------|-----------------------|-------------|--------------|------|------|-------------|--------|
| | HCT-116 | | | U937 | | | NIH3T3 |
| | 12 h | 24 h | 48 h | 12 h | 24 h | 48 h | 24 h |
| 6b | n.d. | n.d. | n.d. | n.d. | n.d. | n.d. | 90 |
| 7a | n.d. | 33.4 ± 0.1 | 15.02 ± 0.12 | n.d. | n.d. | 27.9 ± 0.05 | n.d. |
| 7k | n.d. | 25.7 ± 0.25 | 8.4 ± 0.56 | n.d. | n.d. | 45.5 ± 0.37 | 90 |
| 7g | 13.5 ± 0.2 | 11.6 ± 0.3 | 3.6 ± 0.29 | n.d. | n.d. | 40.6 ± 0.24 | n.d. |

| | | | | | | | |
|---|------|------|------|------|------|------|----|
| 8 | n.d. | n.d. | n.d. | n.d. | n.d. | n.d. | 18 |
|---|------|------|------|------|------|------|----|

n.d. Not determined

To assess the nature of cellular death occurring after **7a**, **7g** and **7k** treatment, Poly(ADP-ribose)-Polymerase (PARP) was evaluated in HCT-116 (Figure 4E,F) and U937 (Figure 5E,F) cell lines. A significant increase of PARP cleavage levels was observed in the samples after 24 h of treatment with **7g** and **7k**, tested at 10 μ M, demonstrating the activation of apoptotic process [29].

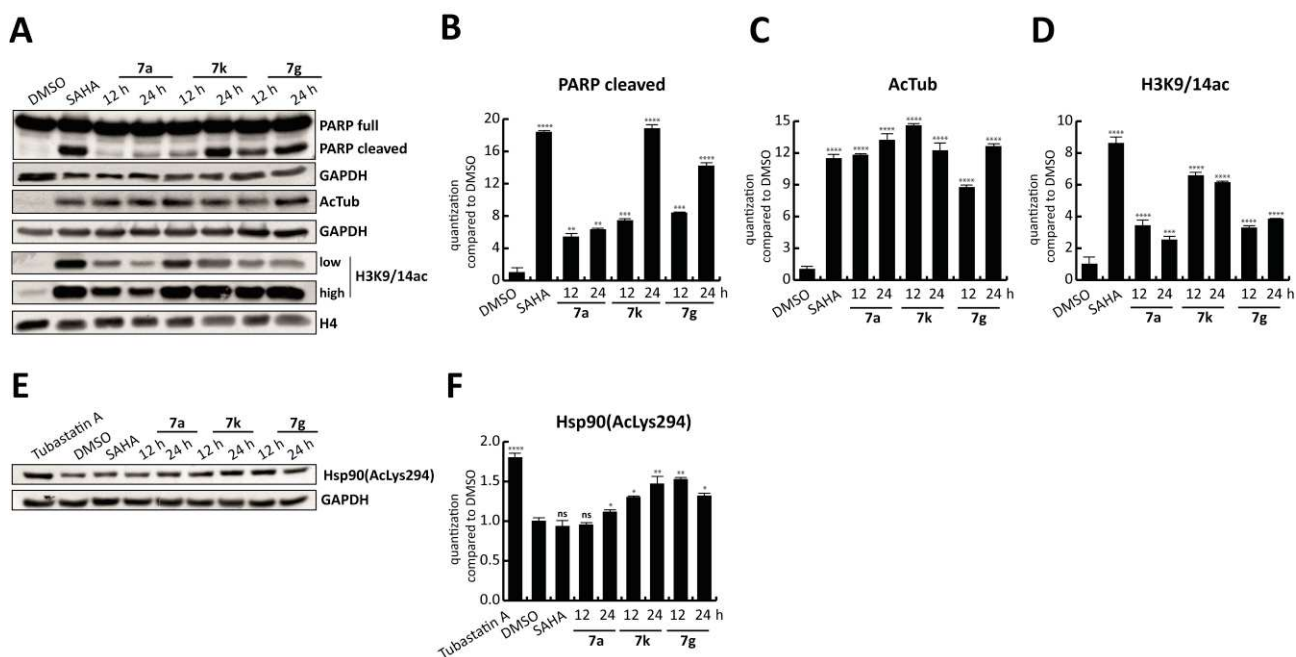


Figure 4. Western blot analysis for cleaved PARP, AcTub, H3K9/14ac and Hsp90(AcLys294) on HCT-116 cancer cell line treated with the compounds **7a**, **7g** and **7k** at 10 μ M for 12 and 24 h. Tubastatin A (5 μ M for 24 h) and SAHA (5 μ M for 24 h) were the positive controls. GAPDH and H4 were used for the normalization. Target levels were quantized using ImageJ software. **** p-value \leq 0.0001, *** p-value \leq 0.001, ** p-value \leq 0.01, * p-value \leq 0.05, ns p-value $>$ 0.05 vs control cells.

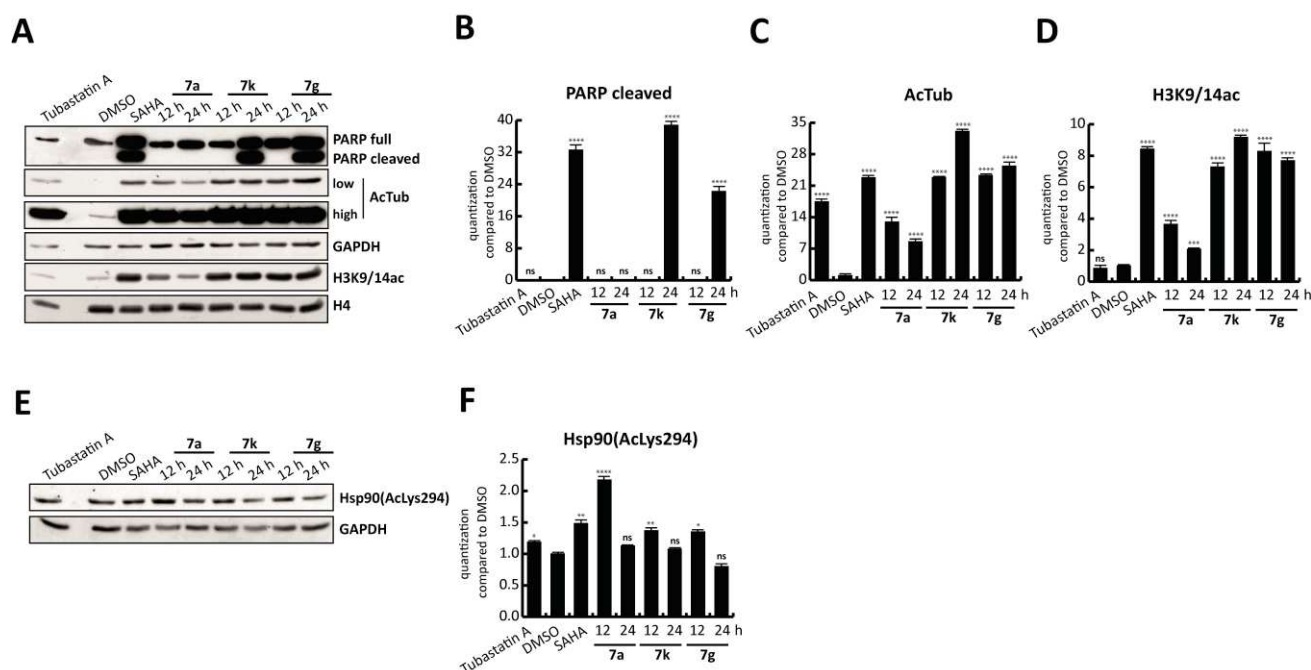


Figure 5. Western blot analysis for cleaved PARP, AcTub, H3K9/14ac and Hsp90(AcLys294) on U937 cancer cell line treated with the compounds **7a**, **7g** and **7k** at 10 μ M for 12 and 24 h. Tubastatin A (5 μ M for 24 h) and SAHA (5 μ M for 24 h) were the positive controls. GAPDH and H4 were used for the normalization. Target levels were quantized using ImageJ software. **** p-value \leq 0.0001, *** p-value \leq 0.001, ** p-value \leq 0.01, * p-value \leq 0.05, ns p-value $>$ 0.05 vs control cells.

To evaluate the capability of the compounds **7a**, **7g** and **7k** to inhibit the HDACs, Western blot studies were conducted in both cell lines analyzing the acetylation levels of alpha-tubulin and of the lysine 9 and 14 of histone 3 (Figure 4 and 5). All molecules, tested at 10 μ M, strongly enhanced the levels of AcTub in HCT-116 (Figure 4C) and U937 (Figure 5C), with a fold \geq 9, indicating the inhibition of cytoplasmic HDACs. The analysis of histone acetylation levels showed that the amount of H3K9/14ac increased after **7a**, **7g** and **7k** treatment, respect to the control, suggesting a possible inhibition of nuclear HDACs may have also occurred. However, in HCT-116 (Figure 4D) compounds **7a** and **7g** appeared to be more selective for cytoplasmic HDACs, increasing the H3K9/14ac of 2/4-fold, compared to **7k** ($>$ 6-fold). In U937 cells (Figure 5D) only compound **7a** showed a low potency against nuclear HDACs.

The interplay between HDAC6 and Hsp90 has been widely demonstrated in the last decade. It was observed that the over-acetylation of Hsp90, due to the inactivation or knockdown of HDAC6, determined the loss of chaperone activity of this protein [30]. Therefore, we decided to evaluate Hsp90(AcLys294) after treatment with **7a**, **7g**, and **7k**. In HCT-116 (Figure 4E, F), but not in U937 (Figure 5E, F), **7a**, **7g** and **7k** increased the levels of Hsp90(AcLys294) when tested at 10 μ M for 12 or 24 h, suggesting the inhibition of HDAC6. In U937, instead, only **7a** raised the Hsp90ac levels respect to the control (Figure 5).

3.4. In silico prediction of selected drug-like properties and experimental evaluation of physico-chemical properties

We predicted the ADME properties and the heart toxicity potential of the newly developed compounds by means of QikProp, a software implemented in Maestro suite (QikProp, version 4.3, Schrödinger, LLC, New York, NY, 2015). The output of the calculation is reported in Table S3. The predicted values for every molecule can be considered acceptable since they were within the recommended range of the software.

Selected parameters were also assessed experimentally. The *in vitro* solubility and chemical stability of selected compounds **6b**, **7e**, and **7k** were measured by means of HPLC methods as reported in previous work from us [31,32]. As expected, the presence of basic groups on compounds **7e,k** improved the solubility profile at pH = 3 with respect to compound **6b**. Gratifyingly, our analysis also revealed that both **7e,k** exhibited a favorable chemical stability profile at acidic pH. In particular, the chemical stability was almost quantitative for the selected compounds with more than 95% of the compound remaining unaltered at pH = 3 after 24 h (Table S4).

3.5. Mutagenicity profile evaluation for **6b**, **7k**, and **8**.

Potential mutagenicity associated with the use of hydroxamic acid-based compounds poses a significant challenge in terms of their drug-like profile [33]. To date, givinostat is the only compound under clinical trials that exhibited no mutagenic effect, while the other FDA approved drugs **1-4** have shown mutagenicity [34]. Therefore, we investigated for compounds **6b**, **7k** and **8** the mutagenic effect in the *Salmonella typhimurium* strains TA98 and TA100. The Ames test is employed to detect potential risks of mutagenicity at the early stages of drug development. The assay can be performed with or without the S9 fraction of rat liver. This latter condition allows an in-depth investigation for evaluating the risk of mutagenicity derived from the metabolites of the compounds under study. After applying both the experimental conditions, no mutagenic effect was observed for compounds **6b**, **7k** and **8** in the *Salmonella typhimurium* strains TA98 and TA100 at all concentrations (5-230 μ M) (Figures S7-S9).

3.6. Lossen rearrangement study on compound **7k**.

It has been observed that the leading cause of mutagenicity associated with the use of HDACi is related to a Lossen's rearrangement involving the hydroxamate group with the formation of the corresponding isocyanate. This intermediate can trigger mutagenicity by damaging the DNA due to its susceptibility to undergo nucleophilic attack [34]. In laboratory, this reaction can be performed on *O*-activated hydroxamic acids under basic conditions. However, under physiological conditions, it has been reported that in case of 2-naphthohydroxamic acid this reaction occurs by the involvement of acetyl-CoA, which activates the oxygen by the addition of an acetyl group [35]. Because of the low acidity of hydroxamic acids, it has been speculated that hydroxamate-based HDACi can reach the catalytic site as neutral molecules and get deprotonated only after a strong metal chelation (e.g. zinc and potassium) [34,36]. In this way, a metal-assisted Lossen's rearrangement may occur leading to the formation of the isocyanate.

In order to check the susceptibility of our compounds to undergo Lossen's rearrangement we investigated **7k** in terms of the formation of the corresponding isocyanate (by checking the conversion to its aniline

counterpart) by exposing it to one equivalent of K_2CO_3 in DMSO at 40 °C (Figures S10, S11). After 18 h we observed by ESI-MS analysis that the predominant peaks were: the starting material (**7k**, $[M+H]^+ = 563.2$) and the corresponding carboxylic acid ($[M+H]^+ = 548.2$, Figure S11). From this study we can assume that the absence of mutagenicity detected in the Ames assay can be explained by a low vulnerability of our compounds to undergo Lossen's rearrangement, thus confirming a safe profile for the HDACi described in this paper.

3.7. Cytotoxic profile evaluation for **6b**, **7g**, **7k** and **8**.

Compounds **6b**, **7k** and **8** were further characterized in a cytotoxicity assay to establish their effect on mouse fibroblasts NIH3T3 cells. Cell viability was measured by the Neutral Red Uptake test and data normalized as % control. TC_{50} values of 90 μM were observed for **6b**, **7k** and 18 μM for **8**, thus indicating a safe profile in normal cells for compounds **6b** and **7k**, while a low cytotoxicity in NIH3T3 cells was observed with compound **8** (Table 3 and Table S5). A second cytotoxicity study was performed on human peripheral blood mononuclear cells (PBMC) after the treatment with compounds **7g** and **7k** for 24 and 48 h. Cell viability was measured by using Guava® ViaCount™ Reagent. From cell viability study, was observed that compound **7k**, after 24 h treatment, exhibited a low cytotoxic action only when tested at 90 μM , thus confirming a safe profile for this compound. On the other hand, compound **7g**, after 24 h treatment, demonstrated a strong reduction in cell viability already when tested at 45 μM (Figure S12, panel A). No significant difference in cytotoxicity were observed when the cells were treated for longer times (48 h, Figure S12, panel B).

4. Conclusion

In this work we describe the synthesis of quinolone-based HDAC inhibitors preferentially targeting the isoform 6. The synthesis of the cap group was achieved by applying a multicomponent reaction involving several substituted isatins, PTSH and a suitable aldehyde. This versatile synthetic strategy could be applied for future scaffold modifications and for the development of optimized analogs. The design of the described molecules was facilitated by applying a computational chemistry approach. The final compounds obtained showed inhibition values in the nanomolar range for HDAC6 with a selectivity index up to 109-fold for HDAC6 over HDAC1. Moreover, selected analogues showed a weak affinity for the *h*HDAC8 enzyme. The most potent HDAC6 inhibitors were subjected to cell-based assays to check their anticancer potential. In particular, compound **7g** gave the best result in terms of cytotoxicity against colon cancer cells, inducing 90% cell death after 48 h at 10 μM , and after 12 h when tested at 50 and 25 μM , by triggering apoptosis. The influence of the compounds on tubulin, histone and Hsp90 acetylation status was evaluated to establish their selectivity towards HDAC6. Notably, all the tested compounds enhanced the levels of AcTub as a result of the inhibition of cytoplasmic HDACs. In HCT-116, **7a** and **7g** showed a lower increase of H3K9/14ac, thus indicating a lower selectivity for nuclear HDACs. Additionally, compounds **7g** and **7k** led to the increase of Hsp90(AcLys294), a selective substrate of HDAC6. By applying HPLC protocols, compound **7k** was found soluble and stable in aqueous solution at pH = 3. Compounds **6b**, **7k** did not display any cytotoxic or

mutagenic profile as assessed by cytotoxicity studies on mouse fibroblasts and Ames test on *Salmonella typhimurium* strains. The absence of mutagenicity was further confirmed by the low susceptibility of compound **7k** to undergo Lossen's rearrangement to generate its isocyanate derivative. Taken together, these data highlight a promising antitumor potential for these quinolone-based HDAC6 selective inhibitors. These evidences may pave the way to the development of more potent and selective optimized hits useful for a H2L transition and for further biological investigation.

5. Experimental data

5.1. General information

Unless otherwise specified, materials were purchased from commercial suppliers and used without further purification. Reaction progress was monitored by TLC using silica gel 60 F254 (0.040–0.063 mm) with detection by UV. Silica gel 60 (0.040–0.063 mm) was used for column chromatography. ¹H NMR and ¹³C NMR spectra were recorded on a Varian 300 MHz spectrometer or a Bruker 400 MHz spectrometer by using the residual signal of the deuterated solvent as internal standard. Splitting patterns are described as singlet (s), doublet (d), triplet (t), quartet (q) and broad (br); the values of chemical shifts (δ) are given in ppm and coupling constants (J) in Hertz (Hz). HPLC were performed with a Shimadzu Prominence apparatus equipped with a scanning absorbance UV-VIS detector (Diode Array SPD-M20A) also equipped with a thermostatic chamber or with Agilent 1100 Series equipped with UV-VIS detector. ESI-MS spectra were performed by an Agilent 1100 Series LC/MSD spectrometer. HRESIMS were carried out by a Thermo Finnigan LCQ Deca XP Max ion-trap mass spectrometer equipped with Xcalibur software, operated in positive ion mode. Infrared (IR) spectra were recorded in the neat on an Agilent Cary 630 Spectrometer FT-IR instrument and are reported in reciprocal centimeters (cm⁻¹). Melting points were detected by a BÜCHI melting point B-450 and reported and °C. The yields are referred to purified products and are not optimized. All moisture-sensitive reactions were performed under argon atmosphere using oven-dried glassware and anhydrous solvents. Final compounds were analyzed by combustion analysis (C, H, N) to confirm purity >95%.

5.2. Chemistry

5.2.1 Methyl 4-((2,3-dioxindolin-1-yl)methyl)benzoate (**10**).

To a solution of isatin (300 mg, 2.03 mmol) in dry DMF, cooled at 0 °C, a 60% dispersion of NaH, in mineral oil (95 mg, 2.38 mmol) was added and stirred for 5 min at 0 °C. Then, methyl 4-(bromomethyl)benzoate (2.34 g, 10.20 mmol) was added and the reaction was allowed to reach 25 °C and stirred for 12 h. Thereafter, a saturated solution of NH₄Cl (5 mL) was added and the mixture was extracted with EtOAc (3 x 5 mL). The combined organic layers were washed with brine, dried over Na₂SO₄ and concentrated *in vacuo*. The residue was used in the next step without further purifications and affording **10** (2.00 g, quantitative yield) as a red solid. ¹H NMR (300 MHz, CDCl₃) δ 8.02 (d, J = 8.3 Hz, 2H), 7.63 (dd, J

= 7.5, 0.8 Hz, 1H), 7.48 (td, $J = 7.8, 1.3$ Hz, 1H), 7.39 (d, $J = 8.5$ Hz, 2H), 7.11 (td, $J = 7.6, 0.8$ Hz, 1H), 6.70 (d, $J = 7.9$ Hz, 1H), 4.98 (s, 2H), 3.90 (s, 3H). ESI-MS m/z : $[M + H]^+$ 296.0.

5.2.2. Ethyl 4-((3-hydroxy-2-oxo-4-phenylquinolin-1(2H)-yl)methyl)benzoate (**11a**).

A solution of benzaldehyde (379 mg, 3.57 mmol) and PTSH (665 mg, 3.57 mmol) in EtOH (17 mL) was stirred at 25 °C for 2 h. After this, **10** (575 mg, 3.57 mmol) and K_2CO_3 (987 mg, 7.14 mmol) were added and the reaction was stirred at 80 °C for 12 h. The solvent was evaporated, and the crude was purified by chromatography on silica gel (20% EtOAc in petroleum ether) giving **11a** (430 mg, 64%) as a red solid. 1H NMR (300 MHz, $CDCl_3$) δ 8.02 (d, $J = 8.3$ Hz, 2H), 7.65 – 6.99 (m, 11H), 5.74 (s, 2H), 4.49 – 4.25 (m, 2H), 1.37 (t, $J = 7.1$ Hz, 3H); ^{13}C NMR (75 MHz, $CDCl_3$) δ 166.2, 159.3, 140.8, 140.7, 133.6, 132.8, 130.8, 130.2, 129.9, 129.7, 128.6, 128.4, 127.5, 126.5, 124.2, 123.3, 122.3, 114.9, 61.0, 46.9, 14.3; ESI-MS m/z : $[M + H]^+$ 400.1; mp 187.3-190.0 °C.

5.2.3. Ethyl 4-((3-hydroxy-2-oxo-4-(pyridin-3-yl)quinolin-1(2H)-yl)methyl)benzoate (**11b**).

Starting from **10** (100 mg, 0.33 mmol) the title compound was obtained following the procedure described to get **11a**. The residue was purified by chromatography on silica gel (2% MeOH in DCM) affording **11b** (43 mg, 32%) as a red solid. 1H NMR (300 MHz, $DMSO-d_6$) δ 9.70 (s, 1H), 8.65 (d, $J = 4.8$ Hz, 1H), 8.57 (s, 1H), 7.92 (d, $J = 8.6$ Hz, 2H), 7.83 (dd, $J = 7.8, 1.9$ Hz, 1H), 7.56 (dd, $J = 7.8, 4.8$ Hz, 1H), 7.44 – 7.23 (m, 4H), 7.21 – 7.00 (m, 2H), 5.74 (s, 2H), 4.27 (q, $J = 7.1$ Hz, 2H), 1.27 (t, $J = 7.1$ Hz, 3H); ESI-MS m/z : $[M + H]^+$ 401.1.

5.2.4. N-Hydroxy-4-((3-hydroxy-2-oxo-4-phenylquinolin-1(2H)-yl)methyl)benzamide (**6a**).

To a solution of **11a** (55 mg, 0.14 mmol) in a 2:1 mixture of DCM (4 mL): MeOH (2 mL), a 50% solution of NH_2OH in water (660 μL , 10.00 mmol) and a 4 M solution of KOH in methanol (1.25 mL, 5.00 mmol) were added dropwise. The reaction was stirred at 25 °C for 3 h, then it was neutralized with 6 N HCl and concentrated *in vacuo*. The residue was purified by chromatography on silica gel (0.1% NH_4OH , 10% MeOH in DCM) affording **6a** (44 mg, 82%) as a white solid. 1H NMR (300 MHz, $DMSO-d_6$) δ 11.14 (s, 1H), 9.36 (s, 1H), 8.98 (s, 1H), 7.75 – 7.24 (m, 11H), 7.11 (d, $J = 4.1$ Hz, 2H), 5.69 (s, 2H); ^{13}C NMR (75 MHz, $DMSO-d_6$) δ 164.4, 158.9, 142.0, 140.2, 134.0, 133.9, 132.2, 130.4, 128.9, 128.2, 127.8, 127.3, 127.0, 125.7, 124.3, 123.1, 122.2, 115.6, 45.9; ESI-MS m/z : $[M - H]^-$ 385.0. FT-IR (neat) ν_{max} 3375, 3291, 3036, 1616, 1566, 1496, 1257, 1015 cm^{-1} ; mp 192.7-195.8 °C, decomposition; Anal. ($C_{23}H_{18}N_2O_4$) C, H, N.

5.2.5. N-Hydroxy-4-((3-hydroxy-2-oxo-4-(pyridin-3-yl)quinolin-1(2H)-yl)methyl)benzamide (**6d**).

Starting from **11b** (20 mg, 0.05 mmol) the title compound was obtained following the procedure described to get **6a**. The residue was purified by chromatography on silica gel (0.1% NH_4OH , 10% MeOH in DCM) affording **15** (16 mg, 84%). 1H NMR (300 MHz, $DMSO-d_6$) δ 11.15 (s, 1H), 9.74 (s, 1H), 8.99 (s, 1H), 8.65 (d, $J = 3.5$ Hz, 1H), 8.57 (s, 1H), 7.83 (d, $J = 7.7$ Hz, 1H), 7.69 (d, $J = 8.1$ Hz, 2H), 7.62 – 7.50 (m, 1H), 7.46

– 7.24 (m, 4H), 7.22 – 6.96 (m, 2H), 5.70 (s, 2H); ¹³C NMR (75 MHz, DMSO-*d*₆) δ 164.3, 158.7, 150.8, 149.4, 142.9, 140.1, 138.2, 133.9, 132.3, 130.0, 127.8, 127.5, 127.0, 125.3, 124.0, 123.4, 121.9, 121.0, 115.7, 46.0; ESI-MS *m/z*: [M - H]⁺ 386.0. Anal. (C₂₂H₁₇N₃O₄) C, H, N.

5.2.6. Ethyl 4-((3-methoxy-2-oxo-4-phenylquinolin-1(2H)-yl)methyl)benzoate (**12a**).

To a solution of **11a** (100 mg, 0.25 mmol) in dry THF (3 mL) cooled at 0 °C, a 60% dispersion of NaH in mineral oil (15 mg, 0.38 mmol) was added. The mixture was stirred at 0 °C for 30 min, then MeI (78 μL, 1.25 mmol) was added. The reaction was allowed to reach 25 °C and stirred for 12 h. After this time a saturated solution of NH₄Cl (5 mL) was added and the mixture was extracted with EtOAc (3 x 5 mL). The combined organic layers were dried over Na₂SO₄ and concentrated in vacuo. The residue was purified by chromatography on silica gel (25% EtOAc in Petroleum ether) affording **12a** (30 mg, 29%) as a colorless oil. ¹H NMR (300 MHz, CDCl₃) δ 8.11 – 7.90 (m, 2H), 7.58 – 7.44 (m, 3H), 7.44 – 7.14 (m, 7H), 7.15 – 6.99 (m, 1H), 5.69 (s, 2H), 4.34 (q, *J* = 7.1 Hz, 2H), 3.80 (s, 3H), 1.35 (t, *J* = 7.1 Hz, 3H); ESI-MS *m/z*: [M + H]⁺ 414.0.

5.2.7. Ethyl 4-((3-(benzyloxy)-2-oxo-4-phenylquinolin-1(2H)-yl)methyl)benzoate (**12b**).

To a solution of **11a** (50 mg, 0.125 mmol) and benzyl bromide (16 μL, 0.137 mmol) in anhydrous DMF (2 mL) was added K₂CO₃ (34 mg, 0.25 mmol) followed by KI (2 mg, 0.01 mmol). Reaction was refluxed for 8 h at 80 °C. Reaction mixture was then partitioned between aqueous saturated NH₄Cl and EtOAc, and the organic layer was washed with a saturated solution of NaHCO₃ (5 mL) and brine (5 mL), dried over Na₂SO₄ and concentrated *in vacuo*. The residue was purified by chromatography on silica gel (25% EtOAc in petroleum ether) affording **12b** (39 mg, 64%) as a pale-yellow oil. ¹H NMR (300 MHz, CDCl₃) δ 8.03 (d, *J* = 8.3 Hz, 2H), 7.56 – 7.40 (m, 3H), 7.40 – 7.13 (m, 10H), 7.13 – 6.94 (m, 3H), 5.73 (s, 2H), 5.15 (s, 2H), 4.37 (q, *J* = 7.1 Hz, 2H), 1.38 (t, *J* = 7.1 Hz, 3H); ESI-MS *m/z*: [M + H]⁺ 490.0.

5.2.8. *N*-Hydroxy-4-((3-methoxy-2-oxo-4-phenylquinolin-1(2H)-yl)methyl)benzamide (**6b**).

Starting from **12a** (30 mg, 0.07 mmol) the title compound was obtained following the procedure described to get **6a**. The residue was purified by chromatography on silica gel (0.1% NH₄OH, 10% MeOH in DCM) affording **6b** (28 mg, 97%) as a white solid. ¹H NMR (300 MHz, CDCl₃) δ 11.15 (s, 1H), 9.00 (s, 1H), 7.69 (d, *J* = 7.9 Hz, 2H), 7.61 – 7.21 (m, 9H), 7.21 – 6.95 (m, 2H), 5.65 (s, 2H), 3.71 (s, 3H); ¹³C NMR (75 MHz, DMSO-*d*₆) δ 164.4, 158.8, 144.8, 140.3, 137.7, 136.4, 133.7, 132.2, 129.7, 129.5, 128.9, 128.6, 127.7, 127.2, 127.0, 123.0, 121.1, 115.6, 60.1, 45.6; ESI-MS *m/z*: [M + H]⁺ 401.0; HRMS-ESI *m/z*: calcd for C₂₄H₂₁N₂O₄⁺ [M+H]⁺: 401.1496; found: 401.1488; FT-IR (neat) *v*_{max} 3217, 2920, 2854, 1719, 1630, 1595, 1456, 1259, 1091, 1016 cm⁻¹; mp 161.0-164.0 °C, decomposition; Anal. (C₂₄H₂₀N₂O₄) C, H, N.

5.2.9. 4-((3-(Benzyloxy)-2-oxo-4-phenylquinolin-1(2H)-yl)methyl)-*N*-hydroxybenzamide (**6c**).

Starting from **12b** (27 mg, 489.56 μmol) the title compound was obtained following the procedure described to get **6a**. The residue was purified by chromatography on silica gel (0.1% NH_4OH , 10% MeOH in DCM) affording **6c** (22 mg, 85%) as a light brown solid. ^1H NMR (300 MHz, $\text{DMSO-}d_6$) δ 11.16 (s, 1H), 9.01 (s, 1H), 7.70 (d, $J = 7.9$ Hz, 2H), 7.59 – 6.81 (m, 16H), 5.70 (s, 2H), 5.07 (s, 2H). ^{13}C NMR (75 MHz, $\text{DMSO-}d_6$) δ 164.4, 159.1, 143.4, 140.3, 138.3, 137.3, 136.5, 133.6, 132.2, 129.8, 129.6, 128.8, 128.6 (2C), 128.5, 128.3, 127.7, 127.2, 127.1, 123.0, 121.2, 115.6, 73.5, 45.6; ESI-MS m/z : $[\text{M} + \text{H}]^+$ 476.9; Anal. ($\text{C}_{30}\text{H}_{24}\text{N}_2\text{O}_4$) C, H, N.

5.2.10. 3-Hydroxy-4-phenylquinolin-2(1H)-one (**13a**).

A solution of benzaldehyde (100 mg, 0.94 mmol) and PTSH (175 mg, 0.94 mmol) in EtOH (5 mL) was stirred at 25 °C for 2 h. After this, isatin (138 mg, 0.94 mmol) and K_2CO_3 (260 mg, 1.88 mmol) were added and the reaction was stirred at 80 °C for 12 h. The solvent was evaporated, and the crude was purified by chromatography on silica gel (20% EtOAc in petroleum ether) giving **13a** (95 mg, 42%) as a brown solid. ^1H NMR (300 MHz, $\text{DMSO-}d_6$) δ 12.19 (s, 1H), 9.16 (s, 1H), 7.57 – 7.35 (m, 3H), 7.34 – 7.18 (m, 4H), 7.09 – 6.94 (m, 2H); ESI-MS m/z : $[\text{M} + \text{Na}]^+$ 260.1.

5.2.11. 3-Hydroxy-4-(pyridin-3-yl)quinolin-2(1H)-one (**13b**).

Starting from 3-pyridinecarboxaldehyde (181 mg, 1.69 mmol) and isatin (500 mg, 1.69), the title compound was obtained following the procedure previously described for compound **13a**. The crude was purified by chromatography on silica gel (5% MeOH in DCM) giving **13b** (180 mg, 45%) as a red solid. ^1H NMR (300 MHz, $\text{DMSO-}d_6$) δ 12.27 (s, 1H), 9.49 (s, 1H), 8.62 (dd, $J = 4.8, 1.7$ Hz, 1H), 8.53 (dd, $J = 2.2, 0.8$ Hz, 1H), 7.85 – 7.71 (m, 1H), 7.62 – 7.46 (m, 1H), 7.42 – 7.25 (m, 2H), 7.17 – 7.05 (m, 1H), 7.05 – 6.94 (m, 1H); ESI-MS m/z : $[\text{M} + \text{H}]^+$ 239.0.

5.2.12. Methyl 4-(((2-oxo-4-phenyl-1,2-dihydroquinolin-3-yl)oxy)methyl)benzoate (**14a**).

To a solution of **13a** (100 mg, 0.42 mmol) in dry DMF (4 mL) methyl 4-(bromomethyl)benzoate (145 mg, 0.63 mmol), KI (7 mg, 0.04 mmol) and K_2CO_3 (116 mg, 0.84 mmol) were added. The reaction mixture was stirred at 80 °C for 12 h. Thereafter the mixture was cooled down to 25 °C and a saturated solution of NH_4Cl (10 mL) was added. The mixture was extracted with EtOAc (10 mL) and the organic layer was washed with a saturated solution of NaHCO_3 (5 mL) and brine (5 mL). Then it was dried over Na_2SO_4 and concentrated *in vacuo*. The crude was purified by chromatography on silica gel (33% EtOAc in petroleum ether) giving **14a** (61 mg, 38%) as a pale brown solid. ^1H NMR (300 MHz, CDCl_3) δ 12.95 (s, 1H), 7.88 (d, $J = 8.0$ Hz, 2H), 7.57 – 7.35 (m, 6H), 7.33 – 7.01 (m, 5H), 5.24 (s, 2H), 3.89 (s, 3H); ^{13}C NMR (75 MHz, CDCl_3) δ 167.0, 161.0, 143.7, 142.2, 140.3, 140.3, 135.5, 133.2, 129.7, 129.4, 129.1, 128.7, 128.3, 127.9, 126.7, 122.8, 120.8, 115.9, 73.4, 57.0; ESI-MS m/z : $[\text{M} + \text{H}]^+$ 386.1; m.p.: 195.0-197.9 °C.

5.2.13. Methyl 4-(((2-oxo-4-(pyridin-3-yl)-1,2-dihydroquinolin-3-yl)oxy)methyl)benzoate (**14b**).

Starting from **13b** (180 mg, 0.76 mmol) the title compound was obtained following the procedure previously described for compound **14a**. The crude was purified by chromatography on silica gel (50% EtOAc in petroleum ether) giving **14b** (60 mg, 20%) as a dark yellow oil. ¹H NMR (300 MHz, CDCl₃) δ 12.82 (s, 1H), 8.71 (dd, *J* = 5.0, 1.7 Hz, 1H), 8.61 – 8.47 (m, 1H), 7.98 – 7.81 (m, 2H), 7.64 – 7.32 (m, 4H), 7.24 – 7.01 (m, 4H), 5.45 – 5.15 (m, 2H), 3.89 (s, 3H); ESI-MS *m/z*: [M + H]⁺ 387.0.

5.2.14. *N*-Hydroxy-4-(((2-oxo-4-phenyl-1,2-dihydroquinolin-3-yl)oxy)methyl)benzamide (**7a**).

To a solution of **14a** (19 mg, 0.049 mmol) in a 2:1 mixture of DCM (2 mL): MeOH (1 mL), a 50% solution of NH₂OH in water (329 μL, 4.90 mmol) and a 4 M solution of KOH in methanol (616 μL, 2.45 mmol) were added dropwise. The reaction was stirred at 25 °C for 3 h, then it was neutralized with 6 N HCl and concentrated *in vacuo*. The crude was purified by chromatography on silica gel (0.1% NH₄OH, 10% MeOH in DCM) giving **7a** (11 mg, 55%) as a white solid. ¹H NMR (300 MHz, DMSO-*d*₆) δ 12.13 (s, 1H), 11.11 (s, 1H), 8.96 (s, 1H), 7.55 (d, *J* = 8.3 Hz, 2H), 7.50 – 7.30 (m, 5H), 7.28 – 7.14 (m, 2H), 7.12 – 7.00 (m, 3H), 7.00 – 6.88 (m, 1H), 5.07 (s, 2H). ¹³C NMR (75 MHz, DMSO-*d*₆) δ 164.3, 159.1, 144.2, 140.6, 138.4, 136.3, 133.7, 132.5, 129.8, 129.1, 128.7, 128.5, 128.0, 127.1, 126.2, 122.5, 120.3, 115.6, 72.8; ESI-MS *m/z*: [M + H]⁺ 387.1; FT-IR (neat) ν_{\max} 3204, 3048, 2858, 1653, 1549, 1279, 1202, 1160, 989 cm⁻¹; mp 204.8-205.4 °C, decomposition; Anal. (C₂₃H₁₈N₂O₄) C, H, N.

5.2.15. *N*-Hydroxy-4-(((1-methyl-2-oxo-4-phenyl-1,2-dihydroquinolin-3-yl)oxy)methyl)benzamide (**7b**).

Step 1: To a solution of **14a** (16 mg, 0.04 mmol) in dry THF (1 mL) cooled at 0 °C, a 60% dispersion of NaH in mineral oil (15 mg, 0.06 mmol) was added. The mixture was stirred at 0 °C for 30 min then MeI (8 μL, 0.12 mmol) was added. The reaction was allowed to reach 25 °C and stirred at this temperature for 12 h. Then a saturated solution of NH₄Cl (5 mL) was added and the mixture was extracted with EtOAc (3 x 5 mL). The combined organic layers were washed with brine, dried over Na₂SO₄ and concentrated *in vacuo*. The crude was purified by chromatography on silica gel (50% EtOAc in petroleum ether) affording *methyl 4-(((1-methyl-2-oxo-4-phenyl-1,2-dihydroquinolin-3-yl)oxy)methyl)benzoate* (16 mg, quantitative yield) as a white solid. ¹H NMR (300 MHz, CDCl₃) δ 7.85 (d, *J* = 6.8 Hz, 2H), 7.57 – 7.32 (m, 5H), 7.32 – 7.17 (m, 3H), 7.17 – 6.95 (m, 3H), 5.13 (s, 2H), 3.95 – 3.79 (m, 6H); ESI-MS *m/z*: [M + H]⁺ 400.1.

Step 2: From *methyl 4-(((1-methyl-2-oxo-4-phenyl-1,2-dihydroquinolin-3-yl)oxy)methyl)benzoate* (22 mg, 0.05 mmol) the title compound was obtained following the procedure previously described for compound **7a**. The crude was purified by chromatography on silica gel (0.1% NH₄OH, 10 % MeOH in DCM) giving **7b** (14 mg, 64%). ¹H NMR (300 MHz, DMSO-*d*₆) δ 11.14 (s, 1H), 8.97 (s, 1H), 7.58-7.47 (m, 7H), 7.35 – 7.13 (m, 3H), 7.06 (dd, *J* = 8.2, 2.4 Hz, 3H), 5.04 (s, 2H), 3.76 (s, 3H) ¹³C NMR (75 MHz, MeOD) δ 166.4, 159.7, 143.0, 140.7, 139.2, 137.0, 133.2, 131.5, 129.4, 129.3, 128.1, 128.0, 127.9, 126.9, 126.5, 122.5, 121.0, 114.5, 73.0, 29.4; ESI-MS *m/z*: [M + H]⁺ 401.0; Anal. (C₂₄H₂₀N₂O₄) C, H, N.

5.2.16. *N*-Hydroxy-4-(((2-oxo-4-phenyl-1-(prop-2-yn-1-yl)-1,2-dihydroquinolin-3-yl)oxy)methyl)benzamide (**7c**).

Step 1: To a solution of **14a** (50 mg, 0.13 mmol) in dry DMF cooled at 0 °C, NaH (60% in mineral oil, 7 mg, 0.194) was added. The reaction was allowed to stir for 30 mins at the same temperature, then propargyl bromide (19 µL, 0.129 mmol) was added. The reaction was allowed to reach 25 °C and stirred for 12 h. After this time, a saturated solution of NH₄Cl (5 mL) was added and the mixture was extracted with EtOAc (3 x 5 mL). The combined organic layers were washed with brine, dried over Na₂SO₄ and concentrated *in vacuo*. The crude was purified by chromatography on silica gel (25% EtOAc in petroleum ether) affording *methyl 4-(((2-oxo-4-phenyl-1-(prop-2-yn-1-yl)-1,2-dihydroquinolin-3-yl)oxy)methyl)benzoate* (31 mg, 56% yield) as a brown solid. ¹H NMR (300 MHz, CDCl₃) δ 7.84 (d, *J* = 7.5 Hz, 2H), 7.63 – 7.37 (m, 5H), 7.34 – 7.19 (m, 3H), 7.19 – 7.11 (m, 1H), 7.08 (d, *J* = 8.0 Hz, 2H), 5.23 (d, *J* = 2.5 Hz, 2H), 5.13 (s, 2H), 3.88 (s, 3H), 2.32 (s, 1H); ESI-MS *m/z*: [M + H]⁺ 424.1

Step 2: From *methyl 4-(((2-oxo-4-phenyl-1-(prop-2-yn-1-yl)-1,2-dihydroquinolin-3-yl)oxy)methyl)benzoate* (30 mg, 0.07 mmol) the title compound was obtained following the procedure previously described for compound **7a**. The crude was purified by chromatography on silica gel (0.1% NH₄OH, 10% MeOH in DCM) giving **7c** (17 mg, 57%) as a brown solid. ¹H NMR (300 MHz, MeOD) δ 11.13 (s, 1H), 8.97 (s, 1H), 7.73 – 7.53 (m, 4H), 7.53 – 7.39 (m, 3H), 7.35 – 7.13 (m, 3H), 7.15 – 6.96 (m, 3H), 5.23 (s, 2H), 5.05 (s, 2H), 3.31 (s, 1H); ¹³C NMR (75 MHz, DMSO-*d*₆) δ 164.3, 158.0, 143.4, 140.5, 138.4, 135.9, 133.4, 132.5, 129.7, 128.8 (2C), 128.7, 128.0, 127.3, 127.1, 123.3, 121.0, 115.6, 79.3, 75.3, 73.1, 32.2; ESI-MS *m/z*: [M + H]⁺ 425.0. mp decomposition; Anal. (C₂₆H₂₀N₂O₄) C, H, N.

5.2.17. *N*-Hydroxy-4-(((1-methyl-2-oxo-4-(pyridin-3-yl)-1,2-dihydroquinolin-3-yl)oxy)methyl)benzamide (**7h**).

Starting from **14b** (15 mg, 0.076 mmol) the title compound was obtained following the procedure previously described for compound **7b**, **Step 1**. The crude was purified by chromatography on silica gel (33% EtOAc in petroleum ether) giving *methyl 4-(((1-methyl-2-oxo-4-(pyridin-3-yl)-1,2-dihydroquinolin-3-yl)oxy)methyl)benzoate* (10 mg, 66%) as a yellow solid. ¹H NMR (300 MHz, CDCl₃) δ 8.68 (dd, *J* = 4.9, 1.7 Hz, 1H), 8.48 (dd, *J* = 2.2, 0.9 Hz, 1H), 7.86 (d, *J* = 8.3 Hz, 2H), 7.62 – 7.32 (m, 4H), 7.23 – 7.03 (m, 4H), 5.31 – 5.06 (m, 2H), 3.89 (s, 3H), 3.86 (s, 3H); ESI-MS *m/z*: [M + H]⁺ 401.1. Starting from *methyl 4-(((1-methyl-2-oxo-4-(pyridin-3-yl)-1,2-dihydroquinolin-3-yl)oxy)methyl)benzoate* (15 mg, 0.076 mmol) the title compound was obtained following the procedure previously described for compound **7a**. The crude was purified by chromatography on silica gel (0.1% NH₄OH, 10% MeOH in DCM) giving **7h** (5 mg, 50%) as a white solid. ¹H NMR (300 MHz, MeOD) δ 8.61 (d, *J* = 4.8 Hz, 1H), 8.32 (s, 1H), 7.74 – 7.45 (m, 6H), 7.30 – 7.01 (m, 4H), 5.12 (d, *J* = 4.9 Hz, 2H), 3.88 (s, 3H); ¹³C NMR (75 MHz, MeOD) δ 166.3, 159.2, 149.3, 148.3, 143.4, 140.2, 138.4, 137.1, 134.8, 131.8, 130.1, 129.5, 128.2, 126.6, 126.2, 123.6, 122.8, 120.2, 114.7, 72.8, 29.2; ESI-MS *m/z*: [M + Na]⁺ 424.0; Anal. (C₂₃H₁₉N₃O₄) C, H, N.

5.2.18. 1-Methylindoline-2,3-dione (**15**) [26].

To a solution of isatin (1.0 g, 6.80 mmol) in dry DMF (4 mL), cooled at 0 °C, a 60% dispersion of NaH, in mineral oil (275 mg, 6.80 mmol) was added and stirred for 5 min at 0 °C. Then, methyl iodide (635 μ L, 10.20 mmol) was added and the reaction was allowed to reach 25 °C and stirred for 12 h. Thereafter, a saturated solution of NH₄Cl (5 mL) was added and the mixture was extracted with EtOAc (3 x 5 mL). The combined organic layers were washed with brine, dried over Na₂SO₄ and concentrated *in vacuo*. The crude was purified by chromatography on silica gel (25% EtOAc in petroleum ether) affording **15** (1.15 g, quantitative yield) as a red solid. ¹H NMR (300 MHz, CDCl₃) δ 7.69 – 7.52 (m, 2H), 7.12 (td, *J* = 7.6, 0.9 Hz, 1H), 6.89 (dd, *J* = 8.6, 0.9 Hz, 1H), 3.25 (s, 3H). The experimental data are consistent with those reported in literature [26].

5.2.19. 4-Cyclohexyl-3-hydroxy-1-methylquinolin-2(1H)-one (**16**).

Starting from **15** (575 mg, 3.57 mmol) and cyclohexanecarboxaldehyde (431 μ L, 3.57 mmol) the title compound was obtained following the procedure described to get **13a**. The residue was purified by chromatography on silica gel (20% EtOAc in petroleum ether) affording **16** (270 mg, 30%) as a white solid. ¹H NMR (300 MHz, CDCl₃) δ 7.92 (d, *J* = 8.2 Hz, 1H), 7.54 – 7.20 (m, 4H), 3.82 (s, 3H), 3.16 (m, 1H), 2.35 – 2.12 (m, 2H), 1.99 – 1.83 (m, 2H), 1.75 (m, 4H), 1.42 (m, 2H); ESI-MS *m/z*: [M + H]⁺ 258.1.

5.2.20. 4-(((4-Cyclohexyl-1-methyl-2-oxo-1,2-dihydroquinolin-3-yl)oxy)methyl)-N-hydroxybenzamide (**8**).

Starting from **16** (270 mg, 1.05 mmol) methyl 4-(((4-cyclohexyl-1-methyl-2-oxo-1,2-dihydroquinolin-3-yl)oxy)methyl)benzoate was obtained following the procedure described to get **14a**. The residue was purified by chromatography on silica gel (33% EtOAc in petroleum ether) affording methyl 4-(((4-cyclohexyl-1-methyl-2-oxo-1,2-dihydroquinolin-3-yl)oxy)methyl)benzoate (317 mg, 74%) as a yellow oil. ¹H NMR (300 MHz, CDCl₃) δ 8.15 – 8.01 (m, 2H), 7.96 (s, 1H), 7.61 (d, *J* = 7.9 Hz, 2H), 7.54 – 7.40 (m, 1H), 7.33 (dd, *J* = 8.6, 1.2 Hz, 1H), 7.22 (t, *J* = 7.6 Hz, 1H), 5.26 (s, 2H), 3.89 (s, 3H), 3.73 (s, 3H), 3.20 (d, *J* = 13.8 Hz, 1H), 2.16 – 1.93 (m, 2H), 1.89 – 1.52 (m, 5H), 1.48 – 1.07 (m, 3H); ¹³C NMR (75 MHz, CDCl₃) δ 167.0, 159.1, 142.9, 140.9, 137.3, 129.7, 129.5, 128.6, 127.9, 126.4, 124.6, 122.1, 120.4, 114.6, 72.7, 52.1, 38.4, 30.6, 29.9, 27.2, 26.1; ESI-MS *m/z*: [M + H]⁺ 406.1; mp 79.1-82.2 °C.

This intermediate (100 mg, 0.25 mmol) was converted into compound **8** following the procedure previously described for the synthesis of compound **7a**. The residue was purified by chromatography on silica gel (0.1% NH₄OH, 10% MeOH in DCM) affording **8** (100 mg, 98%) as a brown solid. ¹H NMR (300 MHz, DMSO-*d*₆) δ 11.21 (s, 1H), 9.01 (s, 1H), 8.04 (d, *J* = 8.2 Hz, 1H), 7.77 (d, *J* = 7.9 Hz, 2H), 7.55 (m, 4H), 7.40 – 7.16 (m, 1H), 5.16 (s, 2H), 3.68 (s, 3H), 3.25 (m, 1H), 2.15 – 1.85 (m, 2H), 1.85 – 0.87 (m, 8H); ¹³C NMR (75 MHz, DMSO-*d*₆) δ 164.4, 158.3, 141.0, 140.5, 137.4, 132.6, 129.3, 128.3, 128.1, 127.4, 125.8, 122.7, 119.8, 115.6, 72.4, 37.7, 30.4, 30.1, 27.0, 26.0; ESI-MS *m/z*: [M + H]⁺ 407.1. HRMS-ESI *m/z*: calcd for C₂₄H₂₇N₂O₄⁺ [M+H]⁺: 407.1965; found: 407.1960; FT-IR (neat) ν_{\max} 3314, 3248, 2919, 2849, 1661, 1618, 1585, 1452, 1206, 1106, 1028 cm⁻¹; mp 197.2-200.0 °C, decomposition Anal. (C₂₄H₂₆N₂O₄) C, H, N.

5.2.21. 4-(Hydroxymethyl)pyridine (**18**).

To a solution of **17** (2.0 g, 18.67 mmol) in methanol (20 mL), cooled at 0 °C, NaBH₄ (706 mg, 18.67 mmol) was added. The reaction was stirred for 2 h and allowed to reach to 25 °C. After the complete consumption of starting material, water (20 mL) was added, solvent was evaporated, and the aqueous residue was extracted with EtOAc (3 x 15 mL). The combined organic layers were filtered over Na₂SO₄ and concentrated *in vacuo* to get **18** (1.60 g, 80%) as a colorless oil. ¹H NMR (300 MHz, CDCl₃) δ 8.52 (dd, *J* = 4.6, 1.5 Hz, 2H), 7.40 – 7.19 (m, 2H), 4.74 (s, 2H), 3.20 (s, 1H).

5.2.22. 4-(Bromomethyl)pyridinium bromide (**19**) [27].

Compound **18** (1.810 g, 16.58 mmol) was dissolved in 48% HBr (16 mL) and stirred at reflux for 4 h. The water was removed *in vacuo* to give a thick gum which was treated with ethanol at 5 °C and then filtered. The white crystals were collected and washed with cold ethanol to get 4-(hydroxymethyl)pyridinium bromide (1.9 g). To a suspension of this salt in chloroform (25 mL) PBr₃ (457 μL, 4.85 mmol) was added, and the mixture was stirred at reflux for 4.5 h. After cooling down to 25 °C, the white precipitate was collected and washed with cold chloroform to give **19** (2.3 g, 93%) as a white solid. ¹H NMR (300 MHz, CDCl₃) δ 8.80 (d, *J* = 6.4 Hz, 2H), 8.00 (d, *J* = 6.4 Hz, 2H), 4.61 (s, 2H). The spectroscopic data are consistent with those reported in literature [27].

5.2.23. 4-(Bromomethyl)benzaldehyde (**21**) [37].

To a solution of 4-(bromomethyl)benzotrile (2.0 g, 10.20 mmol) in dry DCM (40 mL), cooled at -78 °C a 1 M solution of DIBAL-H in DCM (11.2 mL, 11.22 mmol) was slowly added. The reaction was allowed to reach 0 °C in 1 h, then it was slowly quenched with 1 N HCl (20 mL). The mixture was extracted with DCM (3 x 20 mL) and the combined organic layers were washed with NaOH (2 x 20 mL), then dried over Na₂SO₄ and concentrated *in vacuo* affording **21** (2.03 g, quantitative yield) as a white solid that was used in the next step without further purification. ¹H NMR (300 MHz, CDCl₃) δ 10.02 (s, 1H), 7.87 (d, *J* = 8.2 Hz, 2H), 7.56 (d, *J* = 8.1 Hz, 2H), 4.52 (s, 2H). The spectroscopic data are consistent with those reported in literature [37].

5.2.24. 2-(4-(Bromomethyl)phenyl)-1,3-dioxolane (**22**) [37].

To a solution of **21** (2.03 g, 10.20 mmol) in toluene, ethylene glycol (1.1 mL, 20.40 mmol) and PTSA (176 mg, 1.02 mmol) were added. The reaction was stirred at 110 °C for 12 h, then a saturated solution of NaHCO₃ (20 mL) was added. The resulting mixture was extracted with EtOAc (3 x 20 mL) and the combined organic layers were dried over Na₂SO₄ and concentrated *in vacuo*. The crude was purified by chromatography on silica gel (20% EtOAc in petroleum ether) affording **22** (1.7 g, 69%) as a colorless oil. ¹H NMR (300 MHz, Acetone-*d*₆) δ 7.56 – 7.39 (m, 4H), 5.75 (s, 1H), 4.66 (s, 2H), 4.20 – 3.88 (m, 4H). The spectroscopic data are consistent with those reported in literature [37].

5.2.25. 1-Benzylindoline-2,3-dione (**23a**) [26].

To a solution of isatin (300 mg, 2.03 mmol) in dry DMF (2 mL), cooled at 0 °C, a 60% dispersion of NaH in mineral oil (95 mg, 2.38 mmol) was added and stirred for 5 min at 0 °C. Then, benzyl bromide (266 μ L, 2.34 mmol) was added and the reaction was allowed to reach 25 °C and stirred for 12 h. Thereafter, a saturated solution of NH₄Cl (5 mL) was added and the mixture was extracted with EtOAc (3 x 5 mL). The combined organic layers were washed with brine, dried over Na₂SO₄ and concentrated *in vacuo*. The crude was purified by chromatography on silica gel (25% EtOAc in petroleum ether) affording **23a** (358 mg, 74% yield) as a yellow solid. ¹H NMR (300 MHz, CDCl₃) δ 7.67 – 7.55 (m, 1H), 7.47 (td, *J* = 7.8, 1.3 Hz, 1H), 7.41 – 7.24 (m, 5H), 7.08 (t, *J* = 7.6 Hz, 1H), 6.77 (d, *J* = 8.0 Hz, 1H), 4.93 (s, 2H); ¹³C NMR (75 MHz, CDCl₃) δ 183.2, 158.3, 150.7, 138.3, 134.5, 129.1, 128.2, 127.4, 125.4, 123.9, 117.7, 111.0, 44.0; ESI-MS *m/z*: [M + H]⁺ 238.0; mp 129.8-130.8 °C. The spectroscopic data are consistent with those reported in literature [26].

5.2.26. 1-(Pyridin-4-ylmethyl)indoline-2,3-dione (**23b**).

To a solution of **19** (860 mg, 3.39 mmol) in diethyl ether (10 mL) a 10% solution of NaHCO₃ (10 mL) was added. The organic layer was extracted, dried over Na₂SO₄, concentrated *in vacuo* and the residue was dissolved in dry DMF (2 mL). In another flask, a solution of isatin (500 mg, 3.39 mmol) in dry DMF (2 mL), cooled at 0 °C, was treated with a 60% dispersion of NaH in mineral oil (163 mg, 4.07 mmol) and stirred at the same temperature for 30 min. After this time, the previously prepared solution of **19** (free base in dry DMF) was added and the reaction was allowed to reach 25 °C and stirred for 12 h. Then a saturated solution of NH₄Cl (5 mL) was added and the mixture was extracted with EtOAc (3 x 5 mL). The combined organic layers were washed with brine (10 mL), dried over Na₂SO₄ and concentrated *in vacuo*. The crude was purified by chromatography on silica gel (EtOAc) affording **23b** (311 mg, 38% yield) as an orange solid. ¹H NMR (300 MHz, CDCl₃) δ 8.50 (d, *J* = 6.1 Hz, 2H), 7.56 (dd, *J* = 7.5, 1.4 Hz, 1H), 7.51 – 7.34 (m, 1H), 7.20 (d, *J* = 6.2 Hz, 2H), 7.06 (t, *J* = 7.6 Hz, 1H), 6.66 (d, *J* = 7.9 Hz, 1H), 4.88 (s, 2H); ESI-MS *m/z*: [M + H]⁺ 239.0.

5.2.27. 1-Benzyl-3-hydroxy-4-phenylquinolin-2(1H)-one (**24a**).

Starting from benzaldehyde (67 mg, 0.62 mmol) and **23a** (150 mg, 0.62 mmol), the title compound was obtained following the procedure previously described for compound **13a**. The crude was purified by chromatography on silica gel (25% in EtOAc in petroleum ether) giving **24a** (78 mg, 38%) as a brown solid. ¹H NMR (400 MHz, DMSO-*d*₆) δ 9.33 (s, 1H), 7.90 – 6.90 (m, 14H), 5.65 (s, 2H); ESI-MS *m/z*: 328.0.

5.2.28. 3-Hydroxy-4-phenyl-1-(pyridin-4-ylmethyl)quinolin-2(1H)-one (**24b**).

Starting from benzaldehyde (53 mg, 0.62 mmol) and **23b** (120 mg, 0.50 mmol), the title compound was obtained following the procedure previously described for compound **13a**. The crude was purified by chromatography on silica gel (EtOAc) giving **24b** (64 mg, 39%) as a brown solid. ¹H NMR (300 MHz,

CDCl₃) δ 8.58 (d, J = 6.2 Hz, 2H), 7.62 – 7.38 (m, 6H), 7.37 – 7.28 (m, 1H), 7.22 – 7.13 (m, 4H), 7.10 (s, 1H), 5.69 (s, 2H); ESI-MS m/z : [M + H]⁺ 329.

5.2.29. *1-Benzyl-3-hydroxy-4-(pyridin-3-yl)quinolin-2(1H)-one (24c)*.

Starting from 3-pyridinecarboxaldehyde (67 mg, 0.62 mmol) and **23a** (150 mg, 0.62 mmol), the title compound was obtained following the procedure previously described for compound **13a**. The crude was purified by chromatography on silica gel (2% MeOH in DCM) giving **24c** (55 mg, 24%) as a red solid. ¹H NMR (300 MHz, CDCl₃) δ 8.73 (s, 2H), 7.88 – 7.77 (m, 1H), 7.53 – 7.43 (m, 1H), 7.41 – 7.22 (m, 9H), 7.21 – 7.11 (m, 1H), 5.70 (s, 2H); ESI-MS m/z : [M + H]⁺ 329.1.

5.2.30. *3-Hydroxy-4-(pyridin-3-yl)-1-(pyridin-4-ylmethyl)quinolin-2(1H)-one (24d)*.

Starting from 3-pyridinecarboxaldehyde (54 mg, 0.503 mmol) and **23b** (120 mg, 0.503 mmol), the title compound was obtained following the procedure previously described for compound **13a**. The crude was purified by chromatography on silica gel (2% MeOH in DCM) giving **24d** (73 mg, 44%) as a red solid. ¹H NMR (300 MHz, CDCl₃) δ 8.85 – 8.40 (m, 4H), 7.80 (d, J = 7.1 Hz, 1H), 7.55 – 7.38 (m, 1H), 7.37 – 7.25 (m, 2H), 7.24 – 7.00 (m, 4H), 5.66 (s, 2H); ESI-MS m/z : [M + H]⁺ 330.1.

5.2.31. *4-(((1-Benzyl-2-oxo-4-phenyl-1,2-dihydroquinolin-3-yl)oxy)methyl)-N-hydroxybenzamide (7d)*.

Starting from **24a** (78 mg, 0.24 mmol) *methyl 4-(((1-benzyl-2-oxo-4-phenyl-1,2-dihydroquinolin-3-yl)oxy)methyl)benzoate* was obtained following the procedure previously described for compound **14a**. The crude was purified by chromatography on silica gel (50% EtOAc in petroleum ether) giving the intermediate (70 mg, 62%) as a dark yellow oil. ¹H NMR (300 MHz, CDCl₃) δ 7.92 – 7.80 (m, 2H), 7.55 – 7.40 (m, 3H), 7.40 – 7.19 (m, 10H), 7.16 – 6.99 (m, 3H), 5.68 (s, 2H), 5.22 (s, 2H), 3.90 (s, J = 8.5 Hz, 3H); ESI-MS m/z : [M + H]⁺ 476.0. Starting from this intermediate (20 mg, 0.04 mmol) the title compound was obtained following the procedure previously described for compound **7a**. The crude was purified by chromatography on silica gel (0.1% NH₄OH, 10% MeOH in DCM) giving **7d** (9 mg, 45%). ¹H NMR (300 MHz, DMSO-*d*₆) δ 11.14 (s, 1H), 8.97 (s, 1H), 7.63 – 7.19 (m, 14H), 7.19 – 7.00 (m, 4H), 5.64 (s, 2H), 5.10 (s, 2H); ¹³C NMR (75 MHz, DMSO-*d*₆) δ 164.3, 159.0, 143.4, 140.5, 138.2, 137.1, 136.6, 133.6, 132.5, 129.8, 129.6, 129.1, 128.8, 128.6 (2C), 128.1, 127.6, 127.2, 127.1, 123.0, 121.1, 115.7, 73.0, 45.8; ESI-MS m/z : [M + H]⁺ 477.0. FT-IR (neat) ν_{\max} 3259, 2923, 2854, 1719, 1634, 1597, 1453, 1013 cm⁻¹; mp decomposing; Anal. (C₃₀H₂₄N₂O₄) C, H, N.

5.2.32. *N-Hydroxy-4-(((2-oxo-4-phenyl-1-(pyridin-4-ylmethyl)-1,2-dihydroquinolin-3-yl)oxy)methyl)benzamide (7e)*.

Starting from **24b** (71 mg, 0.21 mmol) *methyl 4-(((2-oxo-4-phenyl-1-(pyridin-4-ylmethyl)-1,2-dihydroquinolin-3-yl)oxy)methyl)benzoate* was obtained following the procedure previously described for compound **14a**. The crude was purified by chromatography on silica gel (50% EtOAc in petroleum ether)

giving the intermediate (31 mg, 30%). ¹H NMR (300 MHz, CDCl₃) δ 8.56 (d, *J* = 5.2 Hz, 2H), 7.85 (d, *J* = 8.2 Hz, 2H), 7.52 – 7.41 (m, 3H), 7.31 (m, 4H), 7.19 – 7.00 (m, 6H), 5.65 (s, 2H), 5.17 (s, 2H), 3.89 (s, 3H); ¹³C NMR (75 MHz, CDCl₃) δ 159.8, 159.1, 150.0, 149.1, 143.7, 141.6, 137.9, 136.7, 135.9, 129.6, 129.3, 129.0, 128.9, 128.3, 127.5, 126.9, 126.6, 123.3, 122.8, 120.6, 115.2, 73.1, 52.1, 46.5; ESI-MS *m/z*: [M + H]⁺ 477.0; mp 147.5-150.1 °C. Starting from this intermediate (10 mg, 0.02 mmol) the title compound was obtained following the procedure previously described for compound **7a**. The crude was purified by chromatography on silica gel (0.1% NH₄OH, 10% MeOH in DCM) giving **7e** (8 mg, 90%). ¹H NMR (300 MHz, MeOD) δ 8.48 (d, *J* = 5.2 Hz, 2H), 7.63 – 7.23 (m, 12H), 7.21 – 7.01 (m, 3H), 5.77 (s, 2H), 5.07 (s, 2H); ¹³C NMR (75 MHz, MeOD) δ 168.6, 159.8, 148.9, 147.4, 142.9, 140.6, 139.9, 136.2, 133.1, 131.6, 129.4, 129.3, 129.1, 128.1, 128.0, 127.7, 127.3, 126.5, 122.8, 121.3, 114.7, 73.0, 45.0. ESI-MS *m/z*: [M + H]⁺ 478.0; HRMS-ESI *m/z*: calcd for C₂₉H₂₄N₃O₄⁺ [M+H]⁺: 478,1761; found: 478.1749. FT-IR (neat) *v*_{max} 3479, 3197, 2960, 2855, 1632, 1599, 1377, 1260, 1088, 1009 cm⁻¹; mp decomposition; Anal. (C₂₉H₂₃N₃O₄) C, H, N.

5.2.33. 4-(((1-Benzyl-2-oxo-4-(pyridin-3-yl)-1,2-dihydroquinolin-3-yl)oxy)methyl)-*N*-hydroxybenzamide (**7i**). Starting from **24c** (56 mg, 0.17 mmol) methyl 4-(((1-benzyl-2-oxo-4-(pyridin-3-yl)-1,2-dihydroquinolin-3-yl)oxy)methyl)benzoate was obtained following the procedure previously described for compound **14a**. The crude was purified by chromatography on silica gel (2% MeOH in DCM) giving the intermediate (53 mg, 65%). ¹H NMR (300 MHz, CDCl₃) δ 8.69 (s, 1H), 8.51 (s, 1H), 7.86 (d, *J* = 8.2 Hz, 2H), 7.53 (t, *J* = 10.4 Hz, 1H), 7.46 – 7.20 (m, 8H), 7.20 – 7.01 (m, 4H), 5.67 (s, 2H), 5.37 – 5.12 (m, 2H), 3.89 (s, 3H); ESI-MS *m/z*: [M + H]⁺ 477.0. Starting from this intermediate (53 mg, 0.11 mmol) the title compound was obtained following the procedure previously described for compound **7a**. The crude was purified by chromatography on silica gel (0.1% NH₄OH, 10% MeOH in DCM) giving **7i** (33 mg, 62%). ¹H NMR (300 MHz, DMSO-*d*₆) δ 11.15 (s, 1H), 8.98 (s, 1H), 8.67 (d, *J* = 3.6 Hz, 1H), 8.49 (s, 1H), 7.79 – 7.65 (m, 1H), 7.59 (d, *J* = 8.2 Hz, 2H), 7.54 – 7.38 (m, 3H), 7.38 – 7.20 (m, 5H), 7.20 – 6.96 (m, 4H), 5.66 (s, 2H), 5.18 (s, 2H) ¹³C NMR (75 MHz, DMSO-*d*₆) δ 164.3, 158.8, 150.1, 149.7, 143.9, 140.2, 137.7, 137.0, 136.6, 134.8, 132.7, 129.8, 129.6, 129.2, 128.2, 127.6, 127.2, 127.1, 126.9, 123.9, 123.2, 120.7, 115.9, 73.0, 45.8; ESI-MS *m/z*: [M + H]⁺ 477.0 Anal; (C₂₉H₂₃N₃O₄) C, H, N.

5.2.34. *N*-Hydroxy-4-(((2-oxo-4-(pyridin-3-yl)-1-(pyridin-4-ylmethyl)-1,2-dihydroquinolin-3-yl)oxy)methyl)benzamide (**7j**).

Starting from **24d** (67 mg, 0.20 mmol) methyl 4-(((2-oxo-4-(pyridin-3-yl)-1-(pyridin-4-ylmethyl)-1,2-dihydroquinolin-3-yl)oxy)methyl)benzoate was obtained following the procedure previously described for compound **14a**. The crude was purified by chromatography on silica gel (2% MeOH in DCM) giving the intermediate (31 mg, 32%). ¹H NMR (300 MHz, CDCl₃) δ 8.70 (dt, *J* = 8.3, 4.1 Hz, 1H), 8.63 – 8.42 (m, 2H), 8.11 – 7.94 (m, 1H), 7.85 (d, *J* = 8.2 Hz, 2H), 7.61 – 7.45 (m, 2H), 7.46 – 7.29 (m, 1H), 7.29 – 6.97 (m, 7H), 5.65 (s, 2H), 5.35 – 5.08 (m, 2H), 3.89 (s, 3H). ESI-MS *m/z*: [M + H]⁺ 478.0. Starting from this

intermediate (30 mg, 0.06 mmol) the title compound was obtained following the procedure previously described for compound **7a**. The crude was purified by chromatography on silica gel (0.1% NH₄OH, 10% MeOH in DCM) giving **7j** (18 mg, 60%). ¹H NMR (300 MHz, MeOD) δ 8.63 (d, *J* = 4.1 Hz, 1H), 8.49 (d, *J* = 5.5 Hz, 2H), 8.38 (s, 1H), 7.72 (d, *J* = 7.8 Hz, 1H), 7.62 – 7.34 (m, 5H), 7.30 (d, *J* = 5.6 Hz, 2H), 7.19 (dd, *J* = 8.4, 5.4 Hz, 2H), 7.10 (d, *J* = 8.1 Hz, 2H), 5.78 (s, 2H), 5.25 – 5.03 (m, 2H); ¹³C NMR (75 MHz, MeOD) δ 166.3, 159.3, 149.3, 149.0, 148.5, 148.1, 147.1, 143.3, 140.2, 138.4, 136.2, 135.5, 131.9, 130.0, 129.6, 128.3, 126.7, 123.7, 123.1, 122.0, 120.6, 115.0, 72.9, 45.0; ESI-MS *m/z*: [M + H]⁺ 479.0; Anal. (C₂₈H₂₂N₄O₄) C, H, N.

5.2.36. 1-Benzyl-N-phenylpiperidin-4-amine (**27**) [28].

To a solution of aniline (303 μL, 3.35 mmol) in DCM (10 mL) **26** (800 mg, 4.02 mmol) and AcOH (19 μL, 0.34 mmol) were added. The mixture was stirred at 20 °C for 4 h, then NaBH(OAc)₃ (1.07 g, 5.03 mmol) was added and the reaction stirred at 25 °C for 12 h. After this time a saturated solution of NaHCO₃ (10 mL) was added and the mixture was extracted with DCM (3 x 10 mL). The combined organic layers were dried over Na₂SO₄ and concentrated in vacuo. The residue was purified by chromatography on silica gel (10% EtOAc in petroleum ether) affording **27** (950 mg, 89%) as a white solid. ¹H NMR (300 MHz, CDCl₃) δ 7.58 – 7.30 (m, 5H), 7.30 – 7.15 (m, 2H), 6.84 – 6.71 (m, 1H), 6.71 – 6.58 (m, 2H), 3.60 (s, 2H), 3.36 (m, 1H), 2.92 (m, 2H), 2.36 – 1.99 (m, 4H), 1.68 – 1.42 (m, 2H); ESI-MS *m/z*: [M + H]⁺ 267.1. The spectroscopic data are consistent with those reported in literature [28].

5.2.37. 1-(1-Benzylpiperidin-4-yl)indoline-2,3-dione (**28**) [28].

To a solution of oxalyl chloride (316 μL, 7.14 mmol) in dry DCM (6 mL) cooled at 0 °C, a solution of **27** (950 mg, 3.57 mmol) in DCM (4 mL) was slowly added. The reaction was allowed to reach 25 °C and stirred for 2 h, then the solvent was evaporated. The residue was dissolved in DCM (5 mL), cooled at 0 °C and AlCl₃ (952 mg, 7.14 mmol) was added. The new mixture was stirred at 40 °C for 2 h, then poured on ice and neutralized with a saturated solution of NaHCO₃ (15 mL). The mixture was filtered through paper and extracted with DCM (3 x 10 mL). The combined organic layers were dried over Na₂SO₄ and concentrated in vacuo. The residue was purified by chromatography on silica gel (3% MeOH in DCM) affording **28** (600 mg, 52%) as a red solid. ¹H NMR (300 MHz, CDCl₃) δ 7.72 – 7.48 (m, 2H), 7.46 – 7.15 (m, 6H), 7.09 (m, 1H), 4.34 – 4.05 (m, 1H), 3.57 (s, 2H), 3.04 (d, *J* = 11.3 Hz, 2H), 2.58 – 2.27 (m, 2H), 2.27 – 2.00 (m, 2H), 1.75 (d, *J* = 12.3 Hz, 2H); ¹³C NMR (75 MHz, CDCl₃) δ 183.5, 158.0, 150.3, 138.2, 130.7, 129.1, 128.3, 127.3, 125.6, 123.4, 117.9, 112.0, 62.7, 52.8, 50.9 (2C), 28.1; ESI-MS *m/z*: [M + H]⁺ 321.1; mp 158.1-161.6 °C. The spectroscopic data are consistent with those reported in literature [28].

5.2.38. 4-(((1-(1-Benzylpiperidin-4-yl)-2-oxo-4-phenyl-1,2-dihydroquinolin-3-yl)oxy)methyl)-N-hydroxybenzamide (**7f**).

Compound **28** (200 mg, 0.62 mmol) was submitted to the ring expansion reaction with benzaldehyde (63 μ L, 0.62 mmol) following the same condition described for the synthesis of compound **13a**. The purification of the crude by chromatography on silica gel (5% MeOH in DCM) afforded *1-(1-benzylpiperidin-4-yl)-3-hydroxy-4-phenylquinolin-2(1H)-one* (140 mg, 55%) as a red solid. ^1H NMR (300 MHz, CDCl_3) δ 7.81 (s, 1H), 7.62 – 7.21 (m, 12H), 7.21 – 7.01 (m, 2H), 3.77 – 3.46 (m, 3H), 3.26 – 2.82 (m, 4H), 2.41 – 2.19 (m, 2H), 1.89 – 1.69 (m, 2H).; ESI-MS m/z : $[\text{M} + \text{H}]^+$ 411.1. This intermediate (140 mg, 0.59 mmol) was subjected to the alkylation procedure with methyl 4-(bromomethyl)benzoate (263 mg, 0.88 mmol) previously described for compound **14a**. Purification of the crude by chromatography on silica gel (3% MeOH in DCM) afforded *methyl 4-(((1-(1-benzylpiperidin-4-yl)-2-oxo-4-phenyl-1,2-dihydroquinolin-3-yl)oxy)methyl)benzoate* (50 mg, 15%) as a pale red solid. ^1H NMR (300 MHz, CDCl_3) δ 7.84 (d, $J = 8.3$ Hz, 3H), 7.57 – 7.16 (m, 12H), 7.16 – 6.99 (m, 3H), 5.10 (s, 2H), 3.88 (s, 3H), 3.65 (s, 2H), 3.13 (s, 5H), 2.31 (s, 2H), 1.81 (d, $J = 12.3$ Hz, 2H); ESI-MS m/z : $[\text{M} + \text{H}]^+$ 559.2. This latter intermediate (16 mg, 0.03 mmol) was submitted to the reaction with a 50% solution of NH_2OH in water (190 μ L, 2.87 mmol) previously described for compound **7a**. Purification of the crude by chromatography on silica gel (0.1% NH_4OH , 10% MeOH in DCM) affording **7f** (10 mg, 62%) as a brown solid. ^1H NMR (300 MHz, MeOD) δ 7.89 (s, 1H), 7.69 – 7.26 (m, 11H), 7.26 – 6.91 (m, 6H), 4.97 (s, 2H), 3.72 (s, 2H), 3.17 (d, $J = 12.1$ Hz, 5H), 2.43 (s, 2H), 1.77 (d, $J = 11.7$ Hz, 2H); ^{13}C NMR (75 MHz, MeOD) δ 166.4, 160.2, 143.2, 140.7, 138.9, 136.3, 133.3, 131.5, 129.5, 129.4, 128.7, 128.1, 128.0 (2C), 127.4, 126.5, 122.2, 121.7, 72.8, 62.0, 53.0, 29.3, 26.8; ESI-MS m/z : $[\text{M} + \text{H}]^+$ 560.1; FT-IR (neat) ν_{max} 3209, 2922, 2853, 1722, 1632, 1595, 1455, 1262, 1117, 1011 cm^{-1} ; mp decomposition; Anal. ($\text{C}_{35}\text{H}_{33}\text{N}_3\text{O}_4$) C, H, N.

5.2.39. *1-(4-(1,3-Dioxolan-2-yl)benzyl)indoline-2,3-dione (29)*.

Starting from isatin (500 mg, 3.40 mmol) and **22** (1.24 g, 5.10 mmol) the title compound was synthesized following the same procedure to obtain compound **23a**. The residue was used in the next step without further purifications and affording **29** (1.36 g, quantitative yield) as a red solid. ^1H NMR (300 MHz, CDCl_3) δ 7.68 – 7.56 (m, 1H), 7.56 – 7.30 (m, 5H), 7.09 (td, $J = 7.5, 0.8$ Hz, 1H), 6.80 – 6.66 (m, 1H), 5.78 (s, 1H), 4.94 (s, 2H), 4.22 – 3.91 (m, 4H).

5.2.40. *1-(4-(1,3-Dioxolan-2-yl)benzyl)-3-hydroxy-4-phenylquinolin-2(1H)-one (30a)*.

Starting from **29** (500 mg, 1.62 mmol) the title compound was obtained following the procedure described to get **13a**. The residue was purified by chromatography on silica gel (33% EtOAc in petroleum ether) affording **30a** (310 mg, 48%) as a brown solid. ^1H NMR (300 MHz, CDCl_3) δ 7.70 – 7.46 (m, 6H), 7.46 – 7.26 (m, 5H), 7.26 – 7.02 (m, 2H), 5.81 (s, 1H), 5.72 (s, 2H), 4.25 – 3.94 (m, 4H); ESI-MS m/z : $[\text{M} + \text{H}]^+$ 400.0.

5.2.41. *1-(4-(1,3-Dioxolan-2-yl)benzyl)-3-hydroxy-4-(pyridin-3-yl)quinolin-2(1H)-one (30b)*.

Starting from **29** (500 mg, 1.62 mmol) the title compound was obtained following the procedure described to get **13b**. The residue was purified by chromatography on silica gel (3% MeOH in DCM) affording **30b** (310 mg, 48%) as a brown solid. ¹H NMR (300 MHz, CDCl₃) δ 8.75 (d, *J* = 2.0 Hz, 2H), 8.10 (s, 1H), 7.84 (d, *J* = 7.8 Hz, 1H), 7.60 – 7.42 (m, 3H), 7.40 – 7.25 (m, 5H), 7.25 – 7.06 (m, 1H), 5.80 (s, 1H), 5.72 (s, 2H), 4.23 – 3.92 (m, 4H); ESI-MS *m/z*: [M + H]⁺ 401.0.

5.2.42. *Methyl 4-(((1-(4-(1,3-dioxolan-2-yl)benzyl)-2-oxo-4-phenyl-1,2-dihydroquinolin-3-yl)oxy)methyl)benzoate (31a)*.

Starting from **30a** (310 mg, 0.78 mmol) the title compound was obtained following the procedure described to get **14a**. The residue was purified by chromatography on silica gel (50% EtOAc in petroleum ether) affording **31a** (340 mg, 80%) as a yellow oil. ¹H NMR (300 MHz, CDCl₃) δ 7.85 (d, *J* = 8.3 Hz, 2H), 7.55 – 7.38 (m, 5H), 7.38 – 7.17 (m, 7H), 7.17 – 6.94 (m, 3H), 5.77 (s, 1H), 5.67 (s, 2H), 5.19 (s, 2H), 4.20 – 3.92 (m, 4H), 3.87 (s, 3H); ESI-MS *m/z*: [M + H]⁺ 548.0.

5.2.43. *Methyl 4-(((1-(4-(1,3-dioxolan-2-yl)benzyl)-2-oxo-4-(pyridin-3-yl)-1,2-dihydroquinolin-3-yl)oxy)methyl)benzoate (31b)*.

Starting from **30b** (310 mg, 0.77 mmol) the title compound was obtained following the procedure described to get **14a**. The residue was purified by chromatography on silica gel (33% Petroleum ether in EtOAc) affording **31b** (231 mg, 55%) as a red oil. ¹H NMR (300 MHz, CDCl₃) δ 8.68 (dd, *J* = 5.0, 1.7 Hz, 1H), 8.49 (d, *J* = 2.1 Hz, 1H), 7.85 (d, *J* = 8.3 Hz, 2H), 7.63 – 7.20 (m, 8H), 7.20 – 6.91 (m, 4H), 5.76 (s, 1H), 5.66 (s, 2H), 5.37 – 5.08 (m, 2H), 4.19 – 3.93 (m, 4H), 3.86 (s, 3H); ESI-MS *m/z*: [M + H]⁺ 549.0.

5.2.44. *4-(((1-(4-((Diethylamino)methyl)benzyl)-2-oxo-4-phenyl-1,2-dihydroquinolin-3-yl)oxy)methyl)-N-hydroxybenzamide (7g)*.

To a solution of **31a** (230 mg, 0.62 mmol) in THF (5 mL) a 1 N solution of HCl in water (5 mL) was added. The reaction was stirred at 25 °C for 1 h, then a saturated solution of NaHCO₃ (10 mL) was added and the mixture was extracted with EtOAc (3 x 10 mL). The combined organic layers were dried over Na₂SO₄ and concentrated in vacuo. The residue was used in the next step without further purifications. *Methyl 4-(((1-(4-formylbenzyl)-2-oxo-4-phenyl-1,2-dihydroquinolin-3-yl)oxy)methyl)benzoate* (310 mg, quantitative yield) was obtained as a yellow oil. ¹H NMR (300 MHz, CDCl₃) δ 9.99 (s, 1H), 7.98 – 7.72 (m, 4H), 7.60 – 6.91 (m, 13H), 5.74 (s, 2H), 5.19 (s, 2H), 3.90 (s, 3H). This intermediated was dissolved in DCM (5 mL) and dimethylamine (96 μL, 0.93 mmol) and AcOH (4 μL, 0.06 mmol) were added. This mixture was stirred at 25 °C for 2 h then a NaBH(OAc)₃ (197 mg, 0.93 mmol) was added and the reaction was stirred at 25 °C for 12 h. After this time, a saturated solution of NaHCO₃ (5 mL) was added and the mixture was extracted with DCM (3 x 5 mL). The combined organic layers were dried over Na₂SO₄ and concentrated in vacuo. The residue was purified by chromatography on silica gel (5% MeOH in DCM) affording *methyl 4-(((1-(4-((diethylamino)methyl)benzyl)-2-oxo-4-phenyl-1,2-dihydroquinolin-3-yl)oxy)methyl)benzoate* (204 mg,

59%) as a colorless oil. ¹H NMR (300 MHz, CDCl₃) δ 7.86 (d, *J* = 8.3 Hz, 2H), 7.57 – 7.42 (m, 3H), 7.42 – 7.18 (m, 9H), 7.18 – 6.95 (m, 3H), 5.84 – 5.48 (m, 2H), 5.21 (s, 2H), 3.88 (s, 3H), 3.56 (s, 2H), 2.53 (q, *J* = 7.1 Hz, 4H), 1.04 (t, *J* = 7.1 Hz, 6H); ESI-MS *m/z*: [M + H]⁺ 561.2. Starting from this intermediate (100 mg, 0.18 mmol) the title compound was obtained following the procedure described to get **7a**. The residue was purified by chromatography on silica gel (0.1% NH₄OH, 10% MeOH in DCM) affording **7g** (75 mg, 74%) as a white solid. ¹H NMR (300 MHz, MeOD) δ 7.65 – 7.48 (m, 5H), 7.48 – 7.35 (m, 4H), 7.34 – 7.20 (m, 5H), 7.19 – 6.97 (m, 3H), 5.74 (s, 2H), 5.08 (s, 2H), 3.86 (s, 2H), 2.78 (q, *J* = 7.2 Hz, 4H), 1.16 (t, *J* = 7.2 Hz, 6H); ¹³C NMR (75 MHz, DMSO-*d*₆) δ 164.2, 159.0, 143.5, 140.5, 139.4, 138.2, 136.6, 135.3, 133.6, 132.5, 129.8, 129.6, 129.2, 128.8, 128.6, 128.1, 127.2, 127.1, 126.9, 122.9, 121.1, 115.7, 73.0, 57.0, 46.5, 45.6, 12.0; ESI-MS *m/z*: [M + H]⁺ 562.2. HRMS-ESI *m/z*: calcd for C₃₅H₃₆N₃O₄⁺ [M+H]⁺: 562,2700; found: 562.2678; FT-IR (neat) ν_{\max} 3222, 2963, 2925, 1799, 1719, 1636, 1596, 1454, 1287, 1172, 1121, 1016 cm⁻¹; mp 180.8-182.9 °C, decomposition; Anal. (C₃₅H₃₅N₃O₄) C, H, N.

5.2.45. *4-(((1-(4-((Diethylamino)methyl)benzyl)-2-oxo-4-(pyridin-3-yl)-1,2-dihydroquinolin-3-yl)oxy)methyl)-N-hydroxybenzamide (7k)*.

Starting from **31b** (230 mg, 0.42 mmol) *methyl 4-(((1-(4-((diethylamino)methyl)benzyl)-2-oxo-4-(pyridin-3-yl)-1,2-dihydroquinolin-3-yl)oxy)-methyl)benzoate* was obtained following the procedure described for **7g**. The residue was purified by chromatography on silica gel (10% MeOH in DCM) affording *methyl 4-(((1-(4-((diethylamino)methyl)benzyl)-2-oxo-4-(pyridin-3-yl)-1,2-dihydroquinolin-3-yl)oxy)-methyl)benzoate* (110 mg, 47% (over two steps)) as a brown oil. ¹H NMR (300 MHz, CDCl₃) δ 8.69 (dd, *J* = 4.7, 1.7 Hz, 1H), 8.50 (s, 1H), 7.96 – 7.75 (m, 2H), 7.62 – 7.45 (m, 1H), 7.45 – 6.95 (m, 11H), 5.64 (s, 2H), 5.37 – 5.12 (m, 2H), 3.87 (s, 3H), 3.55 (s, 2H), 2.63 – 2.35 (m, 4H), 1.15 – 0.86 (m, 6H); ESI-MS *m/z*: [M + H]⁺ 562.2. Starting from this intermediate (55 mg, 0.10 mmol) the title compound was obtained following the procedure described to get **7a**. The residue was purified by chromatography on silica gel (0.1% NH₄OH, 10% MeOH in DCM) affording **7k** (45 mg, 80%) as a white solid. ¹H NMR (300 MHz, MeOD) δ 8.63 (dd, *J* = 4.9, 1.7 Hz, 1H), 8.36 (dd, *J* = 2.2, 0.9 Hz, 1H), 7.71 (m, 1H), 7.65 – 7.41 (m, 5H), 7.34 (d, *J* = 8.1 Hz, 2H), 7.25 (d, *J* = 8.1 Hz, 2H), 7.21 – 7.00 (m, 4H), 5.90 – 5.59 (m, 2H), 5.27 – 5.11 (m, 2H), 3.64 (s, 2H), 2.58 (q, *J* = 7.1 Hz, 4H), 1.08 (t, *J* = 7.2 Hz, 6H); ¹³C NMR: (75 MHz, DMSO-*d*₆) δ 164.3, 158.8, 150.0 (2C), 149.7, 143.9, 140.2, 139.0, 137.7, 136.6, 135.3, 134.8, 132.6, 129.8, 129.5, 129.4, 128.2, 127.2, 127.0, 123.9, 123.2, 120.6, 115.9, 73.0, 56.8, 46.4, 45.7, 11.8; ESI-MS *m/z*: [M + H]⁺ 563.2. FT-IR (neat) ν_{\max} 3228, 2958, 2922, 2818, 1638, 1597, 1456, 1307, 1182, 1123, 1019 cm⁻¹; mp 184.5-188.5 °C, decomposition; Anal. (C₃₄H₃₄N₄O₄) C, H, N.

5.3. Molecular Modeling

5.3.1. Proteins and Ligands Preparation

The crystal structures of *h*HDAC6, *h*HDAC1 and *z*fHDAC6 were downloaded from the Protein Data Bank (PDB) with the codes 5EDU, 4BKX and 6THV respectively, and accurately prepared as previously reported

[4,15,38]. The proteins were exploited in the molecular docking calculation. The 3D structures of ligands were built in Maestro 10.1 (Schrödinger, LLC, New York, NY, 2015), and then minimized by means of MacroModel software employing the OPLS-2005 force field. The Generalized-Born/Surface-Area model was employed to simulate the solvent effects using the analytical [39], and no cutoff for nonbonded interactions was selected. Polak-Ribiere conjugate gradient (PRCG) method with 1000 maximum iterations and 0.001 gradient convergence threshold was employed. The quinolone derivatives were treated by LigPrep application (LigPrep version 3.3, Schrödinger, LLC, New York, NY, 2015) in order to generate the most probable ionization state at cellular pH (7.4 ± 0.2) as reported by us previously [40,41]. We used a neutral hydroxamic acid moiety of the quinolone compounds, since the hydroxamic acid proton should not be transferred in HDAC isoforms containing histidines in the binding site close to the reactive metal center, as in the case of HDAC1 and HDAC6.

5.3.2. Molecular Docking and Molecular Properties Prediction

Using the ligands and proteins prepared as above-mentioned we employed Glide software (Glide, version 6.6, Schrödinger, LLC, New York, NY, 2015) to perform the docking studies presented in this paper, applying Glide standard precision (SP) scoring function. Energy grids were prepared using default value of protein atom scaling factor (1.0 \AA) within a cubic box centered on the zinc ion which roughly represents the center of the active sites [14,15]. The ligands were docked into the enzymes after grid generation introducing the metal constraints. The number of poses entered to post-docking minimization was set to 50. Glide SP score was evaluated. Molecular properties were evaluated by means of QikProp (QikProp, version 4.3, Schrödinger, LLC, New York, NY, 2015).

5.2. Solubility and chemical stability studies

5.2.1. HPLC analysis of compounds 6b and 7e,k

For the HPLC analysis a Chromolith HPLC column RP-18 was employed. The runs were performed by a gradient elution starting from a mixture 20% MeCN (0.1% TFA as phase modifier) in H₂O (0.1% TFA as phase modifier) to 90% MeCN (0.1% TFA) in H₂O (0.1% TFA) in 15 min. The flow speed was settled at 1.0 mL/min and the temperature was maintained at 25 °C. The volume of injection of the sample was 10 mL and the wavelength selected for the detection was 254 nm. The retention times obtained following this protocol for compounds **6b** and **7e,k** were 7.3 min, 5.6 min and 3.7 min, respectively.

5.2.2. Solubility assay and chemical stability at 25 °C

A stock solution for each tested compound was prepared dissolving the sample in DMSO to a final concentration of 10 mM. From the stock solution, three samples were prepared: one was used as the standard solution and the other two as the test solutions at pH 3.0 and pH 7.4. The sample concentration of these solutions was 250 μM with a DMSO content of 2.5% (v/v). The standard solution was prepared by dilution of the stock solution in PBS-buffer solution (MeCN/water, 60:40); the dilution of the stock solution in 50

mM acetic acid afforded the samples solution at pH 3.0; and the dilution of the stock solution in 50 mM aqueous PBS-buffer afforded the sample' solution at pH 7.4. These suspension/solutions were sealed and left for 24 h at 25 °C under orbital shaking to achieve “pseudothermodynamic equilibrium”. After that time, the solutions were filtered using PTFE filters and successively diluted 1:2 with the buffer solution used for the preparation of the samples. Then they were analyzed by HPLC/UV/ DAD, using UV detection at 254 nm for quantitation. Solubility was calculated by comparing areas of the sample and of the standard:

$$S = \frac{A_{smp} \times FD \times C_{st}}{A_{st}}$$

S = solubility of the compound (μM); A_{smp} = UV area of the sample solution; FD = dilution factor (2); C_{st} = standard concentration (250 μM); A_{st} = UV area of the standard solution.

For each sample the analysis was performed in triplicate and the solubility result reported was obtained from the average of the three values. The same sample solutions were prepared to evaluate the chemical stability of the compounds after 24 h at 25 °C and analyzed by HPLC/UV/DAD, using UV detection at 254 nm for quantitation. Stability was calculated by comparing the area of the peak at T₀ and the area of the peak of the same solution after 24 h. A stability percentage value was calculated by this method at pH 3.0 and pH 7.4 for each compound by applying the following formula:

$$\%_{remaining} = \frac{AC_{24}}{AC_{T_0}} \times 100$$

AC₂₄ = area of the sample after 24 h at 25 °C; AC_{T₀} = area of the sample at T₀. For each sample the analysis was performed in triplicate and the stability result reported was obtained from the average of the three values.

5.3. Biological data

5.3.1. In vitro testing of HDAC1 and HDAC6

OptiPlate-96 black microplates (PerkinElmer) were employed with an assay volume of 60 μL. Human recombinant HDAC1 (BPS Bioscience, Catalog #: 50051) or human recombinant HDAC6 (BPS Bioscience, Catalog #: 50006) were diluted in incubation buffer (50 mM Tris-HCl, pH 8.0, 137 mM NaCl, 2.7 mM KCl, 1 mM MgCl₂ and 1 mg/mL BSA). A total of 52 μL of this dilution were incubated with 3 μL of different concentrations of inhibitors in DMSO and 5 μL of the fluorogenic substrate ZMAL (Z-(Ac)Lys-AMC) [42,43] (126 μM) at 37 °C. After 90 min incubation time, 60 μL of the stop solution (33 μM Trichostatin A and 6 mg/mL trypsin in trypsin buffer [Tris-HCl 50 mM, pH 8.0, NaCl 100 mM]), were added. After a following incubation at 37 °C for 30 min, the fluorescence was measured on a BMG LABTECH POLARstar

OPTIMA plate reader (BMG Labtechnologies, Germany) with an excitation wavelength of 390 nm and an emission wavelength of 460 nm [43,44].

5.3.2. *In vitro* testing of HDAC8

Recombinant human HDAC8 was purchased as part of the Fluor-de-Lys HDAC8 fluorimetric drug discovery kit (Enzo Life Sciences, No. BMLAK518). Dose-response curves were built for each inhibitor in order to estimate the respective IC₅₀. DMSO concentration was kept constant to 0.5% and, for each compound, a control curve (enzymes incubated with DMSO only) was added. The Fluor-de-Lys substrate was used at 50 μM. A preincubation period of 15 min was chosen to keep safe from the possibility of a slow-binding inhibition. Hence, the compounds, substrate, and enzyme (266 nM) were incubated, and the reaction was allowed to proceed for 1 h at 30 °C; 2 μM TSA within 50 μL of 1× Enzo Developer II was added to quench the reaction and the mixture was further incubated for 1 h at 30 °C. Fluorescence was measured in a plate reader (Varioskan Lux, Thermo Fisher Scientific) with excitation wave length at 370 nm and emission at 450 nm. Data were analyzed by nonlinear regression fit using a generalized form of a dose-response curve:[45]

$$y_{res} = y_{min} + \frac{y_{max} - y_{min}}{\left(1 + \frac{[I]}{IC_{50}}\right)}$$

y_{res} = is the residual activity of the enzyme in the presence of inhibitor at concentration [I]; y_{max} = the maximum observed value for the enzyme at zero inhibitor concentration; y_{min} = the minimum observed value for the enzyme at the highest inhibitor concentration. The model did fit three parameters, namely: IC₅₀, y_{max} , and y_{min} .

In addition, since the total enzyme concentration used in the assay (266 nM) was in the same order of magnitude to the obtained IC_{50s} for two out of three inhibitors (namely, **7g** and **7k**), a more accurate model was chosen to fit the experimental data, ultimately to account for the possibility of a tight-binding interaction. The fit model was in the form of the Morrison equation as implemented in Copeland as reported below [45]:

$$\frac{v_i}{v_0} = 1 - \frac{\sqrt{([E] - [I] - K_i^{app})^2 - 4[E][I]}}{2[E]}$$

v_0 and v_i = were the rate observed in the absence or in the presence of the inhibitor at concentration [I], and [E] was kept fixed at 266 nM. It was assumed that the ratio v_i/v_0 was proportional to the signal (arbitrary fluorescence unit) as obtained by using Fluor-de-Lys kit. This model yields apparent inhibitor constant which should be regarded as a better estimate of interaction with respect to IC₅₀.

5.4. Cell-based Assays

5.4.1 Cell lines

HCT-116, colon cancer cells were propagated in Dulbecco's Modified Eagle's Medium (Euroclone) with 10% fetal bovine serum (FBS; Euroclone), 2 mM L-glutamine (Euroclone), and antibiotics (100 U/ml penicillin, 100 mg/ml streptomycin; Euroclone). U937, histiocytic lymphoma cells were grown in RPMI-

1640 Medium (Euroclone) containing 4.5 g/L glucose (Euroclone) supplemented with 10% FBS (Euroclone), 100 U/mL penicillin-streptomycin (Euroclone), and 2 mM L-glutamine (Euroclone). The cell lines were purchased from ATCC.

5.4.2 MTT assay

Cell viability was determined using the standard Thiazolyl Blue Tetrazolium Bromide [3-(4,5-dimethylthiazol-2-yl)-2,5-diphenyltetrazolium bromide] (MTT; Sigma) assay. A total of 2.5×10^4 cells/well, plated in a 48-well, were treated, in triplicate, with the compounds **7a**, **7k** and **7g** at 50, 25, 10, 5 and 1 μ M for 12, 24 and 48 h. After induction the MTT solution was added at 0.5 mg/ml for 3 h. For HCT-116, adhesion cells, the supernatant was simply removed, whereas for suspension cells, U937, the plate was first centrifuged for 5 min at 1200 rpm. The purple formazan crystals were dissolved in 100 μ l/well of isopropanol (Carlo Erba Reagents) and the absorbance was read at a wavelength of 570 nm with a TECAN M-200 reader (Tecan). The IC₅₀ was analyzed using GraphPad Prism 7.0 software (GraphPad Software).

5.4.3 Total protein extraction

HCT-116 and U937 cells were treated with the compounds **7a**, **7k** and **7g** at 10 μ M for 12 and 24 h. The cells, after treatment, were harvested and washed twice with PBS (Euroclone), and then were lysed in protein extraction buffer containing H₂O with 50 mM Tris HCl pH 8.0 solution, 5 mM EDTA, 1% NP40, 150 mM NaCl, 0.5 % sodium deoxycholate, 0.1% SDS, and 1X protein inhibitor proteinase cocktail before use. The cells were then incubated with the extraction buffer for 15 min at 4°C, centrifuged at 13,000 rpm at 4°C for 30 min, and the supernatant was recovered. Total protein extract was determined using a Bradford assay (Bio-Rad).

5.4.4 Protein histone extraction

After treatment with the compounds **7a**, **7k** and **7g**, at the same conditions used for the total protein extract, HCT-116 and U937 cells were lysed in Triton extraction buffer (TEB) containing PBS with 0.5% Triton X-100 (v/v), 2 mM phenylmethylsulfonyl fluoride, and 0.02% (w/v) NaN₃ at a cell density of 10⁷ cells/mL for 10 min on ice and centrifuged (2,000 rpm at 4 °C for 10 min). The supernatant was removed. Then, the pellet was washed with half the volume of TEB and centrifuged at 2000 rpm at 4 °C for 10 min, and, was suspended in 0.2 N HCl overnight at 4 °C on a rolling table. The samples were centrifuged at 2,000 rpm for 10 min at 4 °C and the supernatant was recovered. The histone protein was determined using a Bradford assay (Bio-Rad).

5.4.5 Western blotting

Western blotting analysis was performed by loading 40 μ g of total protein and 5 μ g for histone protein extract at different concentrations of polyacrylamide gels, depending on the antibodies band. Antibodies used were: PARP (46D11, Cell Signaling), Anti-Acetylated Tubulin (T7451, Sigma), Hsp90(AcLys294) (NBP1-

77944, Bio-Techne SRL), H3K9/14ac (ab232952, Abcam), GAPDH (sc-47724; Santa Cruz Biotechnology), H4 (ab10158, Abcam) Semi-quantitative analysis was performed using ImageJ software.

5.4.6 Statistical Analysis

Graphs represent the mean of three independent experiments with an error bar indicating standard deviation. Differences between the treated cells versus control cells were analyzed using GraphPad Prism 7.0 software (GraphPad Software). Statistical analysis was performed by applying one-way analysis of variance (ANOVA) and Dunnett's multiple-comparison test. Differences between groups were considered to be significant at a p-value of < 0.05. **** p-value \leq 0.0001, *** p-value \leq 0.001, ** p-value \leq 0.01, * p-value \leq 0.05, ns p-value > 0.05 vs control cells.

5.5. Mutagenicity assay: Ames test

The TA100 and TA98 strains of *Salmonella typhimurium* were utilized for mutagenicity assay in absence and presence of metabolic activation, i.e. with and without S9 fraction. The tester strains used were selected because they are sensitive and detect a large proportion of known bacterial mutagens and are most commonly used routinely within the pharmaceutical industry [46,47]. The following specific positive controls were used, respectively, with and without S9 fraction: 2-Nitrofluorene (2-NF) 2 μ g/mL + 4-Nitroquinoline *N*-oxide (4-NQO) 0,1 μ g/mL, and 2-aminoanthracene (2-AA) 5 μ g/mL. Approximately 10^7 bacteria were exposed to 6 concentrations of each test sample ranging from ranging from 8 to 160 μ M, as well as to positive and negative controls, for 90 minutes in medium containing sufficient histidine to support approximately two cell divisions. After 90 minutes, the exposure cultures were diluted in pH indicator medium lacking histidine, and aliquoted into 48 wells of a 384-well plate. Within two days, cells which had undergone the reversion to His grew into colonies. Metabolism by the bacterial colonies reduced the pH of the medium, changing the color of that well. This color change can be detected visually. The number of wells containing revertant colonies were counted for each dose and compared to a zero-dose control. Each dose was tested in six replicates. The material was regarded mutagenic if the number of histidine revertant colonies was twice or more than the spontaneous revertant colonies.

5.6. Cytotoxicity assay on NIH3T3 cell line

Cells (5×10^4) suspended in 1 mL of complete medium were seeded in each well of a 24 well round multidish and incubated at 37 °C in an atmosphere of 5% CO₂. After 24 hours of culture, the culture medium was discharged and test samples, solubilized in DMSO, were added to each well at different concentration values. For the evaluation of cytotoxicity, three experiment repeated in six replicates were performed and all compounds were tested at increasing concentrations ranging from 8 to 160 μ M. The samples were set up in six replicates for each tested concentration. Complete medium was used as negative control. Cell viability and proliferation was evaluated by Neutral Red uptake after 24 hours of incubation with NIH3T3 as follows. First, the following solutions were prepared in order to determine the percentage of viable cells:

1. Neutral Red (NR) stock solution: 0.33 g NR dye powder in 100 ml sterile H₂O
2. NR medium: 1.0 mL NR stock solution + 99.0 routine culture medium pre-warmed to 37 °C
3. NR desorb solution: 1% glacial acetic acid solution + 50% ethanol + 49% H₂O

At the end of incubation, the routine culture medium was removed from each plate and the cells were carefully rinsed with 1 ml pre-warmed D-PBS 0.1 M. Plates were then gently blotted with paper towels. 1.0 ml NR medium was added to each dish and further incubated at 37 °C, 95% humidity, 5.0% CO₂ for 3 hours. The cells were checked during incubation for NR crystal formation. After incubation, the NR medium was removed, and the cells were carefully rinsed with 1 mL pre-warmed D-PBS 0.1 M. PBS was decanted and blotted from the dishes and exactly 1 mL NR desorb solution was added to each sample. Plates were placed on a shaker for 20-45 minutes to extract NR from the cells and form a homogeneous solution. During this step the samples were covered to protect them from light. Five minutes after removal from the shaker, absorbance was read at 540 nm with a UV/visible spectrophotometer (Varian Cary 1E).

5.7. Cytotoxicity assay on human PBMC cell line

Cell viability on human PBMC was determined by using the Guava® ViaCount™ Reagent (Luminex Corporation, US). PBMCs were seeded 1.5 x10⁶/mL in complete medium and treated with 15 μM, 45 μM and 90 μM 7G and 7K compounds or vehicle (DMSO) for 24 h and 48 h. The percentage of viable cells was measured by flow cytometry carried out using GUAVA easyCyte cytometer (Luminex Corporation, US). Analysis was conducted with Guava® ViaCount™ software module (Luminex Corporation, US).

Author contributions

The manuscript was written through contribution of all authors. All authors have given approval to the final version of the manuscript.

Declaration of competing interest

The authors declare that they have no known competing financial interests or personal relationships that could have appeared to influence the work reported in this paper.

Acknowledgement

Authors thank Progetto Dipartimento di Eccellenza DBCF-UNISI 2018-2022. A.P.S. Support from the European Union's Horizon 2020 (EU) Research and Innovation Programme under the Marie Skłodowska-Curie grant agreement No. 721906-TRACT is acknowledged. N.R. Tuscany strategic project POR-FSE 2014-2020, 'Medicina di Precisione e Malattie Rare'(MePreMaRe), (ACE-ESCC). G.R. acknowledges the CNR-CNCCS "Rare, Neglected and Poverty Related Diseases - Schistodiscovery Project" (DSB.AD011.001.003). L.A. Support from the MIUR20152TE5PK; EPICHEMPIO CM1406; VALERE: Vanvitelli per la Ricerca; Campania Regional Government Technology Platform Lotta alle Patologie

Oncologiche: iCURE; Campania Regional Government FASE2: IDEAL. MIUR, Proof of Concept POC01_00043.

Appendix A. Supplementary data

Supplementary data to this article can be found online at [xxxx](#)

References

- [1] T. Li, C. Zhang, S. Hassan, X. Liu, F. Song, K. Chen, W. Zhang, J. Yang, Histone deacetylase 6 in cancer, *J. Hematol. Oncol.* 11 (2018) 111. <https://doi.org/10.1186/s13045-018-0654-9>.
- [2] F. Saccoccia, M. Brindisi, R. Gimmelli, N. Relitti, A. Guidi, A. Prasanth, C. Cavella, S. Brogi, G. Chemi, G. Papoff, D. Herp, M. Jung, G. Campiani, S. Gemma, G. Ruberti, Screening and phenotypical characterization of *Schistosoma mansoni* histone deacetylase 8 (SmHDAC8) inhibitors as multi-stage antischistosomal agents histone deacetylase 8 (Sm HDAC8) inhibitors as multi-stage anti- a Institute b Department c Department, *ACS Infect. Dis.* 6 (2020) 100–113. <https://doi.org/10.1021/acsinfecdis.9b00224>.
- [3] M. Brindisi, A.P. Saraswati, S. Brogi, S. Gemma, S. Butini, G. Campiani, Old but Gold: Tracking the New Guise of Histone Deacetylase 6 (HDAC6) Enzyme as a Biomarker and Therapeutic Target in Rare Diseases, *J. Med. Chem.* 63 (2020) 23–39. <https://doi.org/10.1021/acs.jmedchem.9b00924>.
- [4] Y. Hai, D.W. Christianson, Histone deacetylase 6 structure and molecular basis of catalysis and inhibition, *Nat. Chem. Biol.* 12 (2016) 741–747. <https://doi.org/10.1038/nchembio.2134>.
- [5] E. Landucci, M. Brindisi, L. Bianciardi, L.M. Catania, S. Daga, S. Croci, E. Frullanti, C. Fallerini, S. Butini, S. Brogi, S. Furini, R. Melani, A. Molinaro, F.C. Lorenzetti, V. Imperatore, S. Amabile, J. Mariani, F. Mari, F. Ariani, T. Pizzorusso, A.M. Pinto, F.M. Vaccarino, A. Renieri, G. Campiani, I. Meloni, iPSC-derived neurons profiling reveals GABAergic circuit disruption and acetylated α -tubulin defect which improves after iHDAC6 treatment in Rett syndrome, *Exp. Cell Res.* 368 (2018) 225–235. <https://doi.org/https://doi.org/10.1016/j.yexcr.2018.05.001>.
- [6] Y. Hai, S.A. Shinsky, N.J. Porter, D.W. Christianson, Histone deacetylase 10 structure and molecular function as a polyamine deacetylase, *Nat. Commun.* 8 (2017) 15368. <https://doi.org/10.1038/ncomms15368>.
- [7] M. Duvic, J. Vu, Vorinostat: a new oral histone deacetylase inhibitor approved for cutaneous T-cell lymphoma, *Expert Opin. Investig. Drugs.* 16 (2007) 1111–1120. <https://doi.org/10.1517/13543784.16.7.1111>.
- [8] C. Grant, F. Rahman, R. Piekarz, C. Peer, R. Frye, R.W. Robey, E.R. Gardner, W.D. Figg, S.E. Bates, Romidepsin: a new therapy for cutaneous T-cell lymphoma and a potential therapy for solid tumors, *Expert Rev. Anticancer Ther.* 10 (2010) 997–1008. <https://doi.org/10.1586/era.10.88>.
- [9] M.P. Fenichel, FDA approves new agent for multiple myeloma, *J. Natl. Cancer Inst.* 107 (2015) djv165. <https://doi.org/10.1093/jnci/djv165>.
- [10] R.M. Poole, Belinostat: First Global Approval, *Drugs.* 74 (2014) 1543–1554. <https://doi.org/10.1007/s40265-014-0275-8>.
- [11] K. V Butler, J. Kalin, C. Brochier, G. Vistoli, B. Langley, A.P. Kozikowski, Rational Design and Simple Chemistry Yield a Superior, Neuroprotective HDAC6 Inhibitor, Tubastatin A, *J. Am. Chem. Soc.* 132 (2010) 10842–10846. <https://doi.org/10.1021/ja102758v>.
- [12] M. Morgen, R.R. Steimbach, M. Géraldy, L. Hellweg, P. Sehr, J. Ridinger, O. Witt, I. Oehme, C.J.

- Herbst-Gervasoni, J.D. Osko, N.J. Porter, D.W. Christianson, N. Gunkel, A.K. Miller, Design and Synthesis of Dihydroxamic Acids as HDAC6/8/10 Inhibitors, *ChemMedChem*. 15 (2020) 1163–1174. <https://doi.org/10.1002/cmdc.202000149>.
- [13] M. Géraldy, M. Morgen, P. Sehr, R.R. Steimbach, D. Moi, J. Ridinger, I. Oehme, O. Witt, M. Malz, M.S. Nogueira, O. Koch, N. Gunkel, A.K. Miller, Selective Inhibition of Histone Deacetylase 10: Hydrogen Bonding to the Gatekeeper Residue is Implicated, *J. Med. Chem.* 62 (2019) 4426–4443. <https://doi.org/10.1021/acs.jmedchem.8b01936>.
- [14] M. Brindisi, C. Cavella, S. Brogi, A. Nebbioso, J. Senger, S. Maramai, A. Ciotta, C. Iside, S. Butini, S. Lamponi, E. Novellino, L. Altucci, M. Jung, G. Campiani, S. Gemma, Phenylpyrrole-based HDAC inhibitors: synthesis, molecular modeling and biological studies, *Future Med. Chem.* 8 (2016) 1573–1587. <https://doi.org/10.4155/fmc-2016-0068>.
- [15] M. Brindisi, J. Senger, C. Cavella, A. Grillo, G. Chemi, S. Gemma, D.M. Cucinella, S. Lamponi, F. Sarno, C. Iside, A. Nebbioso, E. Novellino, T.B. Shaik, C. Romier, D. Herp, M. Jung, S. Butini, G. Campiani, L. Altucci, S. Brogi, Novel spiroindoline HDAC inhibitors: Synthesis, molecular modelling and biological studies, *Eur. J. Med. Chem.* 157 (2018) 127–138. <https://doi.org/https://doi.org/10.1016/j.ejmech.2018.07.069>.
- [16] A.K. Ghosh, A.M. Veitschegger, S. Nie, N. Relitti, A.J. Macrae, M.S. Jurica, Enantioselective Synthesis of Thailanstatin A Methyl Ester and Evaluation of in Vitro Splicing Inhibition, *J. Org. Chem.* 83 (2018) 5187–5198. <https://doi.org/10.1021/acs.joc.8b00593>.
- [17] J. Szychowski, J.-F. Truchon, Y.L. Bennani, Natural Products in Medicine: Transformational Outcome of Synthetic Chemistry, *J. Med. Chem.* 57 (2014) 9292–9308. <https://doi.org/10.1021/jm500941m>.
- [18] D. Zhang, A. Kanakkanthara, Beyond the Paclitaxel and Vinca Alkaloids: Next Generation of Plant-Derived Microtubule-Targeting Agents with Potential Anticancer Activity, *Cancers (Basel)*. 12 (2020) 1721.
- [19] S. Yuan, J.V. Gopal, S. Ren, L. Chen, L. Liu, Z. Gao, Anticancer fungal natural products: Mechanisms of action and biosynthesis, *Eur. J. Med. Chem.* 202 (2020) 112502. <https://doi.org/https://doi.org/10.1016/j.ejmech.2020.112502>.
- [20] J.M. Kraus, H.B. Tatipaka, S.A. McGuffin, N.K. Chennamaneni, M. Karimi, J. Arif, C.L.M.J. Verlinde, F.S. Buckner, M.H. Gelb, Second Generation Analogues of the Cancer Drug Clinical Candidate Tipifarnib for Anti-Chagas Disease Drug Discovery, *J. Med. Chem.* 53 (2010) 3887–3898. <https://doi.org/10.1021/jm9013136>.
- [21] G. Balasubramanian, N. Kilambi, S. Rathinasamy, P. Rajendran, S. Narayanan, S. Rajagopal, Quinolone-based HDAC inhibitors, *J. Enzyme Inhib. Med. Chem.* 29 (2014) 555–562. <https://doi.org/10.3109/14756366.2013.827675>.
- [22] R.E. Hawtin, D.E. Stockett, J.A.W. Byl, R.S. McDowell, N. Tan, M.R. Arkin, A. Conroy, W. Yang, N. Osheroff, J.A. Fox, Voreloxin Is an Anticancer Quinolone Derivative that Intercalates DNA and

Poisons Topoisomerase II, PLoS One. 5 (2010) e10186.
<https://doi.org/10.1371/journal.pone.0010186>.

- [23] X. Wang, X. Jiang, S. Sun, Y. Liu, Synthesis and biological evaluation of novel quinolone derivatives dual targeting histone deacetylase and tubulin polymerization as antiproliferative agents, *RSC Adv.* 8 (2018) 16494–16502. <https://doi.org/10.1039/C8RA02578A>.
- [24] A.P. Saraswati, N. Relitti, M. Brindisi, J.D. Osko, G. Chemi, S. Federico, A. Grillo, S. Brogi, N.H. McCabe, R.C. Turkington, O. Ibrahim, J. O’Sullivan, S. Lamponi, M. Ghanim, V.P. Kelly, D. Zisterer, R. Amet, P. Hannon, F. Vanni, C. Ulivieri, D. Herp, F. Sarno, A. Di Costanzo, F. Saccoccia, G. Ruberti, M. Jung, L. Altucci, S. Gemma, S. Butini, D.W. Christianson, G. Campiani, Spiroindoline-Capped Selective HDAC6 Inhibitors: Design, Synthesis, Structural Analysis and Biological Evaluation, *ACS Med. Chem. Lett.* (2020) Just Accepted. <https://doi.org/10.1021/acsmchemlett.0c00395>.
- [25] Y. Tangella, K.L. Manasa, N.H. Krishna, B. Sridhar, A. Kamal, B. Nagendra Babu, Regioselective Ring Expansion of Isatins with in Situ Generated α -Aryldiazomethanes: Direct Access to Viridicatin Alkaloids, *Org. Lett.* 20 (2018) 3639–3642. <https://doi.org/10.1021/acs.orglett.8b01417>.
- [26] M.D. Greenhalgh, S.M. Smith, D.M. Walden, J.E. Taylor, Z. Brice, E.R.T. Robinson, C. Fallan, D.B. Cordes, A.M.Z. Slawin, H.C. Richardson, M.A. Grove, P.H.-Y. Cheong, A.D. Smith, A C=O \cdots Isothiuronium Interaction Dictates Enantiodiscrimination in Acylative Kinetic Resolutions of Tertiary Heterocyclic Alcohols, *Angew. Chemie Int. Ed.* 57 (2018) 3200–3206. <https://doi.org/10.1002/anie.201712456>.
- [27] Z. Liu, Q. Lin, Q. Huang, H. Liu, C. Bao, W. Zhang, X. Zhong, L. Zhu, Semiconductor quantum dots photosensitizing release of anticancer drug, *Chem. Commun.* 47 (2011) 1482–1484. <https://doi.org/10.1039/C0CC04676K>.
- [28] L. Spear, Kerry, U. Campbell, *Heterocyclic Compounds and Methods of Use Thereof*, 2014.
- [29] A.H. Boulares, A.G. Yakovlev, V. Ivanova, B.A. Stoica, G. Wang, S. Iyer, M. Smulson, Role of Poly(ADP-ribose) Polymerase (PARP) Cleavage in Apoptosis: Caspase 3-Resistant PARP Mutant Increases Rates of Apoptosis in Transfected Cells, *J. Biol. Chem.* 274 (1999) 22932–22940. <https://doi.org/10.1074/jbc.274.33.22932>.
- [30] J.J. Kovacs, P.J.M. Murphy, S. Gaillard, X. Zhao, J.-T. Wu, C. V Nicchitta, M. Yoshida, D.O. Toft, W.B. Pratt, T.-P. Yao, HDAC6 Regulates Hsp90 Acetylation and Chaperone-Dependent Activation of Glucocorticoid Receptor, *Mol. Cell.* 18 (2005) 601–607. <https://doi.org/https://doi.org/10.1016/j.molcel.2005.04.021>.
- [31] S. Gemma, C. Camodeca, M. Brindisi, S. Brogi, G. Kukreja, S. Kunjir, E. Gabellieri, L. Lucantoni, A. Habluetzel, D. Taramelli, N. Basilico, R. Gualdani, F. Tadini-Buoninsegni, G. Bartolommei, M.R. Moncelli, R.E. Martin, R.L. Summers, S. Lamponi, L. Savini, I. Fiorini, M. Valoti, E. Novellino, G. Campiani, S. Butini, Mimicking the Intramolecular Hydrogen Bond: Synthesis, Biological Evaluation, and Molecular Modeling of Benzoxazines and Quinazolines as Potential Antimalarial

- Agents, *J. Med. Chem.* 55 (2012) 10387–10404. <https://doi.org/10.1021/jm300831b>.
- [32] A. Grillo, G. Chemi, S. Brogi, M. Brindisi, N. Relitti, F. Fezza, D. Fazio, L. Castelletti, E. Perdona, A. Wong, S. Lamponi, A. Pecorelli, M. Benedusi, M. Fantacci, M. Valoti, G. Valacchi, F. Micheli, E. Novellino, G. Campiani, S. Butini, M. Maccarrone, S. Gemma, Development of novel multipotent compounds modulating endocannabinoid and dopaminergic systems, *Eur. J. Med. Chem.* 183 (2019) 111674. <https://doi.org/10.1016/j.ejmech.2019.111674>.
- [33] P.L. Skipper, S.R. Tannenbaum, W.G. Thilly, E.E. Furth, W.W. Bishop, Mutagenicity of Hydroxamic Acids and the Probable Involvement of Carbamoylation, *Cancer Res.* 40 (1980) 4704 LP – 4708. <http://cancerres.aacrjournals.org/content/40/12/4704.abstract>.
- [34] S. Shen, A.P. Kozikowski, Why Hydroxamates May Not Be the Best Histone Deacetylase Inhibitors—What Some May Have Forgotten or Would Rather Forget?, *ChemMedChem.* 11 (2016) 15–21. <https://doi.org/10.1002/cmdc.201500486>.
- [35] M.S. Lee, M. Isobe, Metabolic Activation of the Potent Mutagen, 2-Naphthohydroxamic Acid, in *Salmonella typhimurium* TA98, *Cancer Res.* 50 (1990) 4300–4307.
- [36] L. Jašíková, E. Hanikýřová, A. Škríba, J. Jašík, J. Roithová, Metal-assisted lossen rearrangement, *J. Org. Chem.* 77 (2012) 2829–2836. <https://doi.org/10.1021/jo300031f>.
- [37] V. Hoffmann, N. Jenny, D. Häussinger, M. Neuburger, M. Mayor, Rotationally Restricted 1,1'-Bis-(phenylethynyl)ferrocene Subunits in Macrocycles, *European J. Org. Chem.* 2016 (2016) 2187–2199. <https://doi.org/10.1002/ejoc.201600158>.
- [38] C.J. Millard, P.J. Watson, I. Celardo, Y. Gordiyenko, S.M. Cowley, C.V. Robinson, L. Fairall, J.W.R. Schwabe, Class I HDACs Share a Common Mechanism of Regulation by Inositol Phosphates, *Mol. Cell.* 51 (2013) 57–67. <https://doi.org/https://doi.org/10.1016/j.molcel.2013.05.020>.
- [39] W.C. Still, A. Tempczyk, R.C. Hawley, T. Hendrickson, Semianalytical treatment of solvation for molecular mechanics and dynamics, *J. Am. Chem. Soc.* 112 (1990) 6127–6129. <https://doi.org/10.1021/ja00172a038>.
- [40] A. Vallone, S. D'Alessandro, S. Brogi, M. Brindisi, G. Chemi, G. Alfano, S. Lamponi, S.G. Lee, J.M. Jez, K.J.M. Koolen, K.J. Dechering, S. Saponara, F. Fusi, B. Gorelli, D. Taramelli, S. Parapini, R. Caldelari, G. Campiani, S. Gemma, S. Butini, Antimalarial agents against both sexual and asexual parasites stages: structure-activity relationships and biological studies of the Malaria Box compound 1-[5-(4-bromo-2-chlorophenyl)furan-2-yl]-N-[(piperidin-4-yl)methyl]methanamine (MMV019918) and analog, *Eur. J. Med. Chem.* 150 (2018) 698–718. <https://doi.org/https://doi.org/10.1016/j.ejmech.2018.03.024>.
- [41] S. Brogi, A. Ramunno, L. Savi, G. Chemi, G. Alfano, A. Pecorelli, E. Pambianchi, P. Galatello, G. Compagnoni, F. Focher, G. Biamonti, G. Valacchi, S. Butini, S. Gemma, G. Campiani, M. Brindisi, First dual AK/GSK-3 β inhibitors endowed with antioxidant properties as multifunctional, potential neuroprotective agents, *Eur. J. Med. Chem.* 138 (2017) 438–457. <https://doi.org/https://doi.org/10.1016/j.ejmech.2017.06.017>.

- [42] B. Heltweg, F. Dequiedt, E. Verdin, M. Jung, Nonisotopic substrate for assaying both human zinc and NAD⁺-dependent histone deacetylases, *Anal. Biochem.* 319 (2003) 42–48. [https://doi.org/https://doi.org/10.1016/S0003-2697\(03\)00276-8](https://doi.org/https://doi.org/10.1016/S0003-2697(03)00276-8).
- [43] D. Wegener, F. Wirsching, D. Riester, A. Schwienhorst, A Fluorogenic Histone Deacetylase Assay Well Suited for High-Throughput Activity Screening, *Chem. Biol.* 10 (2003) 61–68. [https://doi.org/https://doi.org/10.1016/S1074-5521\(02\)00305-8](https://doi.org/https://doi.org/10.1016/S1074-5521(02)00305-8).
- [44] B. Heltweg, J. Trapp, M. Jung, In vitro assays for the determination of histone deacetylase activity, *Methods.* 36 (2005) 332–337. <https://doi.org/https://doi.org/10.1016/j.ymeth.2005.03.003>.
- [45] R.A. Copeland, Reversible Inhibitors, 2000. <https://doi.org/doi:10.1002/0471220639.ch8>.
- [46] D. Purves, C. Harvey, D. Tweats, C.E. Lumley, Genotoxicity testing: current practices and strategies used by the pharmaceutical industry, *Mutagenesis.* 10 (1995) 297–312. <https://doi.org/10.1093/mutage/10.4.297>.
- [47] T.J. Makhafola, E.E. Elgorashi, L.J. McGaw, L. Verschaeve, J.N. Eloff, The correlation between antimutagenic activity and total phenolic content of extracts of 31 plant species with high antioxidant activity, *BMC Complement. Altern. Med.* 16 (2016) 490. <https://doi.org/10.1186/s12906-016-1437-x>.